

**The role of afferent lymph from the gut in the regulation of
the microenvironment and the immune response in the
mesenteric lymph node**

Von der Naturwissenschaftlichen Fakultät der Gottfried Wilhelm Leibniz
Universität Hannover

zur Erlangung des Grades einer
Doktorin der Naturwissenschaften

Dr. rer. nat.

genehmigte Dissertation von

Dipl. Biol. Manuela Ahrendt

geboren am 27.07.1977 in Magdeburg

2009

Referent: Prof. Dr. Walter Müller
Korreferent: Prof. Dr. Reinhard Schwinzer
Tag der Promotion: 08. 06. 2009

Index of contents

List of Abbreviations	- 1 -
Zusammenfassung	- 3 -
Abstract	- 5 -
1. General Introduction	- 6 -
1.1 Organization of lymph nodes	- 6 -
1.2 Differences between lymph nodes	- 8 -
1.3 Immune response	- 9 -
1.4 Oral tolerance	- 12 -
2. The aim of this study	- 14 -
3. Dendritic cell subsets in lymph nodes are characterized by the specific draining area and influence the phenotype and fate of primed T cells	- 16 -
Abstract	- 18 -
3.1. Introduction	- 19 -
3.2. Material and Methods	- 22 -
3.3. Results	- 27 -
3.4. Discussion	- 33 -
3.5. References	- 37 -
3.6. Figures	- 41 -
4. Stromal cells confer lymph node-specific properties by shaping a unique microenvironment influencing local immune responses	- 53 -
Abstract	- 55 -
4.1. Introduction	- 56 -
4.2. Material and Methods	- 59 -
4.3. Results	- 64 -
4.4. Discussion	- 70 -
4.5. References	- 74 -
4.6. Figures	- 79 -
5. Stromal mesenteric lymph node cells are essential for the generation of gut-homing T cells in vivo	- 90 -
Abstract	- 91 -
5.1. Introduction	- 92 -
5.2. Results and Discussion	- 94 -

5.3. Material and Methods	- 102 -
5.4. References	- 107 -
5.5. Figures	- 110 -
6. The mesenteric lymph nodes exhibit a regulatory function in forming a Cholera-toxin specific IgA response in the intestine, whereas the spleen reacts systemically by specific IgM	- 123 -
Abstract	- 124 -
6.1. Introduction	- 125 -
6.2. Material and Methods	- 128 -
6.3. Results	- 133 -
6.4. Discussion	- 137 -
6.5. References	- 141 -
6.6. Figures	- 144 -
7. Lymph node stromal cells strongly influence immune response suppression	- 153 -
Abstract	- 154 -
7.1. Introduction	- 155 -
7.2. Material and Methods	- 158 -
7.3. Results	- 162 -
7.4. Discussion	- 165 -
7.5. References	- 170 -
7.6. Figures	- 175 -
8. General discussion	- 182 -
9. References	- 191 -
10. Contribution	- 200 -
11. Curriculum vitae	- 201 -
12. Publication list	- 203 -
13. Erklärung zur Dissertation	- 205 -
14. Danksagung	- 206 -

List of Abbreviations

Ag	Antigen
CCL	CC chemokine ligand
CCR	CC chemokine receptor
CD	Cluster of differentiation
CT	Cholera toxin
CXCL	CXC chemokine ligand
CXCR	CXC chemokine receptor
DC	Dendritic cells
FoxP3	Forkhead box p3
HEV	High endothelial venules
IFN	Interferon
Ig	Immunoglobulin
IL	Interleukin
LN	Lymph node
LNtx	Transplanted lymph node fragments
LP	Lamina propria
MAdCAM-1	Mucosal addressin cell adhesion molecule-1
MHC	Major histocompatibility complex
mLN	Mesenteric lymph node
mLNtx	Transplanted mesenteric lymph node fragments
mRNA	Messenger ribonucleic acid
OVA	Ovalbumin
pLN	Peripheral lymph node
pLNtx	Transplanted peripheral lymph node fragments

List of Abbreviations

PP	Peyer`s patches
RA	Retinoic acid
RALDH2	Retinal dehydrogenase 2
TGF	Transforming growth factor
Th1 or Th2	Type 1 or Type 2 helper T cells
Treg	Regulatory T cells

Zusammenfassung

Jeden Tag gelangen verschiedene Arten von Antigenen in den Darm. Dort werden sie von Dendritischen Zellen (DC) aufgenommen, die sie über die afferente Lymphe in den mesenterialen Lymphknoten (mLN) transportieren. Im mLN wird entweder eine Immunantwort ausgelöst, wenn das Antigen pathogen ist, oder Toleranz erzeugt, wenn es sich um ein harmloses Antigen handelt. Dieses besondere drainierende Gebiet des mLN führt zu einem einzigartigen Mikroenvironment im mLN im Vergleich zu anderen LN, wie beispielsweise den peripheren Lymphknoten (pLN). Auch wenn sie den gleichen Aufbau mit T- und B-Zell Kompartimenten haben, können doch unterschiedliche Zellpopulationen und unterschiedliche Expressionen von verschiedenen Molekülen gefunden werden.

Um die Frage zu beantworten, ob diese gebietsspezifischen Unterschiede vom LN selber gebildet werden oder vom Lymphfluss beeinflusst werden, wurde ein Transplantationsmodell entwickelt. Dabei wurde der mLN von Ratten und Mäusen entnommen und ein mLN oder ein pLN in das Mesenterium gesetzt. Nach der Regeneration wurden diese transplantierten Fragmente (mLNtx oder pLNtx) auf deren Zellpopulationszusammensetzung, auf das Zytokin- und Chemokinmuster sowie auf deren Fähigkeit untersucht eine spezifische Immunantwort oder mucosale Toleranz auszulösen.

Wir können zeigen, dass die transplantierten LN Fragmente regenerieren, dass die Immunzellen vom Spendertier sind und dass die sesshaften Stromazellen überleben. Weiterhin können wir nachweisen, dass Stromazellen, die das Grundgerüst des LN bilden, einen großen Einfluss auf das Zytokin- und Chemokinmuster im LN haben. Sie scheinen in der Lage zu sein Immunzellen zu manipulieren, wodurch die Induktion einer spezifischen Immunantwort und auch orale Toleranz beeinflusst wird.

Diese Ergebnisse zeigen deutlich, dass Stromazellen ein wichtiger Zelltyp für die Generierung eines einzigartigen Mikroenvironment im LN sind und dass diese Zellen einen Einfluss auf das Gleichgewicht zwischen Immunität und Toleranz haben.

Schlagwörter: Lymphknoten – Transplantation – Stromazellen

Abstract

Every day a huge number of different antigens (Ag) reaching the gut, are taken up by dendritic cells (DC) and transported via the afferent lymphatics into the mesenteric lymph node (mLN). In the mLN, an immune response has to be initiated if the Ag is pathogenic, or tolerance has to be induced if the Ag is harmless. This draining area of the mLN leads to a unique environment within the mLN compared to other LN such as the peripheral lymph node (pLN). Although they have the same architecture with regard to T and B cell compartments, different cell subsets and differences in the expression of various molecules have been identified.

To answer the question whether these site specific differences are LN derived or influenced by the draining area, a transplantation model was established. The mLN of rats and mice was removed and an mLN or a pLN was inserted into the mesentery. After regeneration these transplanted fragments (mLNtx and pLNtx) were analyzed as to their cell subset composition, their cytokine and chemokine pattern and also their ability to induce a specific immune response or mucosal tolerance. Our studies revealed that transplanted LN fragments regenerate and immune cells are host derived, whereas sessile stromal cells survive. Moreover, the stromal cells, which form the backbone of the LN, greatly influence the cytokine and chemokine pattern found in the LN. They seem to be able to educate immune cells, whereby the induction of specific immune responses and also that of oral tolerance are influenced. The results clearly demonstrate that stromal cells are an important cell type for the generation of the unique environment of the LN and that they have an influence on the balance between immunity and tolerance.

Keywords: Lymph nodes – Transplantation – Stromal cells

1. General Introduction

1.1 Organization of lymph nodes

Lymphoid tissues are classified as primary, secondary or tertiary lymphoid organs.

The bone-marrow and the thymus are well known primary lymphoid organs, whereas the function of tertiary lymphoid organs, which are found only in chronically inflamed tissue, is unclear [1, 2]. The spleen and lymph nodes belong to the secondary lymphoid organs. Lymph nodes (LN) are located all over the body in mammals and all have the same architecture in common. LN are encapsulated organs with three different compartmental structures (Fig.1). The first structure, called the cortex or the B cell compartment, is composed of primary and secondary lymphoid follicles.

Primary lymphoid follicles consist of recirculating naïve B cells which proliferate and differentiate after antigen recognition. Then a germinal center develops and the primary follicles turn into secondary lymphoid follicles [3, 4]. The second structure is the paracortex, a T cell rich area with high endothelial venules (HEV). HEV are the entry sites for naïve lymphocytes and activated T cells into the tissue leaving the blood [5-7]. They express the chemokine ligand CCL21, which is a chemotractant for immune cells, expressing the chemokine receptor CCR7 found on T and B cells as well as dendritic cells (DC). Stromal cells surrounding the HEV appear to produce CCL19, the second ligand for CCR7. The interaction of CCR7 with its ligands enables these immune cells to migrate into the LN [7-9]. The third structure is the medulla where effector T cells and memory B cells etc. emigrate via efferent lymphatics [2, 10]. T cells and B cells as well as DC are immune cells which can migrate between blood, lymphoid and nonlymphoid tissue. These cells are the motile cells of the LN [11]. The backbone and therefore the three dimensional architecture

of the LN are formed by stromal cells. Stromal cells are fixed, nonmigrating, nonhematopoietic cells which differ between the T and B cell compartments. Follicular dendritic cells are found in the B cell areas forming a three dimensional sponge like network. They are concerned with the organization of the follicles mediated by CXCL13 and its counterpart CXCR5 and also with the presentation of antigens to B cells [10, 12]. However, fibroblastic reticular cells (FRC) are extensively interconnected cells, forming the framework of the T cell area [10, 13, 14]. They make spaces where immune cells can come into contact with other cells. Furthermore, FRC ensheath thin strands of reticular fibers (RF), called the conduit system, where soluble antigens (Ag) and lymph borne fluid are transported into the lumen of HEV. DC are associated closely with the RF to take up these Ag and present them to T cells [6, 15, 16].

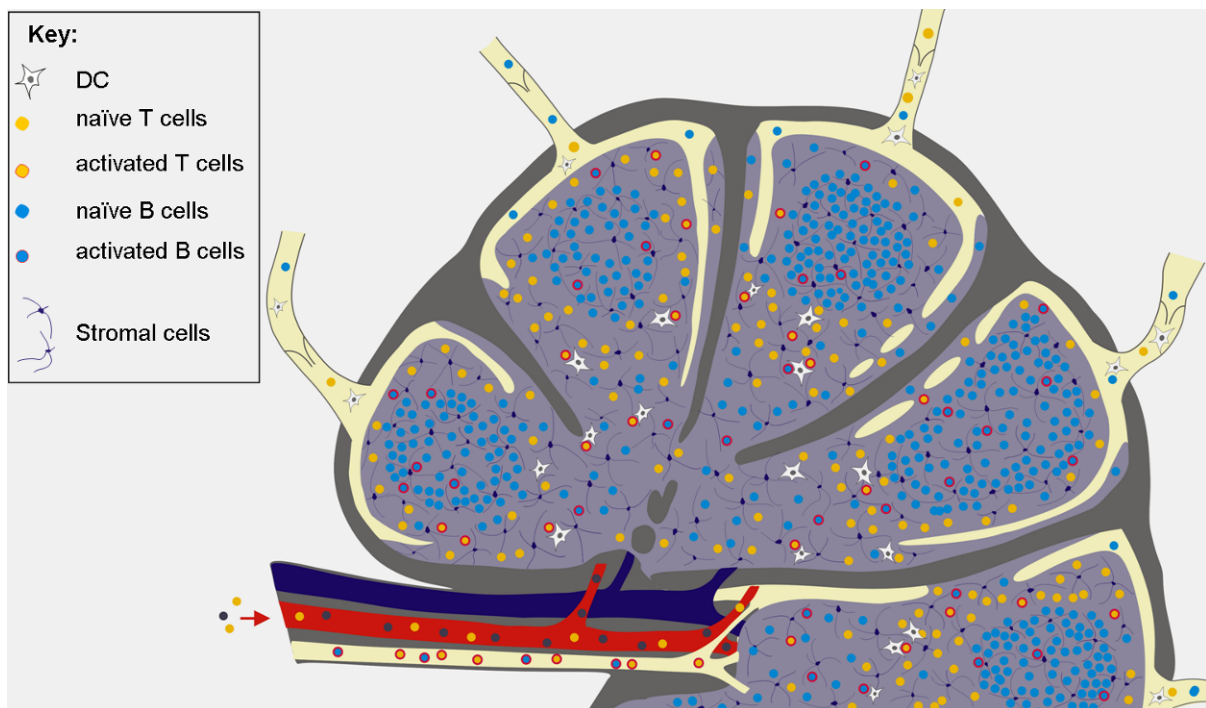


Fig.1 Structure of a lymph node

1.2 Differences between lymph nodes

With respect to their architecture, all LN look identical but on closer inspection differences have been found. LN which drain different areas of the body have been shown to be very different. Immune cells from skin draining LN for example show other surface molecules in comparison with lymphocytes isolated from the gut draining LN. The tissue specific expression pattern of LN has been studied in detail by many groups. They found that lymphocytes of the mesenteric LN (mLN), receiving Ag from the gut, are imprinted to upregulate CCR9 and the adhesion molecule $\alpha_4\beta_7$ integrin on their surface. The specific ligands of these molecules are also exclusively found in the gastrointestinal tract. The mucosal addressin cell adhesion molecule-1 (MAdCAM-1), the ligand for $\alpha_4\beta_7$ integrin is found on HEV in the gut and also in the mLN but could not be detected in peripheral LN (pLN) [7, 8]. However, lymphocytes showing a skin homing pattern are positive for E- and P- selectin ligands and also the chemokine receptor CCR4 which is associated with CCL17 [17].

Furthermore, dendritic cells (DC), coming from the gut show a unique phenotype. Almost all of them show a high expression of the major histocompatibility complex class II (MHCII) and are positive for CD103 and CD11c [18-20]. The enzyme retinal dehydrogenase 2 (RALDH2) is produced only on gut DC [21]. It was shown that RALDH2 is a metabolite in the oxidation of vitamin A to retinoic acid (RA) which is important for the induction of the gut homing molecules on lymphocytes [22, 23]. By contrast DC in pLN are CD103 negative. These DC produce hydroxylases which metabolize vitamin D3 into 1.25(OH)₂D₃, by which T cells upregulate skin homing molecules on their surface. DC in pLN do not express RALDH2 [17, 24, 25].

Additionally, a different cytokine milieu could be found in mLN compared to pLN. The mRNA level of interleukin-4 (IL-4) and transforming growth factor- β (TGF β) was much

higher in mLN, whereas IL-2 and interferon- γ (IFN γ) are decreased compared to pLN [26]. IL-4 for instance has been found to induce the downregulation of skin homing receptors on immune cells. Recently it was shown that in the presence of IL-4 mLN DC upregulate RALDH2, whereby CCR9 expression is induced on lymphocytes while a skin homing pattern is suppressed [27].

Different DC subsets and chemokines within the LN result in a different developmental orientation of CD4⁺ T cells. DC isolated from the mLN have been shown to promote T cells to change to a T helper type 2 (Th2) phenotype while differentiation into a T helper type 1 (Th1) cell is suppressed. An important component for this differentiation process is the cytokine IL-4 which is predominantly found in mLN. Otherwise the differentiation into the Th1 phenotype is supported by IL-2 which is expressed to a greater extent in pLN [20, 26, 28, 29].

1.3 Immune response

Every day pathogens, toxins and food antigens reach the gut and immune responses have to be initiated after recognizing pathogenic antigens (Fig.2). The mLN, draining gut, is the first place where Ag are presented and immune responses are initiated. Therefore, DC in the Peyer's patches (PP) are in close contact to M cells, which are specialized epithelial cells, that bring Ag into the neighbourhood of DC through transcytosis [20, 30]. Directly from the lumen of the gut lamina propria (LP) DC take up Ag and transport them via the afferent lymphatics to the mLN. Soluble Ag are also transported via the afferent lymphatics into the mLN where they are picked up by resident DC. Within the mLN the antigen-loaded DC communicate with T cells as well as B cells to initiate an immune response against the Ag [30].

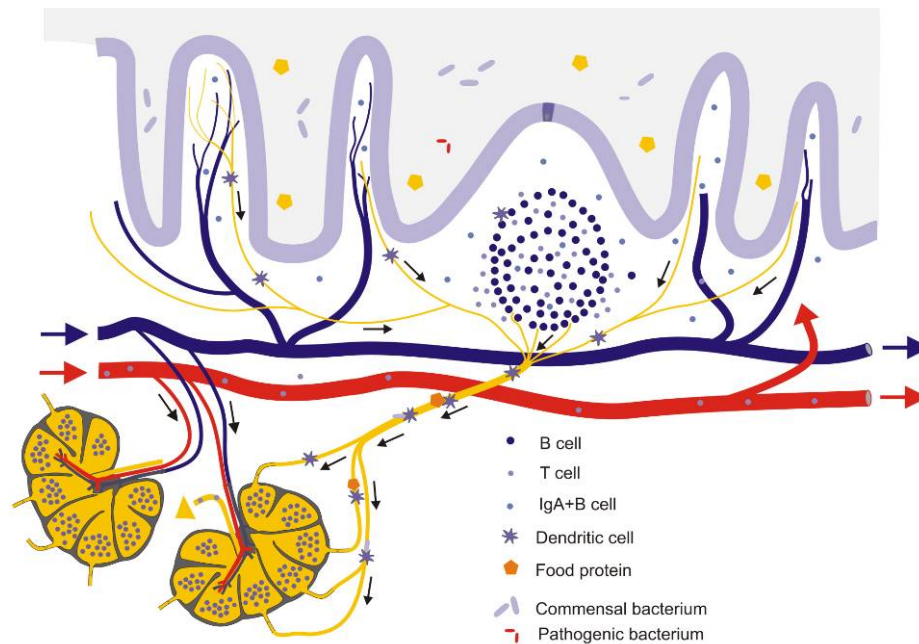


Fig.2 Route of intestinal antigen

From the lumen of the gut, Ag are taken up by DC or by cells within the Peyer's patches and transported into the mLN where an immune response can be induced or tolerance initiated.

DC, after capturing and processing the Ag, present them on their surface as MHC-peptide complexes within the T cell compartment of the mLN. Naïve T cells recirculate through the body from blood to the lymphoid tissue and back searching for their specific Ag. The interaction of T cells and DC leads to the differentiation and proliferation of T cells after successful Ag and co-stimulatory signal recognition [31, 32]. Dependent on the differentiation to Th1 or Th2, different activation markers are induced and different chemokines and cytokines are secreted. For example, Th1 cells produce $\text{IFN}\gamma$ and IL-2, while Th2 cells are characteristic for their production of IL-4 [29, 33]. In the mLN the differentiation into a Th2 phenotype is preferred, whereas CD4^+ T cells in the pLN are primed to a Th1 function [26]. Part of this differentiation process is the loss of LN homing receptors, e.g. CCR7, while gut homing molecules such as CCR9 and $\alpha_4\beta_7$ -integrin, are upregulated on effector T cells primed in the mLN. After that they leave the mLN and migrate to the small

intestine [29, 31-36]. T cells differentiated into T helper cells migrate, by upregulating the chemokine receptor CXCR5, to the B cell areas, where they meet B cells at the border between these two compartments. There, T cells help IgM⁺ B cells via the production of TGFβ to differentiate and proliferate into B cells specific for the immune response by immunoglobulin (Ig) class switching. Changing into IgA producing cells is characteristic for B cells differentiated in the mLN. This switch is promoted by RA produced by mLN DC. The interaction of B cells with DC also results in the upregulation of CCR9 and α₄β₇ integrin for the migration to the LP [10, 37-39]. Thus, the mLN provides the best conditions to quickly and efficiently induce a specific immune response in the draining tissue, the gut.

The newly formed effector lymphocytes provide optimal protection against intestinal pathogens. Ag specific lymphocytes require gut homing molecules to migrate selectively into the LP, where the interaction with CCL25 and MAdCAM-1 ensure the homing. These specific ligands are expressed on the postcapillary endothelial cells to regulate the recruitment into the LP. Effector T cells, which have found their way to the LP, secrete cytokines such as IFNγ or cytolytic proteins such as granzymes to fulfill their protective function [38, 40-42]. B cells, which reached the LP, complete their development by differentiation into IgA producing plasma cells. IgA is the most prominent antibody in the body because of the fact that the secretory IgA (sIgA) is the major isotype in the mucosal secretion. Many possibilities of protection mechanism could be identified to maintain the mucosal barrier by IgA. IgA can be subdivided into low and high affinity IgA. Low affinity IgA prevents the overrun of microorganisms or commensals in the gut, whereas high affinity IgA is produced to protect the host against pathogens. It neutralizes viral proteins on the way through the epithelial cells into the lumen and covers pathogens so that they can easily be identified and eliminated within the PP or the mLN [42-46].

1.4 Oral tolerance

The exclusive environment found in the mLN and in the gut, leads to an optimal and efficient induction of an immune response in this area. It also results in an additional phenomenon called mucosal tolerance. Tolerance is defined as an event where harmless Ag keep the immune response from reacting [47, 48]. The above mentioned antigen-loaded DC migrate via the afferent lymphatics into the mLN. Arriving in the mLN, they present the Ag to T cells. In the case of an immune response, this leads to clonal expansion of Ag specific T cells but in the case of oral tolerance anergy is induced or regulatory cytokine secreting T cells are stimulated [49,50].

Over the years it has been suggested that suppressor CD8⁺ T cells are required for the induction of oral tolerance by cross-presentation with DC [47]. However, depletion of CD8⁺ T cells shows no effect on the induction of oral tolerance, whereas depletion of CD4⁺ T cells prevents oral tolerance [51, 52]. Later studies showed that regulatory CD4⁺ T cells (Tregs) induced by RALDH2 producing DC, are involved in inducing mucosal tolerance [53, 54]. These FoxP3⁺ Tregs suppress the immune response against fed Ag [55, 56].

It is generally accepted that oral tolerance can be induced by feeding high or low doses of Ag. High doses of Ag result in T cell anergy and deletion, whereas low doses of Ag favor tolerance induced by regulatory T cells. After induction of oral tolerance by feeding a high doses of Ag without challenge, tolerized T cells cannot proliferate and enter the B cell follicles because of the absence of CXCR5 expression on their surface [57]. So they are not able to help B cells to proliferate and to switch the Ig class. Later, it has been found that tolerized T cells have the ability to migrate to the B cell area after challenging, but they remain unable to support B cell

proliferation [58]. It is suggested that these tolerized T cells are inefficient in producing cytokines. In μ MT mice which lack B cells, oral tolerance can be induced but suppressor chemokines are not upregulated, while T cell anergy is detected [59]. All this occurs mLN dependently because in the absence of the mLN, tolerance cannot be induced but by transferring mLN T cells from tolerized mice tolerance can be detected [60-62].

2. The aim of this study

Lymph nodes are distributed all over the body. They all have a basic architecture and are populated by the same cell types. Their function is to filter the lymph coming from the draining area and to induce a specific immune response. However, LN are confronted with incoming antigens of different areas. These differences result in different subsets of DC (CD103⁺DC within the mLN), the homing property of lymphocytes (CCR9 and $\alpha_4\beta_7$ on the surface to migrate into the LP) and the cytokine pattern in mLN compared to pLN (more IL-4 and less IL-2).

The elucidation of these differences originate from is still to be investigated. If they are influenced or triggered by the lymph from the draining area, or by components within the LN, for instance the stromal cells, is unknown. Many different components reach the LN via the lymph. This means that cells such as DC, lymphocytes or pathogens migrate from the tissue to the LN while soluble molecules such as cytokines, chemokines or antigens are transported to the LN. Within the LN, flexible immune cells populate the compartments formed by sessile stromal cells. These stromal cells are in close contact to immune cells to regulate their migration within the LN.

To investigate whether the lymph coming from the gut or stromal cells within the LN have an influence on immune cells and their reaction pattern after recognizing an antigen, we established a transplantation model. The mLN of rats and mice were removed and fragments of pLN or mLN were transplanted into the mesentery (Fig.3). The basis of further analysis was studies of regeneration of the transplanted LN fragments. Therefore, the compartment structure, the cell subset composition, the cytokine and chemokine pattern were determined on week 2 to 10. Furthermore, the functions of the regenerated lymph node fragments were investigated. This setup

provided an opportunity to analyze the generation of tissue tropism of T cells. Tolerance was induced to observe the ability in generating oral tolerance against fed antigens by induction of regulatory T cells. To induce an immune response cholera toxin (CT) were administrated orally and later on cell subsets in particular B cells and CT specific antibody were analyzed. Additionally, the role of the mLN on the induction of a CT specific immune response was studied after removing the mLN completely.

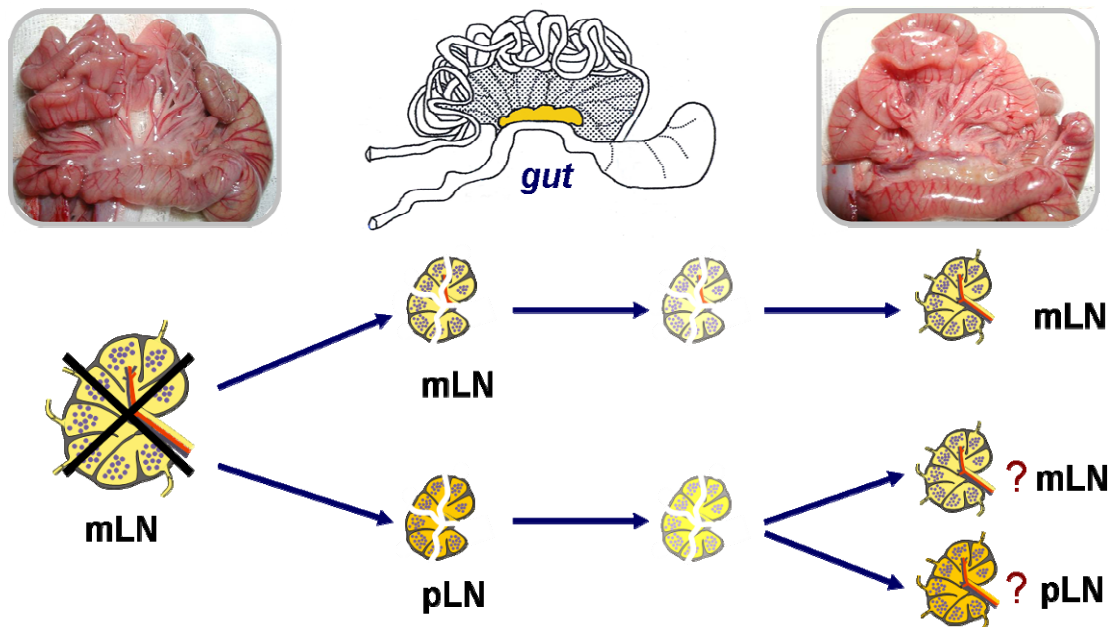


Fig.3 Transplantation model

The mLN of rats and mice were removed and mLN or pLN fragments were inserted into the mesentery. After regeneration the transplanted LN fragments were analyzed for their site-specific expression pattern. Did the transplanted pLN change to the expression pattern of an mLN influenced by the draining area, or did the pLN retain its site-specific expression generated by stromal cells?

3. Dendritic cell subsets in lymph nodes are characterized by the specific draining area and influence the phenotype and fate of primed T cells

Ulrike Bode*, Marc Lörchner*, Manuela Ahrendt*, Maike Blessenohl[?], Kathrin Kalies[?], Anja Claus*, Silke Overbeck^{??}, Lothar Rink^{??} and Reinhard Pabst*

* Functional and Applied Anatomy, Medical School Hannover, Hannover, Germany

? Institute of Anatomy, University of Lübeck, Lübeck, Germany

?? Institute of Immunology, RTWH Aachen, Aachen, Germany

Running Title

Dendritic cell imprinted fate of T cells

Keywords

Dendritic cells, lymph nodes, cytokines, rodents, T lymphocytes,

Abbreviations

MAM: *mycoplasma arthritidis* mitogen; **BrdU:** 5-Bromo-2-deoxy-uridine; **mLN:** mesenteric lymph node; **axLN:** axillary lymph node; **LN:** lymph node

Address correspondence to: Dr. Ulrike Bode; Anatomie II, OE 4120; Medizinische Hochschule Hannover; Carl-Neuberg-Str.1; 30625 Hannover, Germany; Phone: +49-511-532-2989; Fax: +49-511-532-2948; E-Mail: Bode.Ulrike@MH-Hannover.de

Senior author: Prof. Dr. R. Pabst; Anatomie II, OE 4120; Medizinische Hochschule Hannover; Carl-Neuberg-Str.1; 30625 Hannover, Germany; Phone: +49-511-532-6740; Fax: +49-511-532-2948; E-Mail: Pabst.Reinhard@MH-Hannover.de

Abstract

Dendritic cells (DC) are important in differential T cell priming. Little is known about the local priming by DC in the microenvironment of different lymph nodes and about the fate of the imprinted T cells. Therefore, freshly isolated rat DC from mesenteric lymph nodes (mLN) and axillary lymph nodes (axLN) were phenotyped and cultured with blood T cells in the presence of the superantigen *Mycoplasma arthritidis* mitogen (MAM). The phenotype, proliferation and apoptosis of the primed T cells were analyzed. Our data show that a common DC population exists in both mLN and axLN. In addition, region-specific DC with an organotypical marker expression imprinted by the drained area were found. Coculture of T cells with DC from mLN or axLN resulted in a distinct shift in the CD4 and CD8 expression of T cells and their phenotype. Furthermore, when these differentially primed mLN and axLN T cells were injected into recipients, mLN-primed T cells survived longer in other lymphoid organs. The results show that the region-specific DC have a unique phenotype and an impact on the ratio of CD4 : CD8 T cells during an immune response *in vivo*.

3.1. Introduction

Pathogens and other foreign antigens breaching the physical barriers of the body are recognized by a dense network of antigen-presenting cells (APC) that constantly survey the body for non-self antigens. Uptake of foreign antigens by APC induces their maturation and concomitantly their migration into the draining lymph node (LN) via the lymphatic system. Within the LN, T cells scanning APC recognize their cognate antigens, thereby initiating an adaptive immune response [1, 2].

A major cell population of the APC are dendritic cells (DC) [1]. In the periphery, DC are located in the epidermis of the skin. If the physical barrier of the skin breaks down and antigens invade the organism, DC in the skin take up these antigens and migrate via afferent lymphatics into peripheral lymph nodes (pLN) to initiate an immune response [3]. DC in the intestinal mucosa have to fulfill different functions: These DC are sitting in the lamina propria fishing antigen with their dendrites from the lumen of the gut [4]. Antigen-loaded DC migrate via the afferent lymphatics either into the Peyer's patches or into the mesenteric lymph node (mLN) [5]. Here, a decision has to be made whether the antigen is harmful or dangerous. Thus, a DC from the intestinal mucosa plays an important role in initiating an immune response and inducing tolerance [6]. This information has to be imprinted on T cells, because T cells are the effectors and mediators of the defense.

T cell polarization and tissue-specific targeting were deduced from the observation that DC from mLN produce retinoic acid, which is crucial for their ability to imprint T cells to express $\alpha_4\beta_7$ integrin [7]. Similarly, DC isolated from gut-associated lymphoid tissue are able to generate CCR9⁺ effector T cells [8], thereby imprinting T cells with a distinct migratory capacity.

In vitro studies showed that DC of pLN polarize T cells in the direction of becoming T helper type 1 (Th1). By secreting interferon- γ (IFN- γ) and interleukin-2 (IL-2) macrophages in the periphery were activated to internalize the antigen. In contrast, DC from Peyer's patches are able to prime T cells to a Th2 function [9, 10]. By their IL-4 production, Th2 cells help B cells to produce Immunoglobulin A, which is essential for the gut immune system.

However, it is not clear whether DC from mLN and pLN are able to induce differential T-cell function by polarizing T-cell priming into a more "cytotoxic" (CD8) or more "helper" (CD4) direction.

In addition, it is not known whether DC from pLN and mLN have the capacity to influence the survival time of their primed T cells and whether this is dependent on the draining area. First evidence came from studies that showed that effector T cells from mLN survived longer in contact with DC from mLN than with DC from pLN [11].

Superantigens are characterized by their ability to cross-link the major histocompatibility complex (MHC) class II molecules on APC as well as the T-cell receptor (TCR) on T lymphocytes by binding outside the antigen-specific groove of the MHC class II and TCR molecules. Superantigens bring these two critical molecules together to activate more than 2-20% of the whole T-cell pool [12].

Mycoplasma arthritidis mitogen (MAM) is more effective for rodent cells to induce proliferation than other superantigens, e.g. staphylococcal enterotoxin [13].

In this study we focused on the DC populations of the mLN and pLN (axillary LN (axLN)) under steady-state conditions in the rat. The phenotype of DC was analyzed in these two lymph nodes, especially focusing on differences. To functionally differentiate between the DC subsets present in both LN, the DC of mLN and axLN were directly isolated *ex vivo* and then incubated with blood T cells. The superantigen MAM was used to cross-link many T cells with DC.

Since an identical T-cell population was used in the coculture, differences in the priming of T cells directly correlate to the origin of DC isolated from either mLN or axLN. A further aim was to investigate whether the priming of T cells by mLN or axLN DC translates into a biologically different behavior and function of primed T cells *in vivo*. Thus, mLN and axLN primed T cells were adoptively transferred into wild-type recipients and their survival was analyzed *in vivo*.

3.2. Material and Methods

Rats

Rats from the standard inbred strain LEW/Ztm and LEW.7B/Won were bred and maintained at the central animal laboratory of the Medical School Hannover. The LEW.7B strain is identical with the congenic strain originally designated LEW.Ly1 [14]. The RT system is a diallelic polymorphism of the CD45 molecular system. Male animals weighing 180-220g were used for this study, which was approved by the Bezirksregierung Hannover 509c-42502-02/550.

Identification of *ex vivo* DC and their phenotype

The DC were isolated by treatment of LN fragments with 2 mg/ml collagenase D (Hoffmann La Roche, Basel, Switzerland) for 30 min at 37 C°. The enzyme activity was stopped by adding 10 mM EDTA to the cell suspension. The tissue debris was removed by filtering the cell suspension over a nylon filter. The cells were washed and then stained for analysis by flow cytometry. The DC were identified within the T and B cell negative population (Ox12 and R73, phycoerythrin conjugated, Serotec, Oxford, UK) by MHC class II; RT1B (Ox6, FITC conjugated, Serotec) and α_{E2} integrin (CD103) expression (Ox62, biotinylated, Serotec, and PerCP; BD Biosciences, Heidelberg, Germany). The phenotype of DC was characterized using various surface molecules specific for DC by four color staining (APC; BD Biosciences) and analysis by a FACScalibur flow cytometer (BD Biosciences).

Antibodies to phenotype DC subpopulations

For DC phenotyping the following antibodies were used: CD4 (W3/25; Serotec), NKR-P1A (3.2.3., Serotec), α_4 -integrin (HP2/1, Serotec), SIRP (ED9, Serotec), CD80

(BD Biosciences), CD8 (Ox8; Serotec), CD11c (8A2, Serotec), MHC class I (Ox18, Serotec) and IL-2 receptor (Ox39; Serotec).

Quantification of cytokine mRNA among mLN and axLN DC

Total RNA was isolated according to the manufacturer's protocol (Rneasy Kit, Quiagen, Hilden, Germany) and relative cytokine mRNA quantification was done as described in [17]. The primer sequences, the exon localizations, amplicon sizes and gene accession numbers of IL-2, IL-4, IL-10, IL-12p40, IL-15, TGF β -1, IFN- γ were used as described in [17].

Transplantation and regeneration of axLN fragments in the mesentery

The mLN of LEW rats were removed as described in Worbs et al. [6]. Then, mLN fragments or axLN fragments of donor LEW rats were transplanted into this area. Eight weeks after transplantation LN fragments were removed and analyzed for their DC population by flow cytometry.

Generation of mLN and axLN primed T cells

The blood of three LEW.7B/Won rats was sampled. Erythrocytes were removed by adding 25 ml of 150 mM NH₄Cl, 250 μ M EDTA and 10 mM KHCO₃ to 10 ml blood. Then, T cells were isolated by negative selection using the MACS technique following the instructions provided by Miltenyi (Bergisch-Gladbach, Germany). In detail, the blood leukocytes were incubated with mAbs against granulocytes (RP-1, Serotec), monocytes (ED9, Serotec), NK cells (3.2.3., Serotec) and B cells (Ox12, Serotec). For negative selection magnetic beads were used coupled with goat anti-mouse Abs (Miltenyi). The purity was 87 \pm 3 % T cells (n=6).

At the same time the mLN and axLN from 3-4 LEW rats were pooled and the LN were treated with 2 mg/ml collagenase D (Hoffmann La Roche) for 30 min at 37 C $^{\circ}$.

The enzyme activity was stopped by adding 10 mM EDTA to the cell suspension. The tissue debris was removed by filtering the cell suspension over a nylon filter. The cells were washed and then incubated with abs against T and B cells (R73 and Ox12, Serotec). For negative selection magnetic beads were used coupled with goat-anti-mouse Abs (Miltenyi). Then, the DC from mLN and axLN were isolated by negative selection using the MACS technique following the instructions provided by Miltenyi. The purity was analyzed by staining B and T cells (R73 and Ox12, Serotec) combined with an MHC class II (Ox 6, Serotec) and CD103 (Ox62, Serotec) staining. The purity was 90 ± 8 % DC (n=6). The subset of the purified DC was not different from the analyzed DC *ex vivo*. Macrophages were identified by the mAb ED1 (Serotec) in these fractions and <2% were seen among the purified cells. Most contaminating cells were T and B cells not selected by MACS.

The purified T cells and the purified DC were then incubated in a ratio of 1:10 (DC:T cells). To cross-link DC and T cells, 250 ng/ml recombinant superantigen MAM was added to the medium containing RPMI 1640 (Biochrome, Berlin, Germany), 100 units/ml penicillin/streptomycin (Biochrome), 20 mM Glutamin (Biochrome), 20 mM HEPES (ICN Biomedicals GMBH, Eschwege, Germany) and 2-Mercaptoethanol (Merck, Darmstadt, Germany). As a control purified T cells were stimulated by mAbs against the T cell receptor and CD28 *in vitro* as described [18]. After 3 days the cells were harvested and used for phenotyping or injection into recipients.

The phenotype of mLN and axLN primed T cells

T cells which were cultured with purified mLN and axLN DC were harvested 3 days after incubation. To analyze the subset, their phenotype and their proliferation by flow cytometry, three color staining was performed as previously described [11, 16]

Antibodies to phenotype mLN and axLN primed T cells

W3/25 (CD4, phycoerythrin conjugated; Serotec), Ox8 (CD8, biotinylated; Serotec), Ox39 (IL-2 receptor; Serotec), Ox85 (L-selectin, Serotec), HP2/1 (α_4 -integrin, Serotec), WT-1 (LFA-1, Serotec), Ox22 (CD45RC, Serotec) and 1A29 (ICAM-1, Serotec) were used to identify surface molecules. Anti-BrdU (Becton Dickinson (BD) Biosciences) was applied to detect incorporated BrdU.

ELISA of supernatants of cultured mLN and axLN primed T cells

Three days after co-culture of the purified cell populations, the medium was collected and analyzed by ELISA following the instruction guide of BD Biosciences (BD OptEIA Set for rat IFN- γ , IL-4, IL-6 and TNF- α). The optical density was determined in an ELISA-Reader (Bio-TEK Instruments GmbH, Bad Friedrichshall, Germany).

Migration, apoptosis and proliferation of injected mLN and axLN primed T cells

Between $17-42 \times 10^6$ mLN and axLN primed LEW.7B T cells were injected intravenously into LEW recipients. After 3 days 1 mg BrdU /100g weight was given intravenously. One hour later the animals were sacrificed and the injected cells were detected by the mAb His41 (Serotec) against the LEW.7B phenotype via flow cytometry in the mLN axLN and spleen. The percentage of annexin V positive cells among the injected T cells was analyzed by incubation of annexin V-FITC (BD Biosciences, Heidelberg, Germany) and followed analysis in the flow cytometry. The percentage of apoptotic cells was calculated using double staining with propidium iodide and annexin V. Only annexin V single positive cells were counted as apoptotic cells. The percentage of BrdU⁺ cells among the His41⁺ T cells was analyzed by immunohistology [15]. To compare the presence of injected mLN primed T cells in the mLN, axLN and spleen with the presence of axLN primed T cells in these organs, the numbers were calculated in relation to the injected cell number.

Production of recombinant MAM and MAM-GFP

We amplified the MAM gene (*mam*) from the *Mycoplasma arthritidis* Jasmin strain (ATCC 14124; American Type Culture Collection, Rockville, Md.) by PCR. The UGA codons at positions 132, 177 and 178 were converted to UGG codons through PCR using mutagenic primers. *Mam* was directly cloned into the protein fusion expression plasmid vector pGEX4T1 (Amersham, Heidelberg, Germany) without any additional residues. GFP (green fluorescent protein) and MAM-GFP constructs were cloned in the same way. Purification and cleavage of the glutathion-S-transferase-MAM fusion protein were carried out in accordance with the manufacturer's instructions.

Quantification of MAM binding among mLN and axLN DC

As described above mLN and axLN DC were isolated by the MACS technique. Then, the cell populations were incubated either with GFP (0.25 µg/ml) or with MAM-GFP (0.5 µg/ml) for 1h in the dark. FACS staining of MHC class II/ CD103 cells was performed as described above and the cells were then analyzed by three color cytometry. GFP served as a control for MAM-GFP.

3.3. Results

The DC composition of axLN and mLN was unique and influenced by their drainage area

MHCII and CD103 were used to distinguish between mLN and axLN DC. In the axLN, two major subpopulations of MHC class II⁺ cells could be identified based on the expression levels of MHCII and CD103: MHCII^{hi}/CD103⁻ and MHCII⁺/CD103⁻ (Fig.1A). In contrast, in the mLN MHCII^{hi}/CD103⁻ cells were almost absent, while a prominent population, MHCII⁺/CD103⁺ was in the majority in the mLN and only marginally found in the axLN (Fig.1A). The percentages of cells in these three subsets were analyzed. The data clearly show that MHCII⁺/CD103⁻ cells were equally distributed within mLN and axLN, while the MHCII^{hi}/CD103⁻ cells and the MHCII⁺/CD103⁺ cells were specifically present in axLN and mLN, respectively (Fig.1B). To test whether these unique compositions of axLN and mLN DC were influenced by their drainage area, the axLNs were transplanted into the drainage area of the gut. Eight weeks after transplantation, the DC composition of the axLN converted to the mLN pattern (compare Fig.1A to Fig.1C).

The region-specific DC populations of mLN and axLN differed in their cytokine release and phenotype

To find out how these region-specific cell populations differed functionally, their mRNA expression of cytokines and their phenotype were analyzed. Analysis of the cytokine profile by real-time PCR showed that purified DC from mLN produced a different cytokine profile compared to DC from axLN. TGF- β 1 and IL-12 mRNA were produced significantly more among the DC populations from axLN, whereas DC from mLN produced IL-4 mRNA (Fig.2A). Thus, DC from mLN and axLN differed in their

cytokine expression, suggesting that they might exert different priming capabilities on interacting T cells. Focussing on the phenotype of MHCII^{hi} CD103⁻ cells from axLN and MHCII⁺ CD103⁺ cells from mLN the data show the following: First, the two populations were completely different in their observed phenotype. Interestingly, while CD11c expression was found on most mLN MHCII⁺ CD103⁺ cells, MHCII^{hi} CD103⁻ cells from axLN exhibited only a minor CD11c expression (Fig.2B). On the other hand, most MHCII^{hi} CD103⁻ cells from axLN were CD4, NKR-P1A, SIRP and α_4 -integrin positive, while only about half of the MHCII⁺ CD103⁺ cells from mLN exhibited this phenotype pattern (Fig.2C). More than half of the MHCII^{hi} CD103⁻ cells and MHCII⁺ CD103⁺ expressed costimulatory molecules (CD80, Fig.2C), indicating that they were activated. These findings show that the regionally present DC populations were also unique in their phenotype, suggesting that the phenotype is also influenced by the drainage area.

Interestingly, the phenotype of the MHCII⁺ CD103⁻ cells, which were equally distributed between axLN and mLN, was comparable (data not shown). However, the CD11c expression differed significantly between the MHCII⁺ CD103⁻ cells from axLN and those from mLN (axLN 5 \pm 1%; mLN 49.3 \pm 12%, n=6). CD80 was only marginally expressed among these cells (axLN 5.1 \pm 1.2%; mLN 7.4 \pm 1.2%, n=6).

Most MHCII^{hi} CD103⁻ cells from axLN and MHCII⁺ CD103⁺ cells from mLN were able to bind the superantigen MAM

The next question was whether these two region-specific DC populations showed differences in antigen binding as a prerequisite to activate T cells. The superantigen MAM was chosen to analyze differences in the DC-T cell interaction and thereby in the capacity for T-cell activation. First, whether the capacity of binding the

superantigen MAM also differed among the region-specific DC populations from mLN and axLN was investigated.

The data show that nearly all MHCII^{hi} CD103⁻ cells from axLN and MHCII⁺ CD103⁺ cells from mLN were able to bind MAM (Fig.3A). However, looking at the mean fluorescence intensity (Fig.3A), it seems that MAM bound with higher affinity to the DC in axLN compared to mLN. Interestingly, although all DC subsets were MHCII⁺, the MHCII⁺ CD103⁻ cells, which were equally distributed to axLN and mLN and almost comparable in their phenotype, showed only minor MAM binding (Fig.3B). There is a prominent cell population among the MHCII⁺ CD103⁻ from axLN and mLN that did not bind MAM-GFP, but were MHCII⁺ (21±4.4%, n=4). MAM bound RT1D with a higher affinity than RT1B (identified by the mAbs Ox6 used in this study), which are both subclasses of the MHCII molecule (data not shown). Preliminary data suggest MHCII⁺ CD103⁺, which bound MAM-GFP, were more positive for RT1D expression than MHC⁺ CD103⁻ cells. The data indicate that the subpopulations of the DC from mLN and axLN have different expression levels of RT1B and RT1D, which leads to differential affinity of MAM binding.

The same pattern was seen among the DC subsets, when the MHC class I (MHCI) expression was analyzed: a higher MHCI expression was seen in MHCII⁺⁺ CD103⁻ cells from axLN and MHCII⁺ CD103⁺ cells from mLN compared to the MHCII⁺ CD103⁻ from both tissues (Fig.3C).

CD4⁺ and CD8⁺ effector T cells were primed differently by specific DC from mLN and axLN

To test how these specific DC populations from axLN and mLN are able to initiate an immune response and whether they are able to differently influence the direction of the response, blood T cells were cultured with DC from mLN and axLN in the

presence of MAM *in vitro*. First, the phenotype of primed T cells was analyzed after coculture with DC from mLN and axLN. Freshly isolated blood T cells are composed of about 80% CD4⁺ and 20% CD8⁺ T cells (Fig.4A). When these T cells were cultured with mAb stimulation against the TCR and CD28 in the absence of DC, the composition of CD4⁺ and CD8⁺ T cells did not change after stimulation (CD4⁺: 74±1.4%, CD8⁺ : 26±5.7, n=2). Interestingly, coculture with DC from mLN and axLN resulted in a distinct shift in the subset composition of T cells: The mLN-primed T cells were enriched in CD4⁺ T cells compared to the axLN-primed T cells. In contrast, among axLN-primed T cells the CD8⁺ T cells were doubled compared to the initial cell population, indicating that DC from axLN favored activating CD8⁺ T cells (Fig.4A). This was also shown by the absolute numbers of CD8⁺ T cells. While CD8⁺ T cells cultured with DC from mLN were comparable in their numbers before and after culture (before: 8.72 ±0.9 x 10⁶ cells; after: 7.12 ± 1.2 x 10⁶, n=3), CD8⁺ T cells were increased after culture with DC from axLN in comparison to the numbers before culture (before: 12.8 ±2.5 x 10⁶ cells; after: 18.2 ± 5.6 x 10⁶, n=3).

During the last hour of coculture BrdU was added to identify the cells that were in the S phase of the cell cycle at that time-point. The data showed that both the CD4⁺ and the CD8⁺ subsets among the mLN-primed T cells proliferated to a greater extent than axLN-primed T cells at the end of the coculture (Fig.4B). When BrdU was added for the whole culture time nearly all cells had incorporated BrdU during this period, indicating that these observed cells proliferated during culture (data not shown). Apoptosis among the cell populations was comparable (Fig.4C).

The mLN-primed effector CD4⁺ T cells were more activated than axLN-primed cells

Next, it was investigated whether the phenotype of the differentially primed T cells was altered after coculture with specific DC from mLN or axLN. CD4⁺ T cells, which were more numerous in the mLN-primed T-cell population, showed a decrease of L-selectin and CD45RC expression and an increase of IL-2 receptor expression compared to those primed with axLN DC. This shows that mLN CD4⁺ primed T cells were more activated than axLN-primed T cells (Fig.5A). In contrast, this was not the case for CD8⁺ T cells (Fig.5B). Then, whether DC from mLN and axLN induced the blood T-cell population to produce different cytokines was investigated. Therefore, after coculture the supernatants were analyzed for the cytokines IFN- γ , IL-6, TNF- α and IL-4. Whereas mLN-primed T cells produced more IFN- γ , for axLN-primed T cells it was IL-6 (Fig.5C) after MAM stimulation. Blood T cells which were stimulated via mAbs against the TCR and CD28 had decreased levels of IFN- γ compared to those stimulated with mLN and axLN DC (stimulated with mAbs: 551 \pm 57 pg/ml; stimulated in the presence of mLN DC: 4614 \pm 1472 pg/ml and axLN DC: 1267 \pm 211 pg/ml).

Effector T cells primed from mLN DC survived preferentially *in vivo*

Finally, we analyzed whether the differential priming of T cells with regional specific DC from mLN or axLN *in vitro* resulted in a different organ distribution of these T cells after adoptive transfer into wild-type recipients. Adoptively transferred cells were identified by mAb His41, which specifically recognizes cells of LEW.7B origins in LEW recipients (Fig.6A). The distribution pattern was analyzed 3 days after injection, because it had been seen in earlier studies that this was the best time-point to quantify the survival of activated T cells in lymphoid organs in response to their proliferation and cell death [18, 19]. Since the CD4 and CD8 priming of the T cells

during the coculture depended on the source of DC, both subsets were observed with respect to their distribution and survival by flow cytometry. Surprisingly, although identical T-cell numbers were transferred, we observed that both CD4⁺ and CD8⁺ mLN-primed T cells were more frequent in the studied lymphoid organs compared to axLN-primed T cells (Fig.6B and C). In addition, injected CD4⁺ T cells primed from mLN DC had a tendency to be found in higher numbers in mLN, axLN and spleen (Fig.6C). The different cell numbers in these tissues may be caused by differential rates of proliferation and/or apoptosis. Since the proliferation among the injected T cells was comparable (data not shown), the percentage of annexin V-positive cells among the injected T cells was calculated. The data showed that axLN-primed T cells exhibited more apoptotic cells in the mLN and spleen (Fig.6D), suggesting that T cells primed from mLN DC can survive longer than axLN-primed T cells.

3.4. Discussion

DC are important components of the LN microenvironment [20]. Many studies show that they are able to imprint and polarize T cells to produce typical cytokines resulting in alternative T cell function [21, 22].

Our study shows that in normal uninfected animals the mLN and the axLN exhibit distinct DC subsets *in vivo*. Similar organotypic differences between DC in spleen and thymus have been described before [23]. It was shown that MHCII^{hi} cells belong to the Langerhans cell population; these cells reside in their immature state in the epidermis and dermis [3, 24]. This indicates that the MHCII^{hi} CD103⁻ cells, which were exclusively found in the axLN, are Langerhans cells. In the mLN a population of MHCII⁺ CD103⁺ cells was found. Studies in the mouse showed that CD103⁺ DC were predominantly found in the lamina propria of the gut underlining our observations [25, 26]. When we transplanted an axLN into the drainage area of the mLN the DC subset composition of the axLN converted to that of the mLN. Therefore, these region-specific DC subsets are found to be recruited from the drainage area, i.e. the skin and the gut. In addition, these region-specific DC subsets were predominantly CD80⁺ and could bind the superantigen MAM nearly 100%. This indicates that these cells are APC, which were able to stimulate T cells in our *in vitro* system most effectively. However, the MAM binding seems to have a different affinity to DC from axLN and mLN, which may effect T-cell stimulation. Furthermore, the phenotype of these region-specific DC is dependent on the drainage area: the mLN-specific DC mainly produce Th2 cytokines (e.g. IL-4), favoring B-cell development, while the axLN-specific DC produce Th1 cytokines (IL-12) for activating macrophages. It was also found in other species that DC from different sources are able to imprint T cells differently [1, 9, 27]. In addition, in the axLN nearly all of the region-specific DC were

CD4⁺ and SIRP⁺, which has been shown to be a population with a potential to activate T cells [28, 29]. Interestingly these cells also expressed the NKR-P1A receptor. It was shown that DC in the rat expressed the NKR-P1A receptor and that these cells exhibit cytolytic function [23, 30]. However, on the other hand, cross-linking of the receptors leads to IL-12 and IL-1 β cytokine release and induces an activation process on the target cell [31]. In contrast, in the mLN only about 50% of the region-specific DC were CD4⁺ SIRP⁺. It was shown that in the gut-draining lymph two subpopulations exist distinguished by their CD4 and SIRP expression: CD4^{hi} SIRP^{hi} DC are involved in the stimulation of T cells and CD4^{low} SIRP^{low} DC are involved in tolerance mechanism [32, 33, 29].

Another interesting point is that all DC of mLN exhibit a high expression of CD11c compared to those in the axLN. Only a minor population of the DC from axLN display CD11c expression. It was shown that CD11c⁻ cells in the blood belong to the plasmacytoid cell population (pDC), which are specialized cells that secrete cytokines, in particular very large amounts of type I IFNs, in response to viral stimuli [29, 34, 35]. However, it is unknown why pDC are differently distributed throughout the body.

We also identified a DC population in the mLN and axLN, which is MHCII⁺ and CD103⁻. These cells were not region-specific because they were found in both tissues and showed a comparable phenotype. Probably they were resident DC, which are not recruited from the drained area. However, they represent a large population among the DC from both mLN and axLN, and it remains to be studied how these cells influence T-cell priming during stimulation. The CD80 expression indicates that these DC were not in an activated state. Our hypothesis is that they come from the bloodstream into the LN, forming a basic DC pool.

Our data show that the initially identical cell population was differentially primed to induce more activated CD4⁺ T cells (mLN) or more CD8⁺ T cells (axLN). Since T cells stimulated with DC from mLN were more activated, they produced high amounts of IFN- γ by this procedure.

Some studies showed that DC from Peyer`s patches and mLN are able to prime T cells to produce Th2 cytokines [9]. In contrast, the current study suggests that DC alone, which were directly used after mLN isolation and not cultured for expansion, are not able to prime T cells into the Th2 direction. Many other cells are forming the microenvironment of the lymph node, for example the reticular cells [36, 37].

Preliminary data show that other cells, for example stromal cells, are additionally necessary to fulfill T-cell polarization during priming [38]. Furthermore, the lack of induction of a Th2 polarization of mLN-primed T cells may be the results of LEW rat strain and/or MAM as the stimulus, because this strain and this superantigen predominantly develop Th1 responses [39, 40].

Thus, DC, coming from the periphery via the afferent lymphatics into the regional lymph node, are able to determine which T-cell population should be primed.

Therefore, the draining area determines which T-cell function would be supported: the cytotoxic or the helper function.

In addition, the survival of effector T cells, migrating into lymphoid organs after recirculation, is also influenced during the first priming by the region-specific DC: T cells which were stimulated with DC from mLN, survived longer in all lymphoid organs because of decreased apoptosis. Many studies showed that DC from gut-associated lymphoid tissue are able to prime T cells to preferentially express $\alpha_4\beta_7$ integrin and chemokine receptor CCR9 for preferential homing to the gut [26, 41].

Our study shows that priming of T cells by tissue-specific DC is not only involved in selective induction of homing receptors [7, 26, 42], but also in the decision whether

helper or cytotoxic T cells expand and survive. Furthermore, the initial priming by regional DC decides which, where and how effector T cells survive.

In conclusion, we showed that in healthy animals region-specific DC are found in mLN and axLN. They are obviously recruited from the drainage area via the afferent lymph and therefore show a unique area-imprinted phenotype. This specific function of these DC enables the initiation of immune responses of the lymph node in the draining area to prime T cells for an effective response here. In addition, the location of the DC determines whether predominantly helper or cytotoxic T-cell function is favoured and how these cells survive throughout the body. We would argue that not only tissue-specific homing receptor expression of T cells is primed by regional-specific DC but also the fate of these T cells is dependent on the DC pattern they were primed with *in vivo*. Therefore, manipulating the region-specific DC will be a helpful therapeutic concept to reduce autoimmune reactions in the drained tissue.

Acknowledgements

The comments of Jürgen Westermann (Lübeck), Anke Lührmann (Hannover), and Oliver Pabst (Hannover) have been of great help. We thank Dr. M. Leiß, Dräger Medical Ag & Co., Lübeck, Germany for donating a Dräger Vapor 19.n anesthetic vaporizer. The authors also wish to thank Mrs. S. Fiedler and Mrs. F. Weidner for excellent technical assistance and Ms S. Fryk for correction of the English. The work was supported by grants of the Deutsche Forschungsgemeinschaft to U.B. (BO1288/1-2 and SFB621 A10).

3.5. References

1. von Andrian UH, Mempel TR. Homing and cellular traffic in lymph nodes. *Nat. Rev. Immunol.* 2003; 3:867-78
2. Crivellato E, Vacca A, Ribatti D. Setting the stage: an anatomist's view of the immune system. *Trends Immunol.* 2004; 25:210-7
3. Ohl L, Mohaupt M, Czeloth N et al. CCR7 governs skin dendritic cell migration under inflammatory and steady-state conditions. *Immunity* 2004; 21:279-88
4. Niess JH, Brand S, Gu X et al. CX3CR1-mediated dendritic cell access to the intestinal lumen and bacterial clearance. *Science* 2005; 307:254-8
5. Macpherson AJ, Smith K. Mesenteric lymph nodes at the center of immune anatomy. *J. Exp. Med.* 2006; 203:497-500
6. Worbs T, Bode U, Yan S et al. Oral tolerance originates in the intestinal immune system and relies on antigen carriage by dendritic cells. *J. Exp. Med.* 2006; 203:519-27
7. Iwata M, Hirakiyama A, Eshima Y et al. Retinoic acid imprints gut-homing specificity on T cells. *Immunity* 2004; 21:527-38
8. Johansson-Lindbom B, Svensson M, Wurbel MA et al. Selective generation of gut tropic T cells in gut-associated lymphoid tissue (GALT): requirement for GALT dendritic cells and adjuvant. *J. Exp. Med.* 2003; 198:963-9
9. Iwasaki A, Kelsall BL. Freshly isolated Peyer's patch, but not spleen, dendritic cells produce interleukin 10 and induce the differentiation of T helper type 2 cells. *J. Exp. Med.* 1999; 190:229-39
10. Kellermann SA, McEvoy LM. The peyer's patch microenvironment suppresses T cell responses to chemokines and other stimuli. *J. Immunol.* 2001; 167:682-90
11. Bode U, Sahle A, Sparmann G et al. The fate of effector T cells in vivo is determined during activation and differs for CD4+ and CD8+ cells. *J. Immunol.* 2002; 169:6085-91
12. Proft T, Fraser JD. Bacterial superantigens. *Clin. Exp. Immunol.* 2003; 133:299-306
13. Cole BC, Atkin CL. The *Mycoplasma arthritidis* T-cell mitogen, MAM: a model superantigen. *Immunol. Today* 1991; 12:271-6

14. Wonigeit K. Characterization of the RT-Ly-1 and RT-Ly-2 alloantigenic systems by congenic rat strains. *Transplant. Proc.* 1979; 11:1631-5
15. Bode U, Tiedemann K, Westermann J. CD4⁺ effector T cell distribution in vivo: TGF-beta 1/TGF-beta receptor II interaction during activation mediates accumulation in the target tissue by preferential proliferation. *Eur. J. Immunol.* 2004; 34:1050-8
16. Bode U, Sparmann G, Westermann J. Gut-derived effector T cells circulating in the blood of the rat: preferential re-distribution by TGFbeta-1 and IL-4 maintained proliferation. *Eur. J. Immunol.* 2001; 31:2116-25
17. Kalies K, Blessenohl M, Nietsch J et al. T cell zones of lymphoid organs constitutively express Th1 cytokine mRNA: Specific changes during the early phase of an immune response. *J. Immunol.* 2006; 176:741-9
18. Bode U, Wonigeit K, Pabst R et al. The fate of activated T cells migrating through the body: rescue from apoptosis in the tissue of origin. *Eur. J. Immunol.* 1997; 27:2087-93
19. Westermann J, Bode U. Distribution of activated T cells migrating through the body: a matter of life and death. *Immunol. Today* 1999; 20:302-6
20. Mellman I, Steinman RM. Dendritic cells: specialized and regulated antigen processing machines. *Cell* 2001; 106:255-8
21. Banchereau J, Steinman RM. Dendritic cells and the control of immunity. *Nature* 1998; 392:245-52
22. Steinman RM, Hemmi H. Dendritic cells: translating innate to adaptive immunity. *Curr. Top. Microbiol. Immunol.* 2006; 311:17-58
23. Trinite B, Voisine C, Yagita H et al. A subset of cytolytic dendritic cells in rat. *J. Immunol.* 2000; 165:4202-8
24. Czeloth N, Bernhardt G, Hofmann F et al. Sphingosine-1-phosphate mediates migration of mature dendritic cells. *J. Immunol.* 2005; 175:2960-7
25. Annacker O, Coombes JL, Malmstrom V et al. Essential role for CD103 in the T cell-mediated regulation of experimental colitis. *J. Exp. Med.* 2005; 202:1051-61
26. Johansson-Lindbom B, Svensson M, Pabst O et al. Functional specialization of gut CD103⁺ dendritic cells in the regulation of tissue-selective T cell homing. *J. Exp. Med.* 2005; 202:1063-73

27. Mempel TR, Henrickson SE, von Andrian UH. T-cell priming by dendritic cells in lymph nodes occurs in three distinct phases. *Nature* 2004; 427:154-9
28. Turnbull E, MacPherson G. Immunobiology of dendritic cells in the rat. *Immunol. Rev.* 2001; 184:58-68
29. Hubert FX, Voisine C, Louvet C et al. Differential pattern recognition receptor expression but stereotyped responsiveness in rat spleen dendritic cell subsets. *J. Immunol.* 2006; 177:1007-16
30. Josien R, Heslan M, Souillou JP et al. Rat spleen dendritic cells express natural killer cell receptor protein 1 (NKR-P1) and have cytotoxic activity to select targets via a Ca²⁺-dependent mechanism. *J. Exp. Med.* 1997; 186:467-72
31. Poggi A, Rubartelli A, Moretta L et al. Expression and function of NKR1A molecule on human monocytes and dendritic cells. *Eur. J. Immunol.* 1997; 27:2965-70
32. Liu L, Zhang M, Jenkins C et al. Dendritic cell heterogeneity in vivo: two functionally different dendritic cell populations in rat intestinal lymph can be distinguished by CD4 expression. *J. Immunol.* 1998; 161:1146-55
33. Huang FP, Platt N, Wykes M et al. A discrete subpopulation of dendritic cells transports apoptotic intestinal epithelial cells to T cell areas of mesenteric lymph nodes. *J. Exp. Med.* 2000; 191:435-44
34. Yrlid U, Milling SW, Miller JL et al. Regulation of intestinal dendritic cell migration and activation by plasmacytoid dendritic cells, TNF-alpha and type 1 IFNs after feeding a TLR7/8 ligand. *J. Immunol.* 2006; 176:5205-12
35. Yrlid U, Cerovic V, Milling S et al. Plasmacytoid dendritic cells do not migrate in intestinal or hepatic lymph. *J. Immunol.* 2006; 177:6115-21
36. Dudda JC, Martin SF. Tissue targeting of T cells by DCs and microenvironments. *Trends Immunol.* 2004; 25:417-21
37. Katakai T, Hara T, Sugai M et al. Lymph node fibroblastic reticular cells construct the stromal reticulum via contact with lymphocytes. *J. Exp. Med.* 2004; 200:783-95
38. Kraal G, Samsom JN, Mebius RE. The importance of regional lymph nodes for mucosal tolerance. *Immunol. Rev.* 2006; 213:119-30
39. Fournie GJ, Cautain B, Xystrakis E et al. Cellular and genetic factors involved in the difference between Brown Norway and Lewis rats to develop

- respectively type-2 and type-1 immune-mediated diseases. *Immunol. Rev.* 2001; 184:145-60
40. Rink L, Luhm J, Koester M et al. Induction of a cytokine network by superantigens with parallel TH1 and TH2 stimulation. *J. Interferon Cytokine Res.* 1996; 16:41-7
 41. Johansson-Lindbom B, Svensson M, Wurbel MA et al. Selective generation of gut tropic T cells in gut-associated lymphoid tissue (GALT): requirement for GALT dendritic cells and adjuvant. *J. Exp. Med.* 2003; 198:963-9
 42. Mora JR, Bono MR, Manjunath N et al. Selective imprinting of gut-homing T cells by Peyer's patch dendritic cells. *Nature* 2003; 424:88-93

This is the pre-peer-reviewed version of the following article: "Dendritic cell subsets in lymph nodes are characterized by the specific draining area and influence the phenotype and fate of primed T cells", *Immunology*. 2008. Apr;123(4):480-90, which has been published in final form at

<http://www.pubmedcentral.nih.gov/articlerender.fcgi?artid=2433315>

3.6. Figures

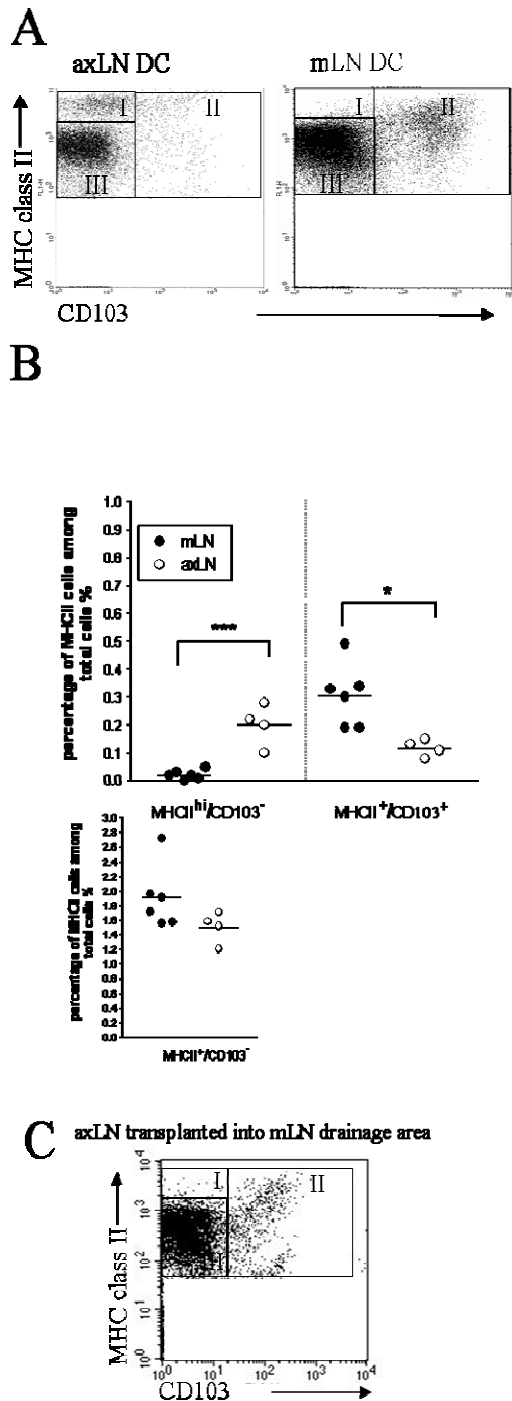


Fig.1: The composition of DC subsets in the mLN is unique and differs from that in the axLN

The subset composition of *ex vivo* DC in mLN and axLN was identified by gating on the T and B cell negative population. Three subpopulations were visualized by MHC

class II⁺ and CD103 expression. **A.** MHCII^{hi}/CD103⁻ (I), MHCII⁺/CD103⁺ (II) and MHCII⁺/CD103⁻ (III). The dot plots clearly show that the MHCII^{hi}/CD103⁻ (I) subpopulation is only present among DC from axLN, while the MHCII⁺/CD103⁺ (II) subpopulation is mostly present in the mLN. **B.** The percentages of cells among the subsets were quantified. Whereas in the mLN more cells were in the MHCII⁺/CD103⁺ (II) subset, the MHCII^{hi}/CD103⁻ (I) subset was only seen in the axLN. Single values are shown. The horizontal lines represent mean values. Asterisks indicate significant differences between DC from mLN and axLN in the students T-test (* p<0.05, *** p<0.001). MHCII⁺/CD103⁻ (III) were equally distributed to mLN and axLN. **C.** 8 weeks after transplantation of an axLN the DC subset composition had converted to the mLN pattern: the MHCII^{hi}/CD103⁻ (I) subset was not seen, whereas the MHCII⁺/CD103⁺ (II) subset was present. The dot plot is representative for three independent experiments.

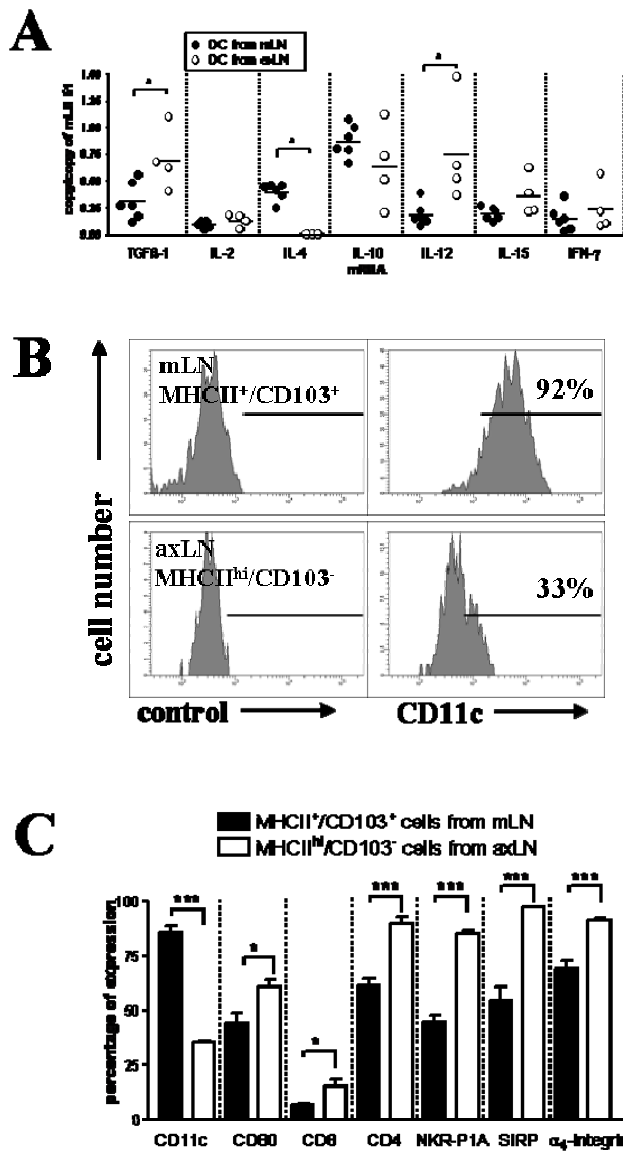


Fig.2: DC from mLN and axLN differ in their cytokine pattern

A. Various cytokine mRNA in purified DC from mLN and axLN were quantified in the real-time PCR. The copies of amplification of cytokine cDNA were related to the measured copies of mLN51, which is constantly produced in mLN and axLN. TGFβ-1 and IL-12 mRNA were produced more by DC from axLN and only DC from mLN produced IL-4 mRNA. Single values of 4-6 independent experiments are shown. The horizontal lines represent mean values. Asterisks indicate significant differences between DC from mLN and axLN in the students T-test (* p<0.05). **B.-C.** The subset composition of DC in mLN and axLN was identified by gating on the T and B cell

negative population and by visualizing the three subpopulations by showing MHC class II⁺ and CD103 expression. Then, the surface expression of various cells was measured on the gated subsets. **B.** The histograms show the CD11c expression among mLN MHCII⁺/CD103⁺ cells and axLN MHCII^{hi}/CD103⁺ cells (left side). The control is shown on the right side. The data show that DC from mLN exhibit more CD11c expression than DC from axLN. **C.** shows means and SEM (n=6-7) of the percentage of surface expression among the subsets. Asterisks indicate significant differences between DC from mLN and axLN in the students T-test (**p<0.001, * p<0.05). The mLN specific (MHCII⁺/CD103⁺) and the axLN specific DC (MHCII^{hi}/CD103⁻) completely differ in their phenotype, while the MHCII⁺/CD103⁻ subsets of mLN and axLN have a similar phenotype (data not shown).

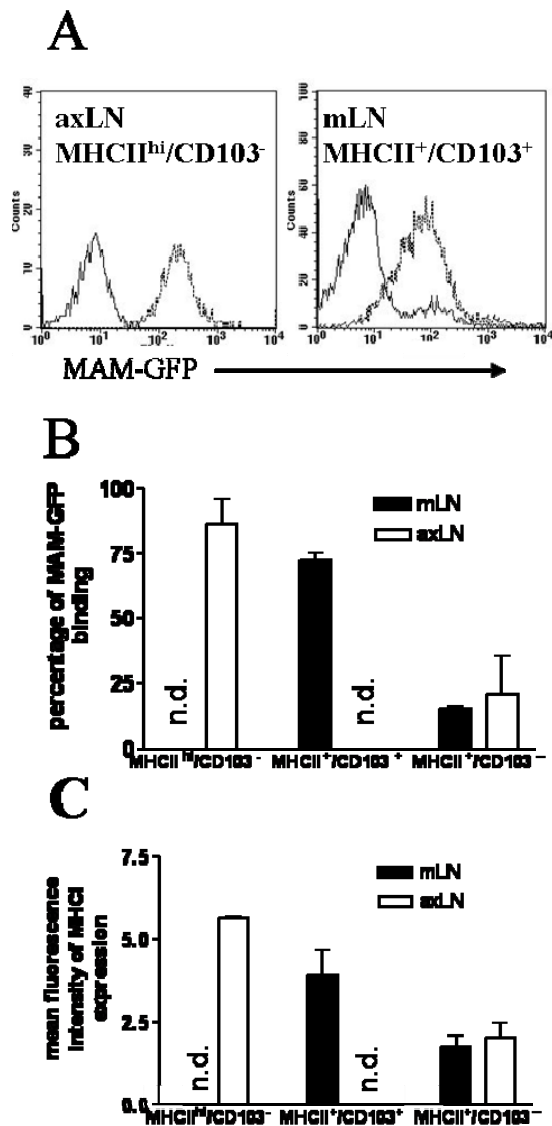


Fig.3: The maximum of MAM binding is seen on the specific DC subsets from mLN and axLN

Purified DC from mLN and axLN were incubated with MAM-GFP, then the binding of MAM-GFP on each subset was analyzed. After gating on each subset, the MAM-GFP binding was analyzed in fluorescence 1. GFP binding served as a control. **A.** The histograms show the binding capacity of MAM (dotted line) among the specific DC subsets of mLN and axLN in comparison to the GFP binding (dark line). **B.** Means and SED are shown from 3 independent experiments. The data show that both specific DC subsets from mLN and axLN had high capacities to bind MAM, while the shared MHCII⁺/CD103⁻ subset can only bind MAM to a minor degree. **C.** MHCII

expression was identified by gating on the DC subsets from mLN and axLN as shown in Fig.1. Means and SED of the mean fluorescence intensity of MHCI expression among the MHCII⁺⁺/CD103⁻, MHCII⁺/CD103⁺ and MHCII⁺/CD103⁻ cells are given from 3 independent experiments. The data document that both specific DC subsets from mLN and axLN had a high expression of MHCI, while the shared MHCII⁺/CD103⁻ subset had a lower expression. (n.d. = not detectable)

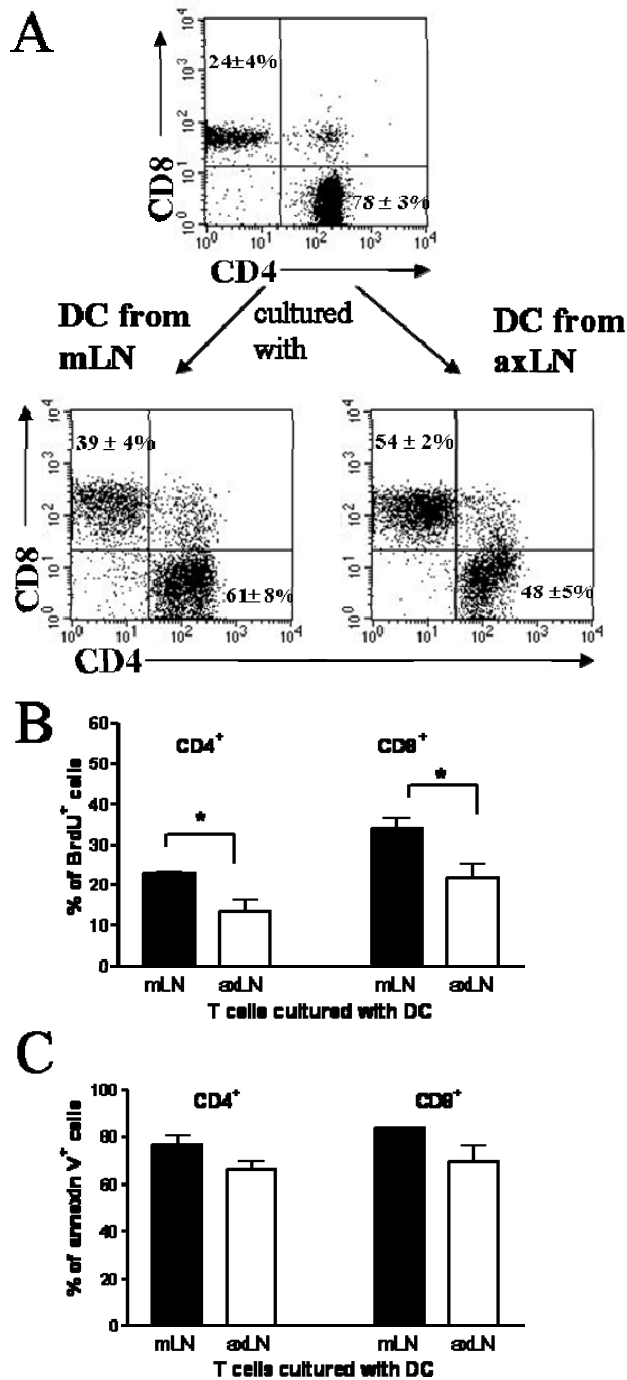


Fig.4: Effector T cells primed by DC from mLN and axLN differ in surface marker expression and effector function

Purified blood T cells were analyzed regarding their subset composition and after culture with purified DC from mLN and axLN the subsets were again analyzed. **A.**

The dot plot shows that the subset composition of mLN and axLN primed T cells had differentially changed after culture (means and SD). **B.-C.** During the last hour of

culture BrdU was added and the percentage of BrdU⁺ cells among the subsets was measured by flow cytometry. In addition, the percentage of annexin V⁺ cells was analyzed among the subsets of mLN and axLN primed T cells. Means and SED are shown from 3 independent experiments. Asterisks indicate significant differences between mLN and axLN of CD4⁺ and CD8⁺ primed T cells in the students T-test (* p<0.05).

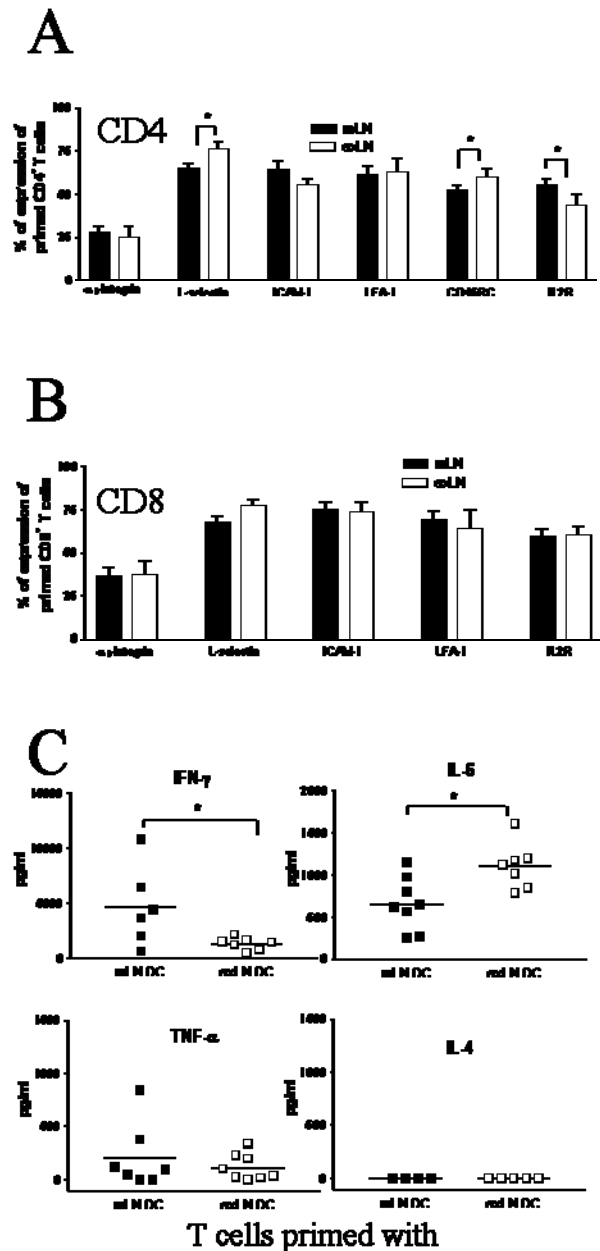


Fig.5: Effector T cells primed by DC from mLN and axLN differ in their cytokine release

Surface expression was measured on mLN and axLN primed effector T cells after culture and before injection into recipients. **A.** The percentage of various markers among CD4⁺ primed T cells. Means and SEM (n=5-6) are given. Asterisks indicate significant differences between surface expression of mLN and axLN primed CD4⁺ T cells in the students T-test (* p<0.05). mLN primed CD4⁺ T cells showed an activated phenotype. **B.** The same analysis was done for mLN and axLN primed CD8⁺ T cells.

No differences were seen between the two populations. **C.** Supernatants of the cultured T cells with DC from mLN and axLN were collected and analyzed by ELISA. Whereas IFN- γ was produced more among the mLN primed T cells after MAM stimulation, production of IL-6 was seen more in the supernatant of axLN primed T cells. Single values of 5-8 independent experiments are shown. The horizontal lines represent mean values.

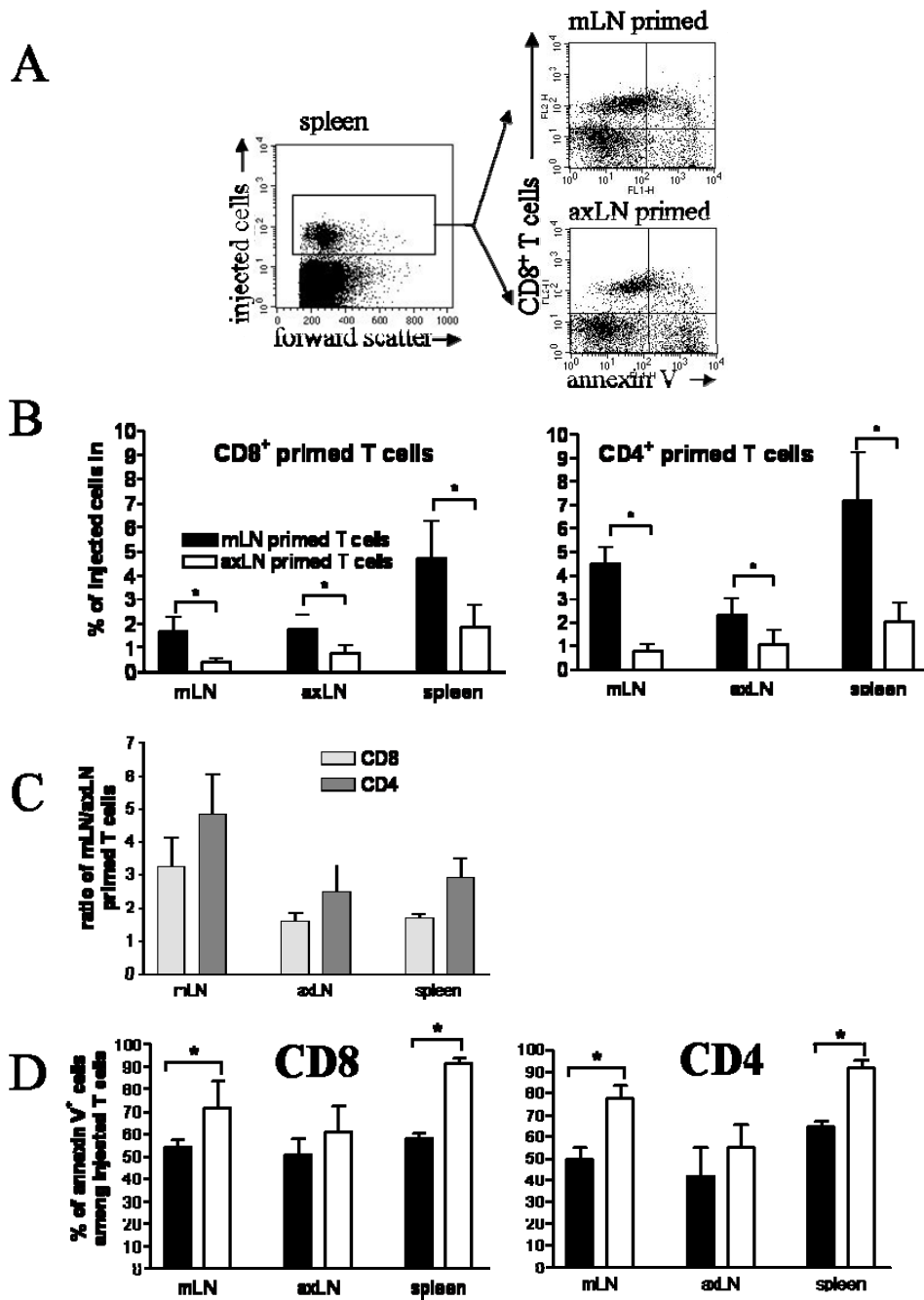


Fig.6: mLN primed effector CD4⁺ T cells preferentially survive *in vivo*

LEW.7B blood T cells were primed with purified DC from either mLN or axLN *in vitro* and injected into LEW recipients. Three days after injection the presence of injected cells was measured in the mLN, axLN and spleen. Apoptotic cells were analyzed by identifying annexin V positive cells among the injected cells by flow cytometry (**D**). **A**. The dot plot shows a staining identifying injected cells (His41⁺ cells) in the spleen. mLN and axLN primed injected CD8⁺ cells were then gated and their annexin V

binding was shown. The dot plots are representative of three independent experiments. **B.** show means and SEM (n=3) of the percentage of injected mLN and axLN primed CD8⁺ and CD4⁺ T cells within the mLN, axLN and spleen. Asterisks indicate significant differences in the students T-test (* p<0.05). The data show that both CD4⁺ and CD8⁺ T cells primed by mLN DC are more frequent in mLN, axLN and spleen than T cells primed by DC from axLN. **C.** To compare the accumulation capacity of CD4⁺ mLN and axLN primed T cells to that of CD8⁺ T cells primed from mLN and axLN, a ratio of the data in B. was calculated (means and SEM, n=3). The data show that on the one hand all injected mLN primed T cells have a higher accumulation capacity than injected axLN primed T cells. On the other hand, injected CD4⁺ primed T cells are more frequently found in mLN, axLN and spleen than injected CD8⁺ primed T cells. **D.** Percentage of annexin V⁺ cells among injected mLN and axLN primed CD8⁺ and CD4⁺ T cells in mLN, axLN and spleen (means and SEM, n=3). Asterisks indicate significant differences in the students T-test (* p<0.05). The data show that both the CD8⁺ and the CD4⁺ T cells primed from axLN have a higher annexin V expression than those primed by mLN DC.

4. Stromal cells confer lymph node-specific properties by shaping a unique microenvironment influencing local immune responses

Manuela Ahrendt*, Swantje Iris Hammerschmidt⁺, Oliver Pabst⁺, Reinhard Pabst*, Ulrike Bode*

* Functional and Applied Anatomy, Hannover Medical School, Hannover, Germany

+Institute of Immunology, Hannover Medical School, Hannover, Germany

Running Title

Transplantation and regeneration of lymph nodes *in vivo*

Keywords

Chemokines, cytokines, stromal cells, lymph nodes, transplantation

Abbreviations

CT, cholera toxin; **FRC**, fibroblastic reticular cells; **MAdCAM-1**, mucosal-addressin cell adhesion molecule 1; **mLN**, mesenteric lymph nodes; **mLNtx**, transplanted mesenteric lymph nodes; **pLN**, peripheral lymph nodes; **pLNtx**, transplanted peripheral lymph nodes; **PP**, Peyer's patches; **RALDH2**, retinal dehydrogenases 2

Address correspondence to: Dr. Ulrike Bode; Anatomie II, OE 4120; Medizinische Hochschule Hannover; Carl-Neuberg-Str.1; 30625 Hannover, Germany; Phone: +49-511-532-2989; Fax:+49-511-532-2948; E-Mail: Bode.Ulrike@MH-Hannover.de

The work was supported by the German Research Foundation (SFB621/A10)

Abstract

Lymph nodes (LN) consist not only of highly motile immune cells coming from the draining area or from the systemic circulation, but also of resident stromal cells building the backbone of the LN. These two cell types form a unique microenvironment which is important for initiating an optimal immune response. The present study asked how the unique microenvironment of the mesenteric lymph node (mLN) is influenced by highly motile cells and/or by the stromal cells.

A transplantation model in rats and mice was established. After resecting the mLN, fragments of peripheral lymph node (pLN) or mLN were inserted into the mesentery. The pLN and mLN have LN-specific properties, resulting in differences of, for example, the CD103⁺ dendritic cell subset, the adhesion molecule mucosal addressin cell adhesion molecule 1, the chemokine receptor CCR9, the cytokine IL-4, and the enzyme retinal dehydrogenase 2.

This new model clearly showed that during regeneration stromal cells survived and immune cells were replaced. Surviving high endothelial venules retained their site-specific expression (mucosal addressin cell adhesion molecule 1). In addition, the low expression of retinal dehydrogenase 2 and CCR9 persisted in the transplanted pLN, suggesting that stromal cells influence the lymph node-specific properties. To examine the functional relevance of this different expression pattern in transplanted animals, an immune response against orally applied cholera toxin was initiated. The data showed that the IgA response against cholera toxin is significantly diminished in animals transplanted with pLN.

This model documents that stromal cells of the LN are active players in shaping a unique microenvironment and influencing immune responses in the drained area.

4.1. Introduction

Lymph nodes (LN) are secondary lymphoid organs in which stimulation and activation of lymphocytes take place and effective immune responses are initiated.

They are connected by the afferent lymphatics from the drained area. Therefore, the function of LN is to filter and monitor the lymph and obtain information about the infection state of the drained area (1, 2).

LN are highly compartmentalized and consist of a unique microarchitecture (2).

However, the cellular composition of the B and T cells is dynamic due to the constant influx and efflux of these cells. Dendritic cells (DC) are loaded with Ag in the periphery and migrate via the afferent lymphatics into the draining LN. Naïve T and B lymphocytes migrate into the LN preferentially via high endothelial venules (HEV) to screen for specific Ag presented by DC. Some stimulated T cells migrate into the B cell area to interact with Ag-specific B cells. Furthermore, activated T and B cells and their descendents leave the LN to spread throughout the body and re-enter the periphery where the specific Ag is present (1, 3).

In addition to these highly motile components, nonhematopoietic cells form a three-dimensional cellular network in the LN. These stromal cells mainly consist of fibroblastic reticular cells (FRC), which can be identified by the Ab ERTR-7 and are also positive for the glycoprotein podoplanin (gp38⁺). It is assumed that due to their interconnection, stromal cells form the skeletal structure of the LN, suggesting that these cells are not motile cells (4-6).

Both the immune cells and the stromal cells are able to produce soluble factors, e.g., cytokines and chemokines. For example, T lymphocytes, which are activated in response to the interaction with Ag-loaded DC, produce a set of cytokines including IL-2, IFN- γ and IL-4 (7). It was shown that stromal cells expressed CCL-19/CCL-21

within the T cell area and HEV of LN (6). Thus, CCR7-positive immune cells are able to migrate into the LN (8).

In addition, it was shown that within the LN immune cells interact with and migrate along the stroma to their compartments (9, 10). However, where and how the interaction takes place, is poorly understood.

The gut is continuously in contact with various numbers of different Ag, for example, food Ag, but also potentially pathogenic microorganisms, toxins and other potentially harmful molecules. To protect the organism against these Ags, immune responses are initiated, resulting in tolerance or protective immune reactions. A characteristic feature of the gut immune system is a preferential response by producing IgA (11). Ag from the gut lumen is taken up by DC and transported into mesenteric lymph nodes (mLN), initiating an immune response in the gut (12, 13). This special location and function requires an exclusive composition of cell subsets, cytokines and chemokines, forming a unique microenvironment in mLN.

mLN-specific properties are as follows: MAdCAM-1 is expressed on HEV, but not on HEV of peripheral lymph nodes (pLN) (14, 15). Naïve T cells, which enter the mLN via HEV, interact with DC arriving via the afferent lymphatics from the gut. These DC preferentially express the retinal dehydrogenases RALDH2 (16, 17). After activation, T cells and also B cells acquire a gut-homing phenotype, including high CCR9 and $\alpha_4\beta_7$ -integrin expression (17-20). Furthermore, DC from the mLN differ from those in pLN in their ability to imprint T cells in the direction of Th2 (7, 21-23), e.g., IL-4 is found at a higher concentration in the mLN compared with the pLN (24). However, it is not known whether this unique microenvironment is due to the highly motile components of the mLN or to stromal cells.

Therefore, we established a model, in which a pLN regenerated in the draining area of the gut, which is ontogenetically occupied by the mLN. Under these *in vivo*

conditions, we are able to study the influence and importance of the draining area and the stromal cells in the *in vivo* situation. For the first time, it has been studied whether LN-specific properties are influenced by the draining area or by stromal cells within the transplanted tissue.

To examine the functional relevance of the altered microenvironment in transplanted LN (LNtx), orally applied cholera toxin (CT) was used as an example of initiation of an immune response in the gut. CT is known as one of the most potent mucosal immunogens causing a strong intestinal IgA response after oral application (25-28). The data presented in this *in vivo* model document the active part played by stromal cells of LN in shaping a unique microenvironment, which is essential for local immune responses.

4.2. Material and Methods

Animals

Rats from the standard inbred strains LEW/Ztm and LEW.7B/Won were bred and maintained at the central animal laboratory of Hannover Medical School. The LEW.7B strain is identical to the congenic strain originally designated LEW.Ly1 (29). The RT system is a diallelic polymorphism of the CD45 molecular system. Male animals with a weight of 180-220g at the beginning of the experiment were used for this study. Furthermore, female C57BL/6 and C57BL/6-Tg (ACTbEGFP) (designated here EGFP mice) mice were bred at the central animal laboratory of Hannover Medical School and were used at a weight of 18-25g. All animal experiments were performed in accordance with the institutional guidelines and had been approved by the Niedersächsisches Landesamt für Verbraucherschutz und Lebensmittelsicherheit (No 33-42502-05/960).

Intestinal surgery

The mLN and pLN were isolated from LEW.7B rats and EGFP mice and used as donors for LEW rats and C57BL/6 mice, respectively (Table 1). Under the combined anesthesia with Ketamine (Gräub AG, Bern, Switzerland) and Domitor (Pfizer, Karlsruhe, Germany) the mLN of the small and large intestine of the host were excised. The donor mLN or axillary and brachial LN were cut into small pieces (about 10 mm³) and then transplanted into this region. These LN fragments were termed mLNtx and pLNtx, respectively. After 2, 4, 6, 8, 10 and 23 weeks 1 mg BrdU/100g weight was given intravenously. One hour later the transplanted LN, mLNtx or pLNtx, were removed and analyzed (n=4-5).

Antibodies for flow cytometry

Cell suspensions from mLNtx and pLNtx were made and about 1×10^6 cells were incubated with biotinylated mAb W3/25 ($CD4^+$ T cells) or Ox8 ($CD8^+$ T cells) and revealed by PerCP. B cells were characterized by Ox12 and a PE –conjugated antibody was used as secondary step. To differentiate between donor and host lymphocytes, mAbs His41 (FITC conjugated) was used analyzed in the FACScan. DC and their subsets were classified as described previously (21). Isotype-matched mAb served as controls. All antibodies were purchased from Serotec, Oxford, UK.

Quantification of mRNA expression among mLNtx and pLNtx

Total RNA of mLNtx, pLNtx and control LN (n= 3) was isolated according to the manufacturer's protocol (Rneasy Kit, Qiagen, Hilden, Germany) and cDNA synthesis was performed with 50 mM oligo primer, 0.1 M DTT, 5x first strand buffer, 10mM dNTP, 35 U/ μ l Rnase inhibitor and 200U/ μ l M-MLV reverse transcriptase (all obtained from Invitrogen, Karlsruhe, Germany) in a total volume of 20 μ l at 37°C for 50 min. With this cDNA quantitative real time PCR was performed using the QuantiTect SYBR-Green protocol from Qiagen. The primer sequences and amplicon sizes of IL-4 (5'-ATGTACCTCCGTGCTTGAAG-3' and 5'-TGAGCGTGGACTCATTAC-3'; 117 bp), IL-2 (5'-CTGAAACTCCCCATGATGCT-3' and 3'-GAAATTTCCAGCGTCTTCCA- 5'; 159 bp), IFN- γ (5'-GCCCTCTCTGGCTGTTACTG-3'and 3'-CTGATGGCCTGGTTGTCTTT-5'; 221 bp), CCR9 (5'-GTGATTCCCCTGGCTCAGA -3' and 5'-CCCCACCAAAGCTTAGTGA -3'; 200 bp), RALDH2 (5'-ACCTATCACCAGGCCTCCTT -3' and 5'-ACAAAATGGGGTTCATTGGA -3'; 174 bp) and GAPDH (5'-GATGACATCAAGAAGGTGGTGA -3' and 5'-ACCAGGAAATGAGCTTCACAAT -3'; 175 bp) for the housekeeping gene were used.

Immunohistochemistry

Cryostat sections of mLN control, mLNtx as well as pLN and pLNtx (n=4-5) were fixed in acetone/methanol solution (1:1, 10 min, -20°C). The alkaline phosphatase anti-alkaline phosphatase (APAAP) technique was used to phenotype B lymphocytes (His14), donor lymphocytes (His41) and adhesion molecules such as HEV (His52, all obtained from Serotec) and mucosal addressin cell adhesion molecule-1 (MAdCAM-1; Ost2, BD Biosciences, Heidelberg, Germany) (30). After incubation with the primary antibodies slides were washed with TBS-Tween (0.05% Tween 20, Serva, Heidelberg, Germany) and incubated with a bridging antibody (rabbit anti-rat, Dako, Hamburg, Germany) and then the APAAP complex (Dako) was applied. Fast blue (Sigma, Munich, Germany) served as a substrate for alkaline phosphatase. Positive and negative controls produced the expected results. All sections were counterstained with hemalaun and mounted in glycergel (Dako). BrdU⁺ cells were determined also using the APAAP technique (24, 31).

Immunofluorescence histochemistry was performed according to standard protocols (32). Briefly, sections were rehydrated in TBST (0.1 M Tris pH 7.5, 0.15 M NaCl, 0.1% Tween-20), pre-incubated with TBST containing 5% rat or mouse serum and stained with fluorescent dye-coupled antibodies (gp38-Cy5, ERTR-7-Cy3, meca79-Cy3, LYVE-1-Cy3 (lymphatic vessel endothelial receptor 1)) in 2.5% serum/TBST. Nuclei were visualized by DAPI staining (1µg/ml DAPI/TBST), and sections were mounted with Fluorescent Mounting Medium (Dako). Images were acquired using an Axiovert 200M microscope with Axiovision software (Carl Zeiss, Jena, Germany).

Identification of T cells in the HEV of mLNtx and pLNtx

Cell suspensions were prepared from LEW.7B mLN. Then 50×10^6 - 100×10^6 cells were injected i.v. into LEW rats (n=3), which had been transplanted 2 and 8 weeks

before (24). One hour later the transplanted LN were removed and frozen in liquid nitrogen and stored at -80°C. Immunohistological staining of the HEV and the injected cells was carried out as described previously (24, 33).

Immunization

Purified cholera toxin (CT, Sigma, Taufkirchen, Germany) was administered as described previously with some modifications: Eight weeks after transplantation LEW rats with mLNtx or pLNtx were immunized orally with 100µg CT (in 0.5ml of 0.01M PBS containing 0.2% gelatine) on day 0 and 14 (25). On day 19 the rats were exsanguinated, cell suspensions were made and gut lavages were collected (n=4-5). For that, the gut was cut into 3 equal pieces, each rinsed with intestinal lavage buffer (0.1 mg/ml trypsin inhibitor, 50 mM EDTA, 0.1% BSA in PBS) and the supernatants frozen immediately at -80°C. Analysis via flow cytometry and ELISA was performed as described below.

ELISA of gut lavage

The concentration of CT-specific IgA (CT-IgA) in the gut lavage of the transplanted rats after CT administration was analyzed in the ELISA (n=5). The plates were coated with 0.1µg/ml CT (Sigma) in PBS overnight at 4°C. After washing, the plates were blocked and samples were added undiluted or to a concentration of 1:512 and incubated 90 min at 37°C. After washing the detection Ab (biotinylated mouse-anti-IgA; BD Biosciences) was added and later detected with HRP (BD biosciences), tetramethylbenzidine (TMB, BD Biosciences) and hydrogen peroxide (1:1) as the substrate. The reaction was stopped with 2N H₂SO₄ (Merck, Darmstadt, Germany). The optical density was analyzed in an ELISA-Reader (Bio-TEK Instruments GmbH, Bad Friedrichshall, Germany).

Data analysis

Calculations, statistical analysis and graphs were performed with the software Graphpad Prism 4.0 (Graphpad Software Inc., San Diego, USA). Statistical differences were calculated in the unpaired t-test and are indicated by *, $P < 0.05$; **, $P < 0.01$; ***, $P < 0.001$.

4.3. Results

mLN or pLN fragments were transplanted into the mesentery after removing the mLN of LEW rats. The LN fragments were removed after different time points, an example of an early time point being 2 wk and of a late time point 8 wk after transplantation.

In LNtx fragments T and B cell areas were transiently disintegrated but regenerated within 8 wk

In LN of untreated animals (control LN), shown in Fig. 1A, the B cell areas were clearly identifiable and separated from T cell zones. Within the B cell areas, germinal centers were visualized by proliferation. Two weeks after transplantation, the T cell and B cell areas were destroyed and only small clusters of B and T cells were seen. Proliferation was distributed over the whole LN fragment and within the B cell clusters germinal centers were not identified (Fig. 1B). However, 8 wk after transplantation, B cells and T cells were found in typical compartments including germinal centers (Fig. 1C). A similar microanatomy was found 23 wk after transplantation, indicating that already after 8 wk the regeneration had been completed (Fig. 1D).

Donor lymphoid cells emigrated from LNtx fragments

To characterize the lymphoid cell subsets in the LNtx fragments, cell suspensions were analyzed characterizing both the host and donor cells. At first, T and B cells within mLNtx and pLNtx were compared to a control mLN. Early after transplantation a significantly increased level of T cells was found which consisted of both CD4⁺ and CD8⁺ T cells (Fig. 2A), whereas B cells were decreased in mLNtx and pLNtx.

However, 8 wk after transplantation, T as well as B cells showed no differences from the mLN control cell subset compositions any longer.

In addition, MHC class II⁺ CD103⁺ cells were analyzed. This cell population, which was shown to be DC, demonstrated a highly decreased incidence within the transplanted fragments compared with DC in control mLN after 2 wk. However, in line with the T and B cells, the percentage of DC was comparable to those of the mLN control 8 wk after transplantation (Fig.2B).

Finally, to observe how many donor cells remained in the LN fragments, the donor cells were quantified. Donor lymphoid cells within the mLNtx declined considerably at 2 and 8 wk after transplantation. Only 2.4% of mLNtx and 1.6% of pLNtx were identified as donor cells after 8 wk (Fig.2C). However, a small population of migrated donor cells was found in secondary lymphoid organs, including the spleen of the recipients, at all time points (data not shown).

The subset composition of DC from pLNtx changed to that of mLN

DC from mLN differed from those of pLN based on the expression levels of MHC class II (MHCII) and CD103 (Fig.3). In the pLN MHCII^{hi}CD103⁻ DC were found, whereas in the mLN MHCII^{hi}CD103⁻ cells were completely absent. In contrast, MHCII⁺CD103⁺ cells were preferentially seen in the mLN (Fig.3). Only mLN-specific DC subsets (MHCII⁺CD103⁺) but not MHCII^{hi}CD103⁻ DC were found in mLNtx and also in pLNtx (Fig.3), demonstrating that the subset composition of pLN DC changed to that of mLNtx.

In addition, in control animals, CD11c expression was different among pLN MHCII^{hi}CD103⁻ and mLN MHCII⁺CD103⁺ cells. Similar to the pattern of the DC subset composition in pLNtx, the CD11c expression was comparable to that of the mLN control (mLN control: 65%; pLNtx: 64±4.4%, n=3).

Stromal cells survived after transplantation

To analyze whether stromal cells also disappeared from the transplanted fragments, mLNtx and pLNtx of EGFP⁺ mice were transplanted into C57BL/6 mice and after 8 wk the LN were removed. GFP⁺ cells were identified in the B cell and T cell area (Fig.4A and B). As was expected from previous results in the rat model, most of the T and B cells were GFP negative, showing that most lymphocytes originated from the host.

Furthermore, the transplanted GFP⁺ LN fragments were stained with the FRC marker gp38 (Fig.4E) and with the fibroblastic marker ERTR-7 (Fig.4F). In contrast to the lymphoid cells, most gp38⁺ and ERTR-7⁺ cells were also GFP⁺ (Fig.4C-H), demonstrating that most of these stromal cells survived after transplantation. This was seen in mLNtx as well as in pLNtx. Interestingly, most of the follicular DC were also GFP⁺ (data not shown), indicating that these cells survived too.

Taken together, complete removal of the mLN and insertion of donor mLN/pLN resulted in destruction of the LN architecture, which was regenerated at 8 wk after transplantation. Therefore, the 8-wk time point was chosen to analyze the microenvironment of regenerated LN fragments.

Reconnection of the LNtx fragments to the blood stream

To analyze the presence of HEV, the LNtx fragments (mLNtx and pLNtx) were stained with a marker for HEV immunohistologically. Within mLNtx as well as pLNtx, HEV were identified (Fig.5A).

To investigate whether these HEV were reconnected to the blood stream and fulfilled their physiological function, naïve mLN lymphocytes from the congenic rat strain (LEW.7B) were isolated and injected i.v. One hour later, the donor cells were found in

the wall of the HEV. Then, EGFP⁺ mice were transplanted into C57BL/6 mice and after 8 wk the transplants were removed and the HEV stained (Fig.5B-D). In these LNtx fragments, GFP⁺ HEV were found, documenting the survival of the donor HEV (Fig.5B-D).

Reconnection of the afferent lymphatics

To ensure that not only the blood vessels were connected to the LNtx fragments, the presence of lymphatics was also checked 8 wk after transplantation. “Berlin blue” was injected into the subserosa of the gut and it was found in the LN fragments as transported via afferent lymphatics to lymph sinuses of mLNtx as well as pLNtx (Fig.5E).

Lymphatic endothelial cells visualized by a staining against the lymphatic endothelial hyaluronan receptor (LYVE-1) within the LNtx fragments were seen (Fig.5F-H). LYVE-1⁺ cells of the sinus are mostly GFP⁺, indicating that these cells also survived during regeneration (Fig.5H).

MAdCAM-1 was not expressed in pLNtx

To identify MAdCAM-1 expression, mLNtx and pLNtx were stained immunohistologically and compared to a control mLN and control pLN. The adhesion molecule MAdCAM-1 was expressed on HEV within the mLN, but not on HEV in pLN (Fig.6A and B). Similarly, MAdCAM-1 expression was found in mLNtx (Fig.6C) but was absent in pLNtx (Fig.6D). This expression pattern was seen at all time points measured (Fig.6E and F).

The drained area influenced IL-4 expression, whereas the expression pattern of CCR9 and RALDH2 was LN-specific

To analyze whether stromal cells or the drained area influenced the cytokine pattern within the LN, various cytokines were quantified via real-time PCR. The expression of IL-4, IL-2 and IFN- γ mRNA differed among mLN and pLN of control animals (34). In detail, IL-4 mRNA was found more in mLN than in pLN. In contrast, IL-2 and IFN- γ mRNA were preferentially detected in pLN.

The IL-4, IL-2 and IFN- γ mRNA in the LN fragments of untreated (under steady-state conditions) and CT-treated animals (immune response) were studied. The different expression of IL-4 in untreated animals was no longer detectable between mLNtx and pLNtx, indicating that IL-4 expression was influenced by the drained area (Fig.7A). In contrast, IFN- γ and IL-2 showed more expression in the pLNtx under steady-state conditions, demonstrating that the expressions of these cytokines were not controlled by the drained area. The differences were increased when CT was given (Fig.7A).

It has been shown that retinal dehydrogenases RALDH1-3 are important for the induction of gut homing receptors. RALDH2 is preferentially expressed in the mLN (16). To test whether this enzyme was dependent on the drained area, RALDH2 expression was quantified via real-time PCR in the LN fragments. The data showed that RALDH2 in mLNtx was expressed similarly compared to the mLN control. In contrast, the RALDH2 expression in pLNtx was at a low level similar to the pLN control (Fig.7B).

Gut tropic T and B cells are positive for the chemokine receptor CCR9 which is influenced by the retinoic acid, the product of RALDH2 (35, 36). Therefore, the CCR9 expression of LN transplants was analyzed. The same pattern was seen for CCR9: The expression in mLNtx was comparable to the mLN control, whereas pLNtx were

as low as the pLN control (Fig.7B). The data document that CCR9 and RALDH2 expression were not influenced by the drained area.

The IgA response in pLNtx was lower than in mLNtx-transplanted rats

Finally, it was analyzed whether these differences in pLNtx influenced a typical gut immune response induced in the draining area of the LNtx fragments. Therefore, the B cell phenotype and response including CT-specific IgA Abs were investigated after an oral dose of CT. The percentage of surface IgA⁺ B cells was much lower in pLNtx compared with mLNtx (Fig.8A). CCR9 expression was decreased on the pLNtx B cells compared with those of mLNtx (Fig.8B). This indicates that gut-specific B cells were reduced in pLNtx after CT treatment. As a result of this reduction, CT-specific IgA Abs were also reduced in pLNtx animals (Fig.8C).

4.4. Discussion

It has been shown that LN transplanted into the s.c. layer of the skin were reconnected to the afferent lymphatics (37-39). However, when a LN was transplanted into the omentum of pigs the LN disappeared and did not regenerate (38). In the present study, it was documented for the first time that LN fragments implanted into the mesentery of mice and rats were regenerated and reconnected to the lymphatic system independent of their origin. Previously, another group suggested that the blood supply of the LNtx alone is not sufficient to establish the LN in this area (38). In our *in vivo* model, both the afferent lymphatics and the blood supply were also regenerated, documented by functional tests in pLNtx and mLNtx. Since these two routes are entry sites of immune cells and soluble molecules, reconnection to the draining area and the blood is a prerequisite of a complete functional regeneration. The present study shows that LNtx fragments were initially destroyed but regeneration was completed 8 wk after transplantation. This period of regeneration was confirmed in recently published data (40).

The donor immune cells disappeared during the first two wk. The host immune cells were able to enter the LN fragments, probably due to the regenerated blood and lymph supply, resulting in a resettlement of the compartments. One type of these highly motile cells are the DC, which migrate from the draining area into the LN. DC from mLN can be distinguished from those from pLN by their different subset composition and expression pattern of surface molecules (e.g. CD103) (21, 22). The results showed that DC from pLNtx had been replaced by DC with a subset composition and phenotype typical for mLN, underlining the generally accepted observation that the DC came from the drained area.

In contrast to the highly motile immune cells, nonhematopoietic cells survived and were not replaced during regeneration of the LNtx. This aspect has not been described before. Nonhematopoietic cells form a three dimensional network building the backbone of the LN. One type of these resident cells forms HEV, which play a critical role in recruiting lymphocytes into LN by expressing homing molecule receptors, e.g., MAdCAM-1 and pLN addressins, and presenting chemokines from the draining area (15, 41). The current study illustrates that HEV not only survived during regeneration but also retain their site-specific expression pattern (such as the absence of MAdCAM-1 expression in pLNtx). This was independent of the reconnected lymph supply which transports Ags and low-weight molecules, e.g., chemokines, from the gut via the conduits to the lumen of HEV.

Another cell population of these nonhematopoietic cells are fibroblastic reticular cells (FRC) identified here by gp38 and ERTR-7 (5, 6). FRC are able to regulate the entry of CCR7⁺ immune cells via CCL19 and CCL21 expression (5, 42), the entry and location of naïve T and B cells within the paracortex of the LN (9) and to produce survival factors which influence naive T homeostasis (6). Finally, it is known that FRC form a cellular sleeve around the conduits by anchoring themselves to the basement membrane and are therefore important structural elements of the LN architecture (43, 44). However, little is known whether FRC as a stromal cell population influence immune responses within the LN.

Our investigations show that stromal cells are involved in the expression pattern of cytokines. During an immune response, cytokines are relevant molecules to drive T cell polarization into a distinct direction. For example, IL-4 is a Th2 cytokine, which is preferentially found in the mLN (34). Our data show that the expression level of IL-4 was influenced by the drained area in steady-state conditions, but also during an immune response. In contrast, IL-2 and IFN- γ were found to be expressed

preferentially in the pLN and their drained area (34). The pattern of IL-2 and IFN γ expression in the pLNtx is unaffected. However, whether the stromal cells themselves express, for example, IL-2, or whether they indirectly influence the motile components to up-regulate these cytokines is not known.

Another important aspect of the present study is that RALDH2 expression in pLNtx was only marginally similar to the situation in control pLN. Retinal dehydrogenases RALDH1-3 are important for the induction of gut-homing receptors. RALDH2 is preferentially expressed on DC in the mLN and not detectable in the pLN (16, 45). Thus, since DC in the pLNtx are host derived, only the stromal cells of the transplanted pLNtx are able to influence indirectly the expression of RALDH2 on these immigrated DC or directly fail to express RALDH2. Preliminary data indicate that FRC within the mLN itself express RALDH2, whereas FRC within the pLN fail to express RALDH1-3 (data not shown).

In response to retinoic acid, T and B cells within the mLN are found to express CCR9 and $\alpha_4\beta_7$ -integrin. Thus, activated T and B cells are imprinted with the gut-homing phenotype to re-enter the gut via their specific expression pattern (19, 46, 47).

Our study shows that pLNtx exhibits an increased number of B cells, expressing minor levels of CCR9. It strongly suggests that the failed RALDH2 expression of pLNtx leads to a decreased CCR9 expression on B cells after initiating an immune response. The functional consequence of this different expression pattern of pLNtx is a lower IgA titer against orally applied CT as seen in mLNtx. Thus, the function of the pLNtx is disturbed, indicated by an impaired immune reaction against Ags coming from the gut.

Taken together, LN consist of both highly motile immune cells and resident nonhematopoietic stromal cells forming the backbone of the LN. When a peripheral

LN was implanted into the mesentery, the highly motile cells disappeared from the LNtx, but the skeletal backbone survived after transplantation. These stromal cells seem to be able to reprogram the highly motile cells in educating them to the organotypical expression pattern. This leads to the situation that a regenerated pLN despite being perfused by the gut lymph still has the LN-specific properties of a pLN. The function of this LN is disturbed, indicated by decreased IgA cells and specific Abs against orally administered Ag, e.g., CT. Thus, stromal cells, as an organotypical skeleton of lymphoid organs, seem to be important for an efficient immune response.

Acknowledgements

The comments of Jutta Schade have been of great help. The authors also wish to thank Nadja Thiessen and Anika Hahn for help with the operations, Frauke Weidner for excellent technical assistance and Sheila Fryk for correction of the English.

4.5. References

1. Tanaka, T., Y. Ebisuno, N. Kanemitsu, E. Umemoto, B. G. Yang, M. H. Jang, and M. Miyasaka. 2004. Molecular determinants controlling homeostatic recirculation and tissue-specific trafficking of lymphocytes. *Int. Arch. Allergy Immunol.* 134:120-134.
2. Crivellato, E., A. Vacca, and D. Ribatti. 2004. Setting the stage: an anatomist's view of the immune system. *Trends Immunol.* 25:210-217.
3. von Andrian, U. H., and T. R. Mempel. 2003. Homing and cellular traffic in lymph nodes. *Nat. Rev. Immunol.* 3:867-878.
4. Gretz, J. E., A. O. Anderson, and S. Shaw. 1997. Cords, channels, corridors and conduits: critical architectural elements facilitating cell interactions in the lymph node cortex. *Immunol. Rev.* 156:11-24.
5. Lammermann, T., and M. Sixt. 2008. The microanatomy of T-cell responses. *Immunol Rev.* 221:26-43.
6. Link, A., T. K. Vogt, S. Favre, M. R. Britschgi, H. Acha-Orbea, B. Hinz, J. G. Cyster, and S. A. Luther. 2007. Fibroblastic reticular cells in lymph nodes regulate the homeostasis of naive T cells. *Nat. Immunol.* 8:1255-1265.
7. Iwasaki, A., and B. L. Kelsall. 1999. Freshly isolated Peyer's patch, but not spleen, dendritic cells produce interleukin 10 and induce the differentiation of T helper type 2 cells. *J. Exp. Med.* 190:229-239.
8. Ohl, L., G. Bernhardt, O. Pabst, and R. Forster. 2003. Chemokines as organizers of primary and secondary lymphoid organs. *Semin. Immunol.* 15:249-255.
9. Bajenoff, M., J. G. Egen, L. Y. Koo, J. P. Laugier, F. Brau, N. Glaichenhaus, and R. N. Germain. 2006. Stromal cell networks regulate lymphocyte entry, migration, and territoriality in lymph nodes. *Immunity.* 25:989-1001.
10. Katakai, T., T. Hara, M. Sugai, H. Gonda, and A. Shimizu. 2004. Lymph node fibroblastic reticular cells construct the stromal reticulum via contact with lymphocytes. *J. Exp. Med.* 200:783-795.
11. Brandtzaeg, P. 2007. Induction of secretory immunity and memory at mucosal surfaces. *Vaccine.* 25:5467-5484.
12. Macpherson, A. J., and K. Smith. 2006. Mesenteric lymph nodes at the center of immune anatomy. *J. Exp. Med.* 203:497-500.

13. McGhee, J. R., J. Kunisawa, and H. Kiyono. 2007. Gut lymphocyte migration: we are halfway 'home'. *Trends Immunol.* 28:150-153.
14. Iizuka, T., T. Tanaka, M. Suematsu, S. Miura, T. Watanabe, R. Koike, Y. Ishimura, H. Ishii, N. Miyasaka, and M. Miyasaka. 2000. Stage-specific expression of mucosal addressin cell adhesion molecule-1 during embryogenesis in rats. *J. Immunol.* 164:2463-2471.
15. Berlin, C., E. L. Berg, M. J. Briskin, D. P. Andrew, P. J. Kilshaw, B. Holzmann, I. L. Weissman, A. Hamann, and E. C. Butcher. 1993. Alpha 4 beta 7 integrin mediates lymphocyte binding to the mucosal vascular addressin MAdCAM-1. *Cell.* 74:185-195.
16. Iwata, M., A. Hirakiyama, Y. Eshima, H. Kagechika, C. Kato, and S. Y. Song. 2004. Retinoic acid imprints gut-homing specificity on T cells. *Immunity.* 21:527-538.
17. Mora, J. R., and U. H. von Andrian. 2008. Differentiation and homing of IgA-secreting cells. *Mucosal Immunol.* 1:96-109.
18. Campbell, D. J., and E. C. Butcher. 2002. Intestinal attraction: CCL25 functions in effector lymphocyte recruitment to the small intestine. *J. Clin. Invest.* 110:1079-1081.
19. Pabst, O., L. Ohl, M. Wendland, M. A. Wurbel, E. Kremmer, B. Malissen, and R. Forster. 2004. Chemokine receptor CCR9 contributes to the localization of plasma cells to the small intestine. *J. Exp. Med.* 199:411-416.
20. Svensson, M., J. Marsal, A. Ericsson, L. Carramolino, T. Broden, G. Marquez, and W. W. Agace. 2002. CCL25 mediates the localization of recently activated CD8alpha(+) lymphocytes to the small-intestinal mucosa. *J. Clin. Invest.* 110:1113-1121.
21. Bode, U., M. Lorchner, M. Ahrendt, M. Blessenohl, K. Kalies, A. Claus, S. Overbeck, L. Rink, and R. Pabst. 2008. Dendritic cell subsets in lymph nodes are characterized by the specific draining area and influence the phenotype and fate of primed T cells. *Immunology* 123:480-490.
22. Ardavin, C., P. Martinez del Hoyo, Martin, F. Anjuere, C. F. Arias, A. R. Marin, S. Ruiz, V. Parrillas, and H. Hernandez. 2001. Origin and differentiation of dendritic cells. *Trends Immunol.* 22:691-700.
23. Bode, U., M. Lorchner, R. Pabst, K. Wonigeit, S. Overbeck, L. Rink, and J. Hundrieser. 2007. The superantigen-induced polarization of T cells in rat

- peripheral lymph nodes is influenced by genetic polymorphisms in the IL-4 and IL-6 gene clusters. *Int. Immunol.* 19:81-92.
24. Bode, U., A. Sahle, G. Sparmann, F. Weidner, and J. Westermann. 2002. The fate of effector T cells *in vivo* is determined during activation and differs for CD4⁺ and CD8⁺ cells. *J. Immunol.* 169:6085-6091.
 25. Schmucker, D. L., C. K. Daniels, R. K. Wang, and K. Smith. 1988. Mucosal immune response to cholera toxin in ageing rats. I. Antibody and antibody-containing cell response. *Immunology.* 64:691-695.
 26. Elson, C. O., and W. Ealding. 1984. Cholera toxin feeding did not induce oral tolerance in mice and abrogated oral tolerance to an unrelated protein antigen. *J. Immunol.* 133:2892-2897.
 27. Elson, C. O., and W. Ealding. 1984. Generalized systemic and mucosal immunity in mice after mucosal stimulation with cholera toxin. *J. Immunol.* 132:2736-2741.
 28. Cox, E., F. Verdonck, D. Vanrompay, and B. Goddeeris. 2006. Adjuvants modulating mucosal immune responses or directing systemic responses towards the mucosa. *Vet. Res.* 37:511-539.
 29. Wonigeit, K. 1979. Characterization of the RT-Ly-1 and RT-Ly-2 alloantigenic systems by congenic rat strains. *Transplant. Proc.* 11:1631-1635.
 30. Walter, S., B. Micheel, R. Pabst, and J. Westermann. 1995. Interaction of B and T lymphocyte subsets with high endothelial venules in the rat: binding *in vitro* does not reflect homing *in vivo*. *Eur. J. Immunol.* 25:1199-1205.
 31. Bode, U., K. Wonigeit, R. Pabst, and J. Westermann. 1997. The fate of activated T cells migrating through the body: rescue from apoptosis in the tissue of origin. *Eur. J. Immunol.* 27:2087-2093.
 32. Worbs, T., U. Bode, S. Yan, M. W. Hoffmann, G. Hintzen, G. Bernhardt, R. Forster, and O. Pabst. 2006. Oral tolerance originates in the intestinal immune system and relies on antigen carriage by dendritic cells. *J. Exp. Med.* 203:519-527.
 33. Bode, U., C. Duda, F. Weidner, M. Rodriguez-Palmero, K. Wonigeit, R. Pabst, and J. Westermann. 1999. Activated T cells enter rat lymph nodes and Peyer's patches via high endothelial venules: survival by tissue-specific proliferation and preferential exit of CD8⁺ T cell progeny. *Eur. J. Immunol.* 29:1487-1495.

34. Bode, U., G. Sparmann, and J. Westermann. 2001. Gut-derived effector T cells circulating in the blood of the rat: preferential re-distribution by TGFbeta-1 and IL-4 maintained proliferation. *Eur. J. Immunol.* 31:2116-2125.
35. Mora, J. R., and U. H. von Andrian. 2006. T-cell homing specificity and plasticity: new concepts and future challenges. *Trends Immunol.* 27:235-243.
36. Agace, W. W. 2006. Tissue-tropic effector T cells: generation and targeting opportunities. *Nat. Rev. Immunol.* 6:682-692.
37. Pabst, R., and H. J. Rothkotter. 1988. Regeneration of autotransplanted lymph node fragments. *Cell Tissue Res.* 251:597-601.
38. Mebius, R. E., P. R. Streeter, J. Breve, A. M. Duijvestijn, and G. Kraal. 1991. The influence of afferent lymphatic vessel interruption on vascular addressin expression. *J. Cell Biol.* 115:85-95.
39. Cupedo, T., W. Jansen, G. Kraal, and R. E. Mebius. 2004. Induction of secondary and tertiary lymphoid structures in the skin. *Immunity.* 21:655-667.
40. Tammela, T., A. Saaristo, T. Holopainen, J. Lyytikka, A. Kotronen, M. Pitkonen, U. Abo-Ramadan, S. Yla-Herttuala, T. V. Petrova, and K. Alitalo. 2007. Therapeutic differentiation and maturation of lymphatic vessels after lymph node dissection and transplantation. *Nat. Med.* 13:1458-1466.
41. Miyasaka, M., and T. Tanaka. 2004. Lymphocyte trafficking across high endothelial venules: dogmas and enigmas. *Nat. Rev. Immunol.* 4:360-370.
42. Bajenoff, M., J. G. Egen, H. Qi, A. Y. Huang, F. Castellino, and R. N. Germain. 2007. Highways, byways and breadcrumbs: directing lymphocyte traffic in the lymph node. *Trends Immunol.* 28:346-352.
43. Gretz, J. E., C. C. Norbury, A. O. Anderson, A. E. Proudfoot, and S. Shaw. 2000. Lymph-borne chemokines and other low molecular weight molecules reach high endothelial venules via specialized conduits while a functional barrier limits access to the lymphocyte microenvironments in lymph node cortex. *J. Exp. Med.* 192:1425-1440.
44. Sixt, M., N. Kanazawa, M. Selg, T. Samson, G. Roos, D. P. Reinhardt, R. Pabst, M. B. Lutz, and L. Sorokin. 2005. The conduit system transports soluble antigens from the afferent lymph to resident dendritic cells in the T cell area of the lymph node. *Immunity.* 22:19-29.
45. Mora, J. R., M. Iwata, B. Eksteen, S. Y. Song, T. Junt, B. Senman, K. L. Otipoby, A. Yokota, H. Takeuchi, P. Ricciardi-Castagnoli, K. Rajewsky, D. H.

- Adams, and U. H. von Andrian. 2006. Generation of gut-homing IgA-secreting B cells by intestinal dendritic cells. *Science*. 314:1157-1160.
46. Johansson-Lindbom, B., M. Svensson, M. A. Wurbel, B. Malissen, G. Marquez, and W. Agace. 2003. Selective generation of gut tropic T cells in gut-associated lymphoid tissue (GALT): requirement for GALT dendritic cells and adjuvant. *J. Exp. Med.* 198:963-969.
47. Johansson-Lindbom, B., M. Svensson, O. Pabst, C. Palmqvist, G. Marquez, R. Forster, and W. W. Agace. 2005. Functional specialization of gut CD103+ dendritic cells in the regulation of tissue-selective T cell homing. *J. Exp. Med.* 202:1063-1073.

Reprinted from *The Journal of Immunology*, 181, "Stromal cells confer lymph node-specific properties by shaping a unique microenvironment influencing local immune responses", page 1898-1907, authors are Manuela Ahrendt, Swantje Iris Hammerschmidt, Oliver Pabst, Reinhard Pabst and Ulrike Bode.
Copyright 2008. The American Association of Immunologists, Inc.

4.6. Figures

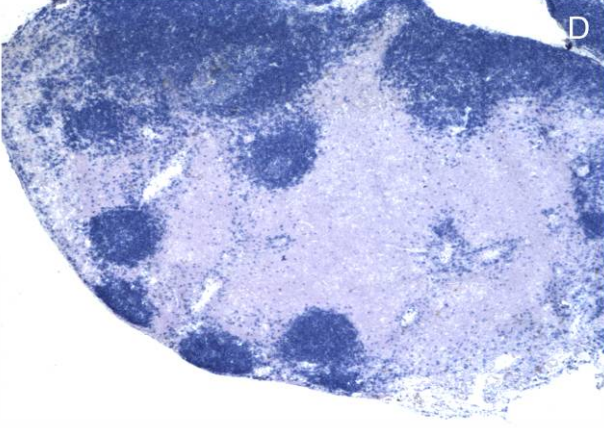
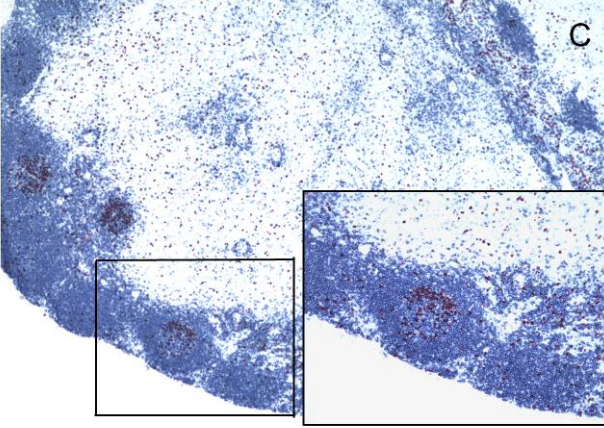
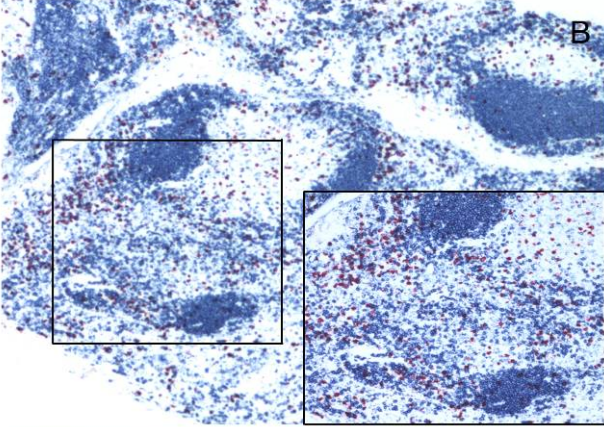
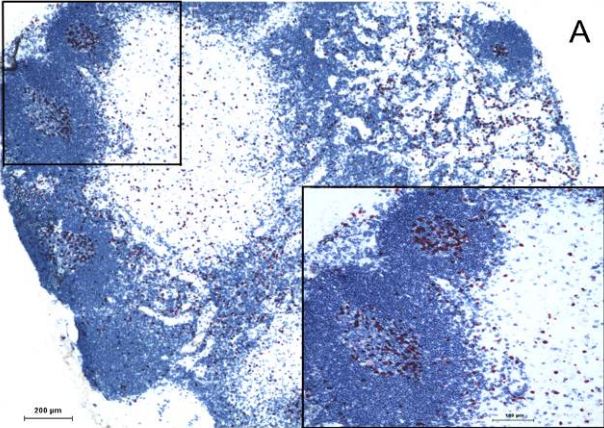


Fig.1: The lymph node architecture is destroyed after transplantation, but regenerate within 8 weeks

Cryosections of transplanted rat mLN and pLN were stained with mAbs against B cells (**A.-D.**, dark blue) and incorporated BrdU (**A.-C.**, red) (n=4-5). The inserts (right side) show the area in the left box in a higher magnification **A**. The mLN of an untreated animal shows a typical compartmental structure, and germinal centers visualized by proliferation are present. **B**. Two weeks after transplantation the architecture of the compartments is destroyed. Only small clusters of B and T cells are seen and germinal centers are absent. Eight weeks (**C.**), but also 23 weeks (**D.**) after transplantation large B and T cell areas are again found, comparable to the control mLN. In addition, germinal centers are present both in pLNtx and mLNtx.

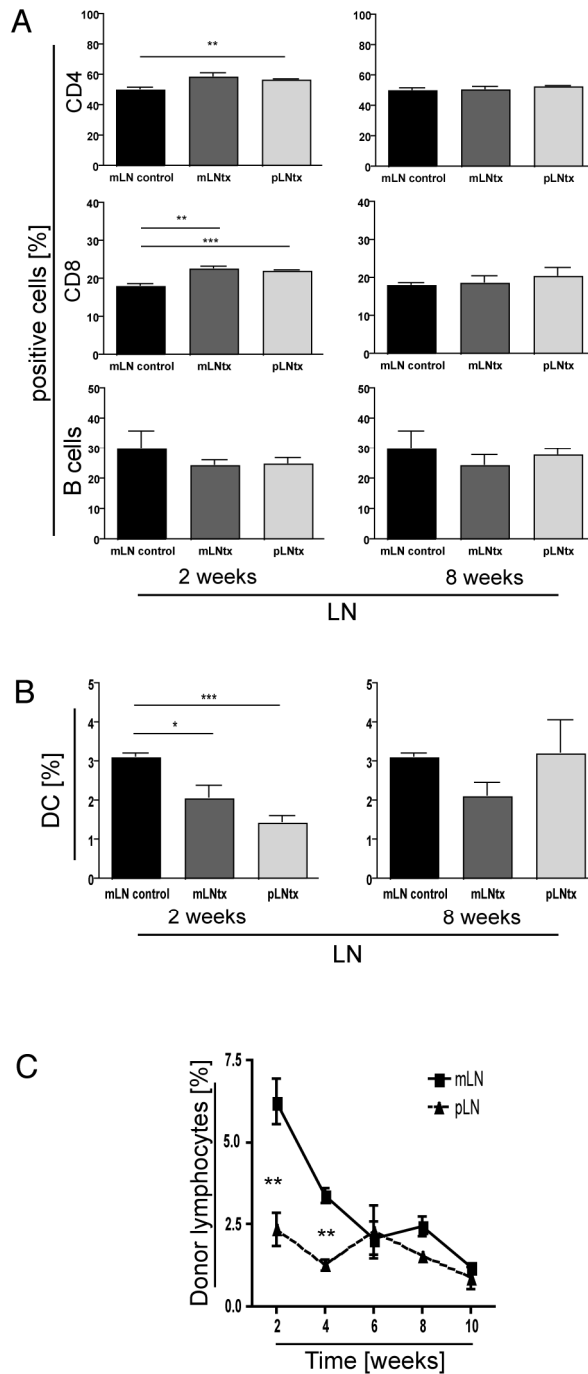


Fig.2: Donor immune cells leave the transplanted LN fragments

A. mLNtx and pLNtx were analyzed for their cell populations by flow cytometry. After 2 weeks there is a relative increase of both CD4⁺ and CD8⁺ T cells compared to mLN of control animals. In contrast, there is a decrease in the B cells and DC in mLNtx as well as pLNtx compared to mLN control. Eight weeks after transplantation the cell composition of both types of transplanted fragments is comparable to the mLN

control. Means and standard error are given (n=3-5) and significant differences in the unpaired t-test are indicated by **, P< 0.01; ***, P< 0.001.

B. After 2 weeks there is a significant decrease of these DC in mLNtx as well as pLNtx compared to mLN control. However, 8 weeks after transplantation both types of transplanted fragments no longer show significant differences. Means and standard error are given (n=3-5) and significant differences in the unpaired t-test are indicated by *, P< 0.05; ***, P< 0.001.

C. Donor lymphocytes of LEW.7B transplanted LN were detected within the LNtx over time by staining with the mAb His41 and analyzing via flow cytometry. mLNtx show significantly more donor cells than pLNtx 2 and 4 weeks after transplantation. Means and standard error are given from 4 independent experiments (significant differences in the unpaired t-test are indicated by **, P<0.01).

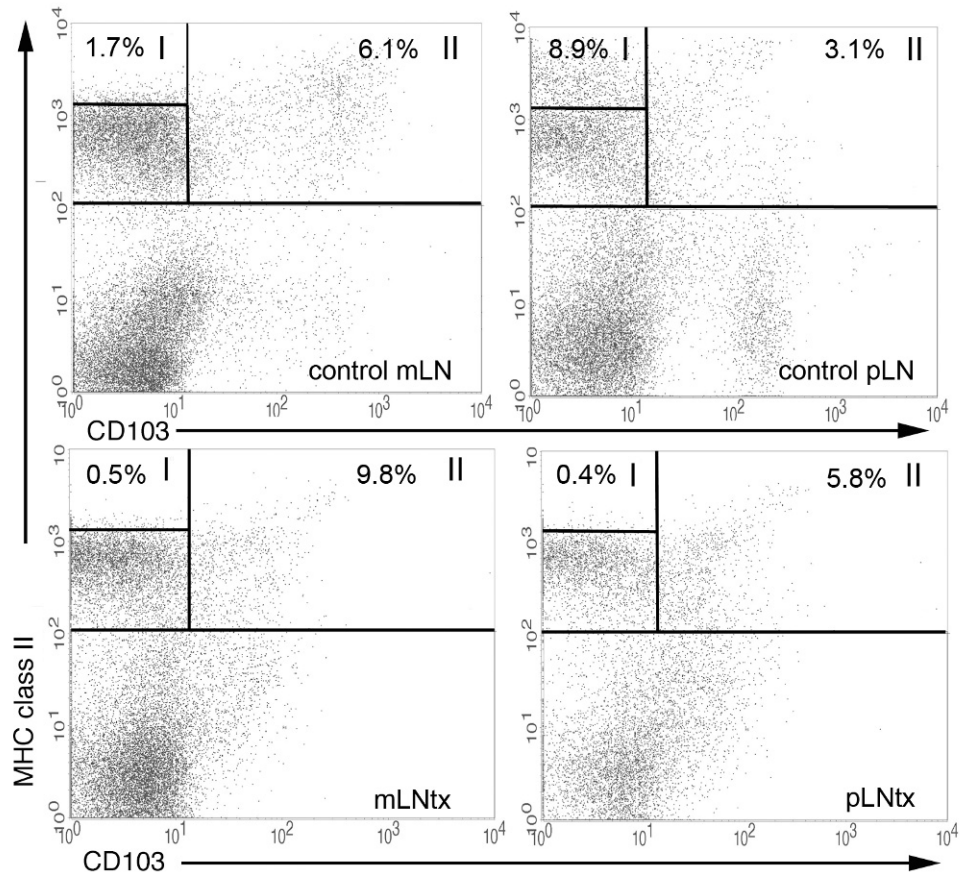


Fig.3: Eight weeks after transplantation DC of pLNtx exhibit the phenotype of mLN DC

mLNtx and pLNtx were analyzed by gating on the T and B cell negative population for their MHCII⁺CD103⁺ DC population by flow cytometry. Dot plots from DC of the mLN and pLN control as well as mLNtx and pLNtx are shown. In the control mLN and also in mLNtx and pLNtx MHCII⁺CD103⁺ DC are found (region II), whereas MHCII^{hi}CD103⁻ cells (region I) are only detected among the population of control pLN DC. The dot plots represent three independent experiments.

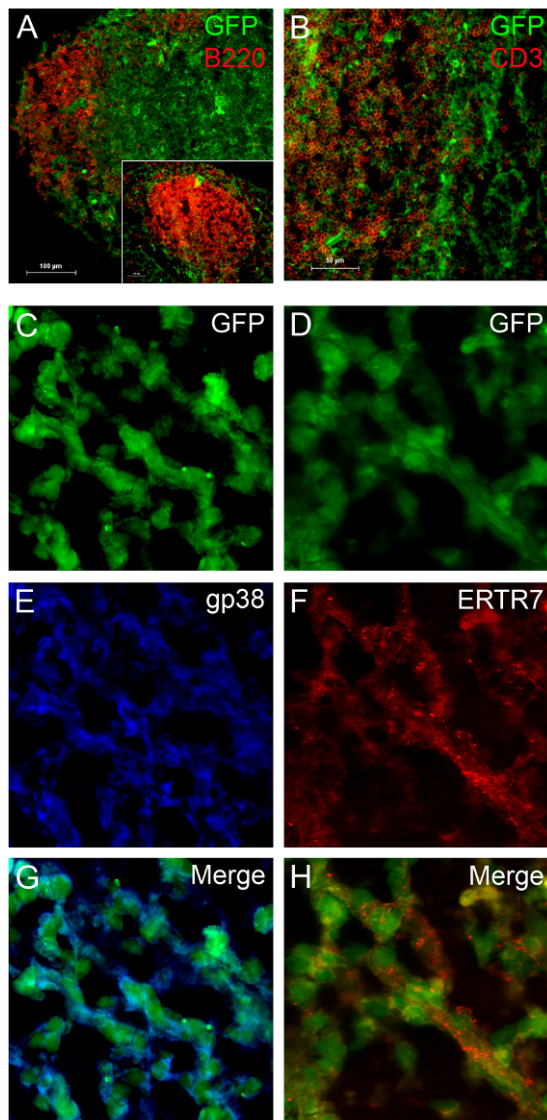


Fig.4: Fibroblastic reticular cells survive after transplantation

A.-H. LN of EGFP⁺ mice (green) were transplanted into C57BL/6 mice and removed 8 weeks later (n=3). **A.-B.** B and T cell subsets of the transplanted LN fragments were analyzed by fluorescent staining. GFP⁺ cells are seen in both the B cell area (A. red) and in the T cell area (B. red). The insert shows a typical B cell follicle (red) in the B cell area. While GFP⁺ immune cells disappear from the regenerated LN fragment, stromal cells survive and are seen as remaining GFP⁺ cells.

C.-H. Stromal cells of the transplanted fragments were analyzed by immunofluorescent staining with gp-38 and ERTR-7. Donor cells (green) are found within mLNTx as well as pLNTx (**C. and D.**). **E.** shows staining with gp38 (blue), and **F.**

staining with ERTR-7 (red). The merging of C. and E. and also of D. and F. shows that most FRC are GFP⁺.(G. and H.). Nearly all gp38 and ERTR-7⁺ cells are GFP⁺.

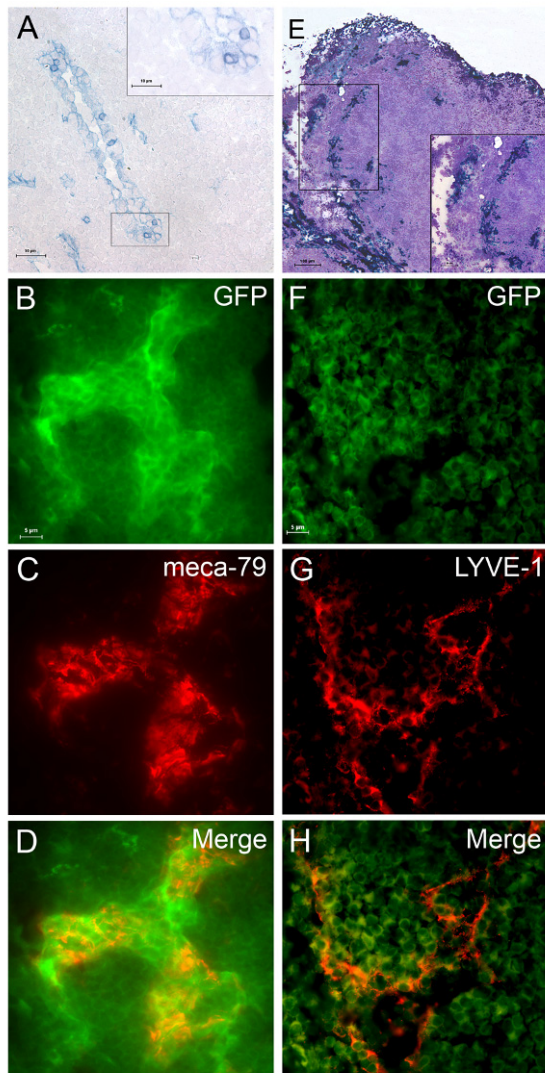


Fig.5: The transplanted lymph node fragments are connected to the blood vessels and lymphatics

Eight weeks after transplantation mLNTx and pLNTx were excised and the presence of HEV (Fig. A-D) and lymphatics (E-H) was analyzed. **A.** Lymphocytes of the congenic LEW.7B strain were injected into transplanted LEW rats, which were exsanguinated 1h after injection. Cryosections of the transplanted mLN and pLN fragments (LNTx) were stained for HEV (light blue) and donor cells (dark blue). The insert shows a

higher magnification. Injected cells are found in the LNtx and in the wall of the HEV (n=3) **B**. Lymph node fragments of EGFP⁺ mice were transplanted into C57BL/6 mice and 8 weeks after transplantation mLNtx and pLNtx were removed and the HEV were identified immunohistologically. In both LNtx GFP⁺/HEV⁺ cells are found (**B-D**). **E**. Eight weeks after transplantation the dye “Berlin blue” was injected into the subserosa of the gut. Berlin blue can only be transported via the lymph. The dye is found in the lymph vessels and also in the sinus of the LNtx. The insert shows a higher magnification. **F-H**. Lymph node fragments of EGFP⁺ mice were transplanted into C57BL/6 mice and 8 weeks after transplantation mLNtx and pLNtx were removed and stained for lymphatic endothelial cells (LYVE-1) (n=2). LYVE-1 is present in the marginal lymphatic sinus in pLNtx and also in mLNtx. Most of these cells are GFP⁺ (**E-H**).

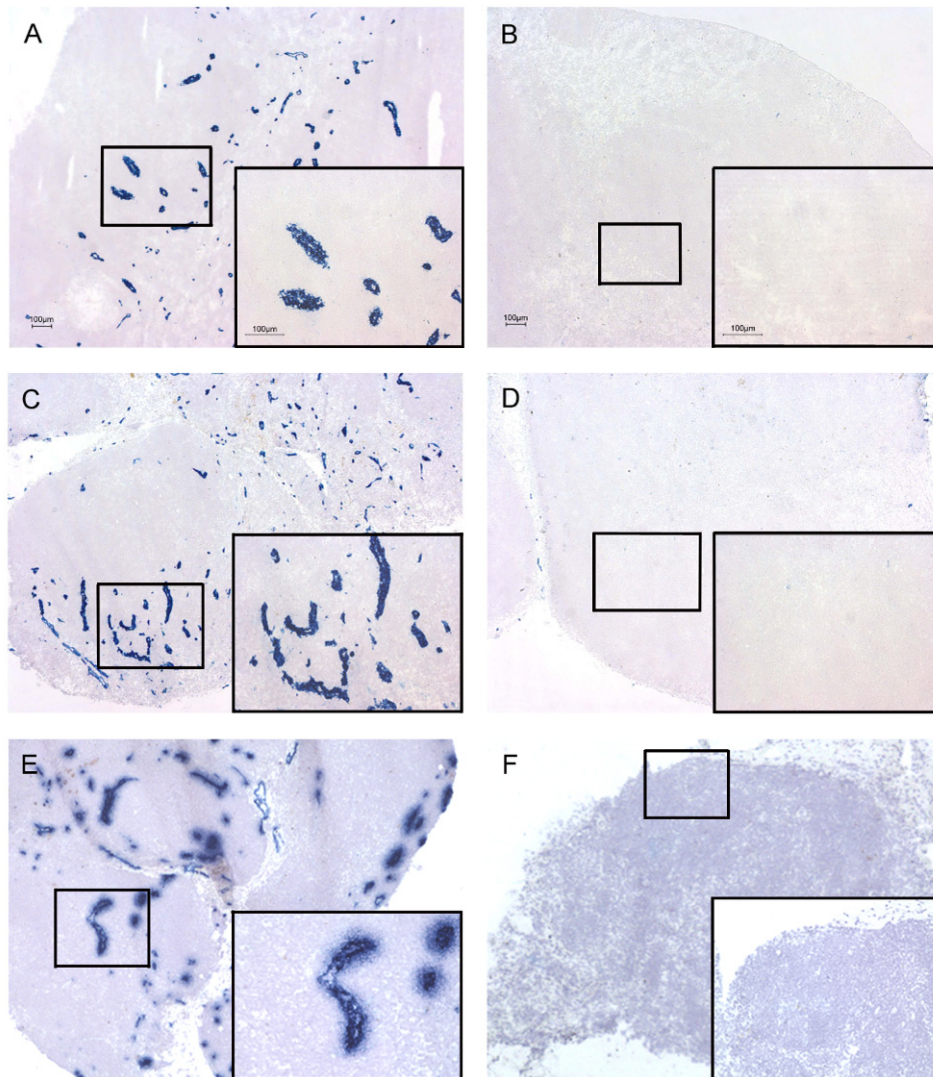


Fig.6: MAdCAM-1 expression is not influenced by the drained area

A.MLN and **B.** pLN of control animals as well as mLNtx and pLNtx were analyzed by immunohistological staining against MAdCAM-1 eight weeks (**C. and D.**) and 23 weeks (**E. and F.**) after transplantation. MAdCAM-1 is detected in the control mLN as well as the mLNtx but not in the pLN control. Over a period of 23 weeks MAdCAM-1 expression is not detected in pLNtx (**F.**) (n=4-5). The inserts show a higher magnification.

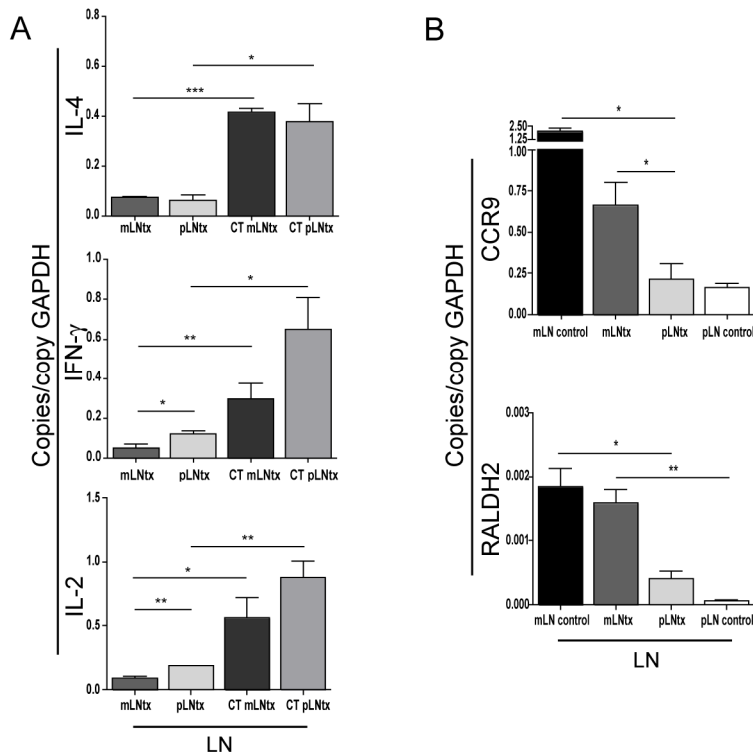


Fig.7: The expression pattern of Th1 cytokines, CCR9 and RALDH2 is LN specific

Eight weeks after transplantation cholera toxin (CT) was given orally. The mLNtx and pLNtx were excised, mRNA isolated and real time PCR in triplets was performed. Untreated mLNtx and pLNtx were also analyzed. The data are normalized to the housekeeping gene GAPDH for rats and given from 3 animals. Significant differences in the unpaired t-test are indicated by *: $P < 0.05$; **: $P < 0.01$.

A. Eight weeks after transplantation IL-4 is detected in both types of transplanted fragments on similar expression levels and at a higher amount after CT treatment. In contrast, the expression of IFN- γ and IL-2 is significantly increased in pLNtx compared to mLNtx in untreated animals. After CT treatment both cytokines are strongly upregulated in mLNtx and to a greater extent in pLNtx. **B.** CCR9 expression in mLNtx and pLNtx is expressed similarly compared to the mLN and pLN control, respectively. The same is valid for RALDH2 expression.

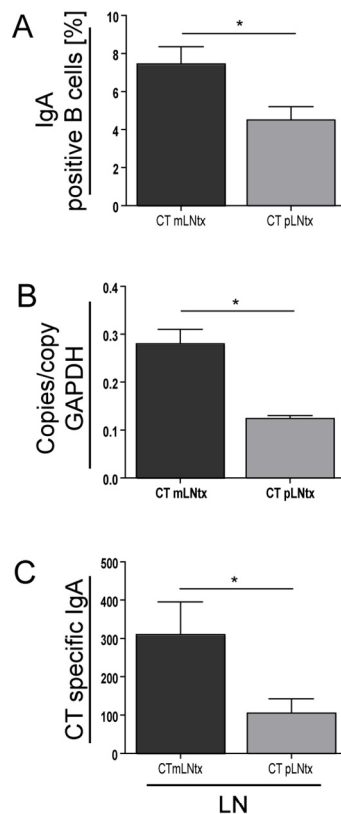


Fig.8: CCR9⁺ B cells are less increased in pLNtx after CT administration

Eight weeks after transplantation cholera toxin (CT) was administered and mLNtx and pLNtx were excised. **A.** Cell suspensions were made and IgA⁺ B cells were analyzed by flow cytometry. The percentage of surface IgA⁺ B cells is much lower in pLNtx compared to mLNtx. **B.** B cells were separated via positive selection using the MACS technique, mRNA was isolated and real time PCR in triplets for CCR9 was performed. The data are normalized to the housekeeping gene GAPDH for rats and given from 2 animals. Significant differences in the unpaired t-test are indicated by *: P < 0.05. CCR9 expression is lower among the pLNtx B cells compared to those of mLNtx **C.** The gut was lavaged to perform a CT-specific IgA ELISA. The data show significantly higher CT-specific IgA levels in mLNtx than pLNtx. Means and standard error are given from 5-8 independent experiments (significant differences in the unpaired t-test are indicated by *: P < 0.05).

5. Stromal mesenteric lymph node cells are essential for the generation of gut-homing T cells in vivo

Swantje I. Hammerschmidt¹, Manuela Ahrendt², Ulrike Bode², Benjamin Wahl¹, Elisabeth Kremmer³, Reinhold Förster¹ and Oliver Pabst¹

¹ Institute of Immunology, Hannover Medical School, 30625 Hannover, Germany

² Institute of Anatomy, Hannover Medical School, 30625 Hannover, Germany

³ Institute of Molecular Immunology, National Research Center for Environment and Health, 81377 Munich, Germany

© Hammerschmidt et al., 2008. Originally published in **The Journal of Experimental Medicine**, doi: 10.1084/jem.20080039.

Running Title

stroma cells dictate the generation of gut-homing

Keywords

Intestine, mesenteric lymph nodes, tissue tropism, $\alpha_4\beta_7$ -integrin, CCR9

Address correspondence to: Dr. Oliver Pabst; Institute of Immunology; Hannover Medical School; Carl-Neuberg Strasse 1; 30625 Hannover, Germany; Tel.: +49-511-5329725; Fax: +49-511-5329722; E-mail: Pabst.Oliver@MH-Hannover.de

Abstract

T cells primed in the gut-draining mesenteric lymph nodes (mLN) are imprinted to express $\alpha_4\beta_7$ -integrin and chemokine receptor CCR9, thereby enabling lymphocytes to migrate to the small intestine. *In vitro* activation by intestinal dendritic cells (DC) or addition of retinoic acid (RA) is sufficient to instruct expression of these gut-homing molecules. We report that *in vivo* stroma cells, but not DC, allow the mLN to induce the generation of gut tropism. Peripheral LN (pLN) transplanted into the gut mesenteries fail to support the generation of gut-homing T cells, even though gut-derived DC enter the transplants and prime T cells. DC that fail to induce $\alpha_4\beta_7$ -integrin and CCR9 *in vitro* readily induce these factors *in vivo* upon injection into mLN afferent lymphatics. Moreover, uniquely mesenteric but not pLN stroma cells express high levels of RA-producing enzymes and support induction of CCR9 on activated T cells *in vitro*. These results demonstrate a hitherto unrecognized contribution of stromal cell delivered signals, including RA, on the imprinting of tissue tropism *in vivo*.

5.1. Introduction

Seminal observations demonstrated that lymphocytes isolated from gut-associated lymphoid tissues (GALT) preferentially home to mucosal tissues, whereas lymphocytes isolated from skin-draining LN are biased to enter cutaneous sites (1, 2). Since then the molecular mechanisms underlying these divergent homing properties have been studied in exquisite detail (for a recent review see (3)). The migration of antigen-experienced T cells into the intestine requires $\alpha_4\beta_7$ -integrin and the chemokine receptor CCR9. $\alpha_4\beta_7$ -Integrin interacts with mucosal vascular addressin cell adhesion molecule 1, which is uniformly expressed by intestinal venules and β_7 -integrin-deficient cells are impaired in entering the intestine (4, 5). Expression of the CCR9 ligand CCL25 builds up a gradient with highest expression in the proximal small intestine, low expression in the ileum and no detectable expression in the colon (6). Consistently, homing of T cells into the proximal small intestine more stringently depends on CCL25-CCR9 interaction compared to homing into the ileum (7). In contrast, the migration of effector T cells into the skin requires expression of E- and P-selectin ligand and the chemokine receptor CCR4, which endow T cells to interact with the respective ligands expressed in the skin (8). Thus the anatomical site of T cell activation and expansion determines the array of homing factors, including chemokine receptors and integrins, expressed by antigen-experienced T cells. The particular combination of these homing factors specifically targets antigen-experienced T cells to different lymphoid and extralymphoid tissues expressing the respective ligands.

Numerous studies indicated that DC play a decisive role in the imprinting of tissue tropism. *In vitro* stimulation by GALT-derived DC is sufficient to induce expression of

$\alpha_4\beta_7$ -integrin and CCR9 on T cells (9, 10), whereas DC isolated from skin-draining LN confer expression of CCR4 and enzymes required for E- and P-selectin ligand synthesis (11, 12). Such differential function of GALT and peripheral LN (pLN) DC has recently been suggested to reflect their differential ability to produce the vitamin A metabolite retinoic acid (RA). RA is sufficient to direct expression of $\alpha_4\beta_7$ -integrin and CCR9 *in vitro* irrespective of the origin of the antigen-presenting DC (13). Moreover, addition of RA antagonists impairs up-regulation of gut-homing factors after priming by GALT DC (13). Thus, availability of RA supports the generation of gut-homing T cells, and GALT DC can act as a source for RA *in vitro*. However, at present the *in vivo* function of DC-delivered signals in imprinting gut-homing remains speculative. In this paper, we use LN transplantations and DC injection into mesenteric LN (mLN) afferent lymphatics to reveal a hitherto unrecognized essential role of stroma cell-derived signals, including RA, on the generation of tissue tropism *in vivo*.

5.2. Results and Discussion

mLN but not pLN stroma cells support the generation of gut-homing T cells *in vivo*.

To study the role of LN stroma cells in the generation of gut-homing effector T cells, mLN were excised from WT mice and replaced by either pLN or mLN fragments isolated from EGFP mice. 8 wk after surgery, transplanted LN (Tx-LN) could be identified by their EGFP expression (Fig.1, A and B). In line with previous observations, we noted that Tx-LN displayed normal tissue architecture and cellular composition ((14) and Fig.S1), and were connected to gut-draining afferent and LN efferent lymphatics (not depicted (15)). Fluorescent microscopy on T cell zones in Tx-LN revealed that EGFP expression colocalized with gp38 (Fig.1C) and ER-TR7 (Fig.1D), which are both expressed by LN stroma cells, whereas EGFP⁺ cells showed no overlap with anti-B220 and anti-CD3 staining (not depicted). Similar results were obtained when cells isolated by collagenase digestion of Tx-LN were analyzed by flow cytometry. Few B and T cells, as well as DC, expressed EGFP (Fig.1E). Flow cytometry of CD45⁻gp38⁺ stroma cells revealed almost 50% EGFP⁻ cells (Fig.1E). Because immunohistology showed that in the T cell zones of Tx-LN the vast majority of stroma cells expressed EGFP, this indicates that donor- and host-derived stroma cells are unevenly distributed in the various compartments of the transplant. In conclusion, a major population of donor-derived nonhematopoietic stroma cells survived in the Tx-LN, whereas the vast majority of hematopoietic cells were constituted by host cells.

To investigate the type of tissue tropism generated in such chimeric Tx-LN, TCR transgenic OT-I or OT-II T cells were fluorescently labeled with CFSE and adoptively transferred into nonmanipulated or transplanted recipients. The frequency of

adoptively transferred cells homing into Tx-LN was comparable to endogenous mLN (unpublished data), indicating that Tx-LN were properly vascularized and equipped with the molecular machinery enabling efficient lymphocyte entry. On the subsequent day, mice were fed with a single dose of Ova, and a group of nontransplanted mice received a single s.c. injection of Ova. 3 d after antigen delivery, cells were isolated from gut-draining endogenous mLN or Tx-LN as well as endogenous skin-draining pLN and analyzed by flow cytometry. In line with previous reports, we observed that in nontransplanted WT mice, feeding of Ova induced T cell proliferation preferentially in the gut-draining mLN but not pLN (16). Expectedly, OT-I T cells proliferating in the endogenous mLN acquired a gut-homing phenotype, characterized by up-regulation of $\alpha_4\beta_7$ -integrin and CCR9 (Fig.2A and B). Expression of $\alpha_4\beta_7$ -integrin gradually increased with progressing cell divisions, whereas CCR9 was highly expressed already after one or two rounds of cell division (Fig.2B). Similarly, OT-II T cells up-regulated $\alpha_4\beta_7$ -integrin and CCR9 expression in the mLN after antigen feeding (Fig.2C), even though expression levels were lower compared to OT-I T cells. S.c. antigen delivery preferentially resulted in T cell proliferation in the draining inguinal LN, accompanied by no apparent expression of $\alpha_4\beta_7$ -integrin and CCR9 (Fig.2A and B).

Comparison of these results obtained from the endogenous LN with the Tx-pLN revealed striking differences: T cells primed in Tx-pLN failed to up-regulate $\alpha_4\beta_7$ -integrin and CCR9. In contrast, grafted Tx-mLN were indistinguishable from endogenous mLN in respect to their ability to promote the generation of gut-homing T cells (Fig.2A-C). Notably, oral administration of Ova readily induced proliferation of T cells in Tx-pLN and Tx-mLN comparable to endogenous mLN (Fig.2A). Expanding T cells down-regulated CD62L and up-regulated CD44 in Tx-pLN and Tx-mLN to a similar extent, which is indicative for their effector status (Fig.S2). However, because

their small size, neither Tx-pLN nor Tx-mLN were able to direct normal numbers of primed OT-I T cells into the small intestine.

Because the induction of T cell proliferation after oral antigen application depends on DC-bound antigen transport (16, 17), the efficient induction of T cell proliferation indicates that gut-derived DC readily entered Tx-LN. Consistently, we observed that compared to endogenous pLN, Tx-pLN contained increased frequencies of DC expressing CD103⁺, which is indicative of their origin in the small intestinal lamina propria (Fig.S3A). Moreover, orally applied latex beads appeared in Tx-mLN as well as Tx-pLN (Fig.S3B), a process which requires the active cell-bound transport of the beads. Thus, even though gut-derived DC initiated T cell priming in Tx-pLN and Tx-mLN, divergent homing molecules were induced on the expanding T cells. In particular, gut-derived DC that effectively induce a gut-homing phenotype *in vitro* are insufficient to sustain the generation of a gut tropism in Tx-pLN *in vivo*. This suggests that in Tx-LN, donor-derived factors, which are retained after transplantation, essentially shape the type of tissue tropism generated.

Notably, flow cytometry revealed a significant fraction of EGFP⁻ host-derived stroma cells in Tx-LN (Fig.1E). Thus we cannot rule out that EGFP⁻ host-derived stroma cells might have seeded the Tx-LN. Transplantation of LN fragments requires puncturing and tearing of the LN capsule before insertion into the mesenterium to allow for proper engraftment and vascularisation of the transplants. Thus, rebuilding of the capsule and ingrowth of the vasculature most likely will involve substantial contribution of EGFP⁻ host cells. However, apparently these cells are not able to overcome the dominant effect of EGFP⁺ donor-derived stroma on the type of tissue tropism generated in Tx-LN. Moreover, immunohistology showed that in the T cell zones, i.e., at the site of T cell priming, indeed the vast majority of gp38⁺ stroma cells is donor-derived. We therefore suggest that nonhematopoietic stromal elements are

essential for the generation of gut-homing T cells in gut-draining mLN and that these stromal elements differ between pLN and mLN, thereby providing a structural basis for the divergent generation of tissue tropism observed in these LN *in vivo*.

BM-DC and spleen-derived DC induce gut-homing T cells *in vivo* but not *in vitro*.

Analyzing the potential of distinct DC subsets to generate gut-homing T cells *in vivo* requires uncoupling the origin of the DC from their usual destination, i.e., the draining LN. To this aim, we established a new method to inject DC directly into the mLN afferent lymphatics (intralymphatic (i.l.) injection). After oil feeding, the small intestine was exposed by surgery and the mLN afferent lymphatics were located. 10^5 BM-DC was injected into two separate lymphatic vessels opening into the distal aspect of the mLN chain using a fine glass capillary (Fig.3A and B). Injection of Ova-loaded BM-DC readily induced proliferation of only antigen-specific adoptively transferred T cells, indicating that no overt unspecific T cell proliferation was induced. Moreover, DC defective in antigen presentation in the context of either MHC class I or class II failed to provoke T cells proliferation (Fig.3C). Thus, T cell proliferation upon i.l. injection of BM-DC reflects the direct priming by the injected DC and does not result from antigen passed on to LN resident DC.

We next explored the phenotype of T cells primed in the mLN upon i.l. injection of DC. As described in the previous paragraph, antigen-loaded DC were injected into mLN afferent lymphatics of WT recipients that previously received CFSE-labeled Ova-specific DO11.10 cells. 3 d later, cells were isolated from the mLN and analyzed for the expression of $\alpha_4\beta_7$ -integrin, CCR9, and E- and P-selectin ligand. For comparison, another group of mice received 10^6 DC-injected s.c., and cells isolated from the skin-draining pLN were analyzed. Strikingly, BM-DC that fail to induce CCR9

on T cells *in vitro* (Fig.4B and (9)), efficiently induced CCR9 after i.l. injection *in vivo* (Fig.4A and B). Similarly, *in vitro* expression of $\alpha_4\beta_7$ -integrin is induced by BM-DC only after prolonged culture (3, 18) but was rapidly induced *in vivo* (Fig.4A and B). Thus, T cells primed by BM-DC *in vitro* largely differ with respect to their homing properties from T cells primed by BM-DC *in vivo*. We next extended our experiments to primary DC. DC were isolated from spleen or mLN of WT mice and loaded with Ova peptide *in vitro*. Expectedly, only mLN-derived DC induced a gut-homing phenotype on T cells *in vitro* (unpublished data). In contrast, both mLN- and spleen-derived DC induced considerable up-regulation of CCR9 and $\alpha_4\beta_7$ -integrin upon i.l. injection (Fig.4C and D). In line with these observations, i.p. injection of BM-DC has also been reported to induce expression of $\alpha_4\beta_7$ -integrin on antigen specific proliferating T cells in the mLN (18). This indicates that even though mLN-derived DC might be more efficient in inducing CCR9 (Fig.4C and D) compared to spleen-derived DC, the LN environment and not the origin of DC determines the generation of gut-homing T cells *in vivo*.

Stroma cells in mLN express RALDH and support the induction of CCR9 *in vitro*.

Because RA can mimic the effects of GALT DC *in vitro* and addition of RA antagonists counteracts the ability of GALT DC to generate gut-homing T cells, it is tempting to speculate that stroma cells might directly or indirectly influence RA levels in LN. To determine a potential contribution of stromal cells to RA production, we compared the expression of the RA producing enzymes RALDH1, 2 and 3 in purified stroma cells and CD103⁺ and CD103⁻DC isolated from mLN or pLN. Stroma cells were sorted as CD45⁻CD24⁻gp38⁺ cells to >95% purity and contained no detectable DC (unpublished data). As published previously, RALDH2 expression was

substantially higher in CD103⁺ mLN DC compared to their CD103⁻ counterparts (Fig.5A and (19)). Surprisingly, CD103⁻ pLN DC showed elevated expression levels of RALDH2. This indicates that RALDH2 expression by DC does not necessarily correlate with expression of CD103 or with their ability to instruct CCR9 expression on activated T cells. Interestingly, comparison of RALDH expression between pLN- and mLN-derived stroma cells revealed striking differences. Exclusively mLN-derived stroma cells showed robust expression of RALDH2, whereas expression of this enzyme was virtually absent from pLN stroma cells (Fig.5A). Moreover, expression of RALDH1 and 3 was substantially higher in mLN- compared to pLN-derived stroma cells (Fig.5A). In contrast, no differences were observed in expression of the Vitamin A metabolizing alcohol dehydrogenases ADH1, ADH4 and ADH5 (unpublished data). Next, we directly assessed the ability of LN stroma to support the generation of gut-homing T cells. Because cell sorting of primary LN cell suspensions did not yield sufficient cells for functional assays, LN were enzymatically digested and the resulting cell suspensions plated. Nonadherent cells were repeatedly removed and after 10 d of culture, a dense monolayer of LN-adherent cells with most cells resembling fibroblasts was obtained. Flow cytometry revealed that the vast majority of all cells in such cultures were CD45⁻ and expressed gp38. In contrast, only a minor population of hematopoietic cells was observed (2.4±2.2% of all cells expressed CD11b and 1.5%±1.4% of cells coexpressed CD11c and MHCII, n=7) and real-time PCR assays did not show any expression of MHCII. Thus, we suggest that such cultures of LN-adherent cells do not contain functionally relevant populations of DC or macrophages and can be used as a substitute for primary isolates of LN stroma cells. Interestingly, OT-I T cells activated by anti-CD3/CD28 stimulation readily up-regulated expression of CCR9 in the presence of adherent cells cultured out of mLN but not pLN (Fig.5B and C). Up-regulation of CCR9 was dependent on the presence

of retinol, suggesting that the ability of mLN but not pLN stroma-adherent cells to metabolize retinol was responsible for the induction of CCR9 (Fig.5B and C). We therefore suggest that the particular ability of mLN to support the generation of gut-homing T cells, at least in part, relies on the ability of mLN stroma cells to produce RA.

RA is well known to act as a signalling molecule eliciting RA-dependent responses throughout tissues, as exemplified by the rescue of morphogenetic defects in RALDH2-deficient embryos by low chimerism with WT cells (20). Moreover, RA can enhance its own production by up-regulation of the enzymatic machinery regulating RA levels. Thus the combined function of LN-resident stroma cells and migrating DC, both of which express high levels of RALDH genes, might integrate to shape the unique properties of LN, including the particular ability of mLN to direct effector T cells into the gut.

In line with this idea, we observed that BM-DC failed to induce expression of CCR9 upon i.l. injection in the mLN of CCR7-deficient mice (Fig.5E). CCR7-deficient mice are characterized by impaired steady-state migration of DC, have a strongly reduced population of CD103⁺ DC in their mLN (16, 21) and residual CD103⁺ DC in the mLN of CCR7-deficient mice almost completely lack expression of RALDH2 (Fig.5D). Up-regulation of $\alpha_4\beta_7$ -integrin, as well as expression of RALDH genes by mLN stroma cells was not significantly altered in CCR7-deficient mice (Fig.5D and E). Therefore, *in vivo*, the generation of gut tropism, i.e. expression of CCR9, appears to require instructive signals by both mLN resident stroma cells and DC. These signals are likely to include the agonistic effects of RA on the induction of CCR9 and $\alpha_4\beta_7$ -integrin and appear to influence proliferating T cells in trans. In contrast, RA provided in cis by the antigen-presenting DC appears to play a subordinate role, as revealed by the ability of RALDH2-negative spleen DC to induce CCR9 after i.l. injection and

the inability of Tx-pLN to support the induction of gut tropic T cells. Still, RA provided *in cis* by the antigen-presenting DC might add to the net regulation of tissue tropic factors as reflected by the more potent activity of mLN-derived DC to induce CCR9 compared with spleen-derived DC after i.i. injection.

Recently, an additional role for RA has been reported in the generation of regulatory T cells (19, 22-24). Interestingly, conversion of naïve T cells into regulatory T cells occurs more efficiently in GALT than other tissues (19, 23), raising the possibility that regulation of RA levels by LN stroma cells does not only affect tissue tropisms but, moreover, might influence the balance between effector and regulatory T cell generation.

In conclusion, we suggest that *in vivo* gut-homing T cells can only be generated in a permissive LN environment that is determined by resident stroma cells and DC.

Resident stroma cells might produce negative signals that impair the generation of gut-homing T cells in Tx-pLN. Additionally, mLN stroma cells deliver positive signals, including RA, that support the induction of $\alpha_4\beta_7$ -integrin and CCR9 on T cells by DC that fail to promote this process *in vitro*. Under physiological conditions stroma cells and DC might cooperate in shaping a LN environment that in the mLN is distinguished by high levels of RA, favouring the induction of gut-homing molecules. This balance is perturbed by LN transplantation and i.i. injection, revealing the major influence of stromal cells in LN function.

5.3. Material and Methods

Mouse strains

C57BL/6, C57BL/6-Tg(Tcra Tcrb)1100Mjbj (designated here as OT-I mice, OT-I T cells selectively recognize Ova peptide presented in the context of MHC class I), C57BL/6-Tg(Tcra Tcrb)425Cbn-Ptprc^a (designated here as OT-II Ly5.1 mice, OT-II T cells selectively recognize Ova peptide presented in the context of MHC class II), B6.C-H2^{bm1} (designated here as bm1-mice, bm-1 mice carry a mutated H2-K molecule and can not present Ova peptide in the context of MHC class I), B6;129-H2^{dlab1} (designated here as MHC class II-deficient-mice), C57BL/6-Tg(ACTbEGFP) (designated here as EGFP-mice; these mice constitutively express EGFP in all cells under the control of the chicken β -actin promoter), BALB/c and BALB/c – Tg(DO11.10) were bred at the central animal facility of Hannover Medical School under specific pathogen-free conditions. BALB/c mice were purchased from Charles River (Germany). All experiments have been approved by the institutional review board and the “Niedersächsisches Landesamt für Verbraucherschutz und Lebensmittelsicherheit“.

Antibodies and reagents

The following antibodies, fusion proteins and conjugates were used in this study: anti-CD11c-APC (HL3), anti-MHCII (1A^b)-bio (AF6-120.1), anti-V β 5.1, 5.2 TCR-bio (MR9-4), anti-V α 2-PE (B20.1), anti- α 4 β 7 (DTAK32), CD45.2-PerCp-Cy5.5 (104) (all BD Biosciences), anti-DO11.10 TCR-bio (KJ1-26) (Caltag), ER-TR7 (BMA), recombinant mouse E-Selectin/Fc chimera and recombinant mouse P-Selectin/Fc chimera (R&D Systems). Anti-CD4 (RmCD4.2), anti-CD3 (17A2), anti-CD8 β (RmCD8-2), anti-B220 (TIB146), anti-CCR9 (7E7) and anti-gp38 (8.1.1) antibodies

were produced in our laboratory. Cy3 and Cy5 conjugates (Amersham) as well as Pacific Orange conjugates (Invitrogen) were prepared as recommended by the manufacturer. Biotinylated antibodies were recognized by streptavidin coupled to PerCp (BD Biosciences). Anti-CCR9 and anti- $\alpha_4\beta_7$ were detected using mouse anti-rat-Cy5 (Jackson Immuno Research). E-Selectin/Fc chimera and P-Selectin/Fc chimera were detected with goat anti-human-Cy5 (Jackson Immuno Research).

Intestinal surgery

Under the combined anesthesia with Ketamine and Rompun, mesenteric lymphadenectomy was carried out by microdissection along the length of the superior mesenteric artery to aortic root. mLN or pLN (inguinal, axillary and brachial LN) were isolated from EGFP-mice and grafted into the site of the removed mLN. Mice were used for experiments eight weeks after transplantation. Immunohistology of grafted LN was performed as described (25).

Adoptive cell transfer

Cells were isolated from DO11.10, OT-II Ly5.1 or OT-I transgenic mice expressing TCR recognizing Ovalbumin (Ova), labelled with CFSE as described previously (16) and i.v. transferred into syngenic recipients. Mice received a single dose of 100 mg Ova by gavage. BM-DC were prepared as previously described (26) and loaded with antigen by addition of 1 mg/ml Ova during the maturation. BM-DC were washed thoroughly and injected intra lymphatic (i.l.) or s.c. into adoptively transferred recipients. For s.c. transfers, 10^6 DC were injected into the dorsal flank. Mice receiving DC i.l. were gavaged with 200 μ l olive oil 1h before surgery for better visualization of mesenteric lymph vessels. Under the combined anaesthesia with Ketamine and Rompun, mLN afferent lymphatics were exposed and 10^5 DC in a

volume of 2x1 µl were injected with a fine glass needle into two separate lymph vessels.

Cell isolation

For isolation of DC lymphoid organs were digested at 37° for 45 min with 0.5 mg/ml Collagenase A and 50 U/ml DNase I (both Roche) in RPMI 1640/10%FCS. Red blood cells were lysed and CD11c⁺ cells were enriched by CD11c MicroBeads using AutoMACS (Miltenyi), yielding an average purity of 70% MHCII⁺CD11⁺ DC. Enriched DC suspensions were pulsed with 1 µg/ml OVA peptide (323-329) binding to MHC class II for 1h at 37° and washed thoroughly before i.l. injection. For isolation of stroma cells LN were digested at 37° for 60 min with 0.1 mg/ml Liberase Blendzyme 2 and 50 U/ml DNase I (both Roche). Hematopoietic cells were depleted by anti-CD45 anti-CD11c MACS negative selection and purified by FACS sorting (FACSAria, BD Biosciences) as DAPI⁻CD45⁻CD24⁻gp38⁺ cells for isolation of RNA. Alternatively, digested lymph node cell suspensions were cultured in DMEM/10%FCS/PS for 10 days. Medium was exchanged every second day to remove non-adherent cells from the cultures.

In vitro cocultures

10⁵ CFSE-labelled OT-I cells were activated by adding 10⁵ antigen-loaded DC. For stroma cell cocultures, 2.5x10⁵ CFSE-labelled purified CD8⁺ OT-I cells (CD8⁺ T Cell Isolation Kit, Miltenyi) were activated with CD3/CD28 beads (Dynal) in the absence or presence of 50nM retinol or 5nM RA (both Sigma).

Real-time PCR

RNA was isolated using the Absolutely RNA Microprep Kit (Stratagene) and converted into cDNA (Superscript II reverse transcriptase, Invitrogen) using random hexamer primers. Expression of GAPDH and RALDH1, 2 and 3 was analyzed using a Lightcycler 2.0 Roche and SYBR Premix Ex Taq Kit (Takara). The following primers were used: RALDH1 fwd: CTCCTCTCACGGCTCTTCA, RALDH1 rev: AATGTTTACCA CGCCAGGAG, RALDH2 fwd: CATGGTATCCTCCGCAATG, RALDH2 rev: GCGCA TTTAAGGCATTGTAAC, RALDH3 fwd: AACCTGGACAAAGCACTGAAG, RALDH3 rev: AATGCATTGTAGCAGTTGATCC, GAPDH fwd: TGCACCACCAACTGCTTAG.

Statistical analysis

Statistical analysis was performed with GraphPadPrism software. All significant values were determined using the unpaired two-tailed t test, error bars represent SD. Statistical differences for the mean values are indicated as follows: *, $p < 0.05$; **, $p < 0.01$; ***, $p < 0.001$

Online Supplemental Material:

Fig.S1: Tx-LN display normal cellular composition and lymph node architecture.

Fig.S2: Proliferating T cells in Tx-LN gain a phenotype indicative for activated T cells.

Fig.S3: Gut-derived DC enter Tx-LN.

Acknowledgements

This work was supported by Deutsche Forschungsgemeinschaft Grants, SFB621-A1 to R.F. and SFB621-A11 to O.P. We thank Georg Behrens for providing MHC class II-deficient-mice and Immo Prinz, Andreas Krueger and William W. Agace for discussion and comments on the manuscript. The authors have no conflicting financial interests.

5.4. References

1. McDermott, M.R., and J. Bienenstock. 1979. Evidence for a common mucosal immunologic system. I. Migration of B immunoblasts into intestinal, respiratory, and genital tissues. *J. Immunol.* 122:1892-1898.
2. Cahill, R.N., D.C. Poskitt, D.C. Frost, and Z. Trnka. 1977. Two distinct pools of recirculating T lymphocytes: migratory characteristics of nodal and intestinal T lymphocytes. *J. Exp. Med.* 145:420-428.
3. Agace, W.W. 2006. Tissue-tropic effector T cells: generation and targeting opportunities. *Nat. Rev. Immunol.* 6:682-692.
4. Wagner, N., J. Lohler, E.J. Kunkel, K. Ley, E. Leung, G. Krissansen, K. Rajewsky, and W. Müller. 1996. Critical role for beta7 integrins in formation of the gut-associated lymphoid tissue. *Nature* 382:366-370.
5. Lefrancois, L., C.M. Parker, S. Olson, W. Muller, N. Wagner, M.P. Schon, and L. Puddington. 1999. The role of beta7 integrins in CD8 T cell trafficking during an antiviral immune response. *J. Exp. Med.* 189:1631-1638.
6. Ericsson, A., K. Kotarsky, M. Svensson, M. Sigvardsson, and W. Agace. 2006. Functional characterization of the CCL25 promoter in small intestinal epithelial cells suggests a regulatory role for caudal-related homeobox (Cdx) transcription factors. *J. Immunol.* 176:3642-3651.
7. Stenstad, H., M. Svensson, H. Cucak, K. Kotarsky, and W.W. Agace. 2007. Differential homing mechanisms regulate regionalized effector CD8alpha beta+ T cell accumulation within the small intestine. *Proc. Natl. Acad. Sci. U. S. A.* 104:10122-10127.
8. Austrup, F., D. Vestweber, E. Borges, M. Lohning, R. Brauer, U. Herz, H. Renz, R. Hallmann, A. Scheffold, A. Radbruch, and A. Hamann. 1997. P- and E-selectin mediate recruitment of T-helper-1 but not T-helper-2 cells into inflamed tissues. *Nature* 385:81-83.
9. Johansson-Lindbom, B., M. Svensson, M.A. Wurbel, B. Malissen, G. Marquez, and W. Agace. 2003. Selective generation of gut tropic T cells in gut-associated lymphoid tissue (GALT): requirement for GALT dendritic cells and adjuvant. *J. Exp. Med.* 198:963-969.

10. Mora, J.R., M.R. Bono, N. Manjunath, W. Weninger, L.L. Cavanagh, M. Roseblatt, and U.H. Von Andrian. 2003. Selective imprinting of gut-homing T cells by Peyer's patch dendritic cells. *Nature* 424:88-93.
11. Mora, J.R., G. Cheng, D. Picarella, M. Briskin, N. Buchanan, and U.H. von Andrian. 2005. Reciprocal and dynamic control of CD8 T cell homing by dendritic cells from skin- and gut-associated lymphoid tissues. *J. Exp. Med.* 201:303-316.
12. Dudda, J.C., J.C. Simon, and S. Martin. 2004. Dendritic cell immunization route determines CD8+ T cell trafficking to inflamed skin: role for tissue microenvironment and dendritic cells in establishment of T cell-homing subsets. *J. Immunol.* 172:857-863.
13. Iwata, M., A. Hirakiyama, Y. Eshima, H. Kagechika, C. Kato, and S.Y. Song. 2004. Retinoic acid imprints gut-homing specificity on T cells. *Immunity* 21:527-538.
14. Wolvers, D.A., C.J. Coenen-de Roo, R.E. Mebius, M.J. van der Cammen, F. Tirion, A.M. Miltenburg, and G. Kraal. 1999. Intranasally induced immunological tolerance is determined by characteristics of the draining lymph nodes: studies with OVA and human cartilage gp-39. *J. Immunol.* 162:1994-1998.
15. Ahrendt, M., Hammerschmidt, S., Pabst, O., Pabst, R., Bode, U. 2008. Stromal cells confer lymph node-specific properties by shaping a unique microenvironment influencing local immune responses. *J. Immunol.* 181: 1989-1907.
16. Worbs, T., U. Bode, S. Yan, M.W. Hoffmann, G. Hintzen, G. Bernhardt, R. Forster, and O. Pabst. 2006. Oral tolerance originates in the intestinal immune system and relies on antigen carriage by dendritic cells. *J. Exp. Med.* 203:519-527.
17. Pabst, O., G. Bernhardt, and R. Forster. 2007. The impact of cell-bound antigen transport on mucosal tolerance induction. *J. Leukoc. Biol.* 82:795-800.
18. Dudda, J.C., A. Lembo, E. Bachtanian, J. Huehn, C. Siewert, A. Hamann, E. Kremmer, R. Forster, and S.F. Martin. 2005. Dendritic cells govern induction and reprogramming of polarized tissue-selective homing receptor patterns of T cells: important roles for soluble factors and tissue microenvironments. *Eur. J. Immunol.* 35:1056-1065.

19. Coombes, J.L., K.R. Siddiqui, C.V. Arancibia-Carcamo, J. Hall, C.M. Sun, Y. Belkaid, and F. Powrie. 2007. A functionally specialized population of mucosal CD103⁺ DCs induces Foxp3⁺ regulatory T cells via a TGF-beta and retinoic acid-dependent mechanism. *J. Exp. Med.* 204:1757-1764.
20. Vermot, J., N. Messaddeq, K. Niederreither, A. Dierich, and P. Dolle. 2006. Rescue of morphogenetic defects and of retinoic acid signaling in retinaldehyde dehydrogenase 2 (Raldh2) mouse mutants by chimerism with wild-type cells. *Differentiation* 74:661-668.
21. Ohl, L., M. Mohaupt, N. Czeloth, G. Hintzen, Z. Kiafard, J. Zwirner, T. Blankenstein, G. Henning, and R. Forster. 2004. CCR7 governs skin dendritic cell migration under inflammatory and steady-state conditions. *Immunity* 21:279-288.
22. Mucida, D., Y. Park, G. Kim, O. Turovskaya, I. Scott, M. Kronenberg, and H. Cheroutre. 2007. Reciprocal TH17 and regulatory T cell differentiation mediated by retinoic acid. *Science* 317:256-260.
23. Sun, C.M., J.A. Hall, R.B. Blank, N. Bouladoux, M. Oukka, J.R. Mora, and Y. Belkaid. 2007. Small intestine lamina propria dendritic cells promote de novo generation of Foxp3 T reg cells via retinoic acid. *J. Exp. Med.* 204:1775-1785.
24. Benson, M.J., K. Pino-Lagos, M. Roseblatt, and R.J. Noelle. 2007. All-trans retinoic acid mediates enhanced T reg cell growth, differentiation, and gut homing in the face of high levels of co-stimulation. *J. Exp. Med.* 204:1765-1774.
25. Pabst, O., H. Herbrand, T. Worbs, M. Friedrichsen, S. Yan, M.W. Hoffmann, H. Korner, G. Bernhardt, R. Pabst, and R. Forster. 2005. Cryptopatches and isolated lymphoid follicles: dynamic lymphoid tissues dispensable for the generation of intraepithelial lymphocytes. *Eur. J. Immunol.* 35:98-107.
26. Czeloth, N., G. Bernhardt, F. Hofmann, H. Genth, and R. Forster. 2005. Sphingosine-1-phosphate mediates migration of mature dendritic cells. *J. Immunol.* 175:2960-2967.

5.5. Figures

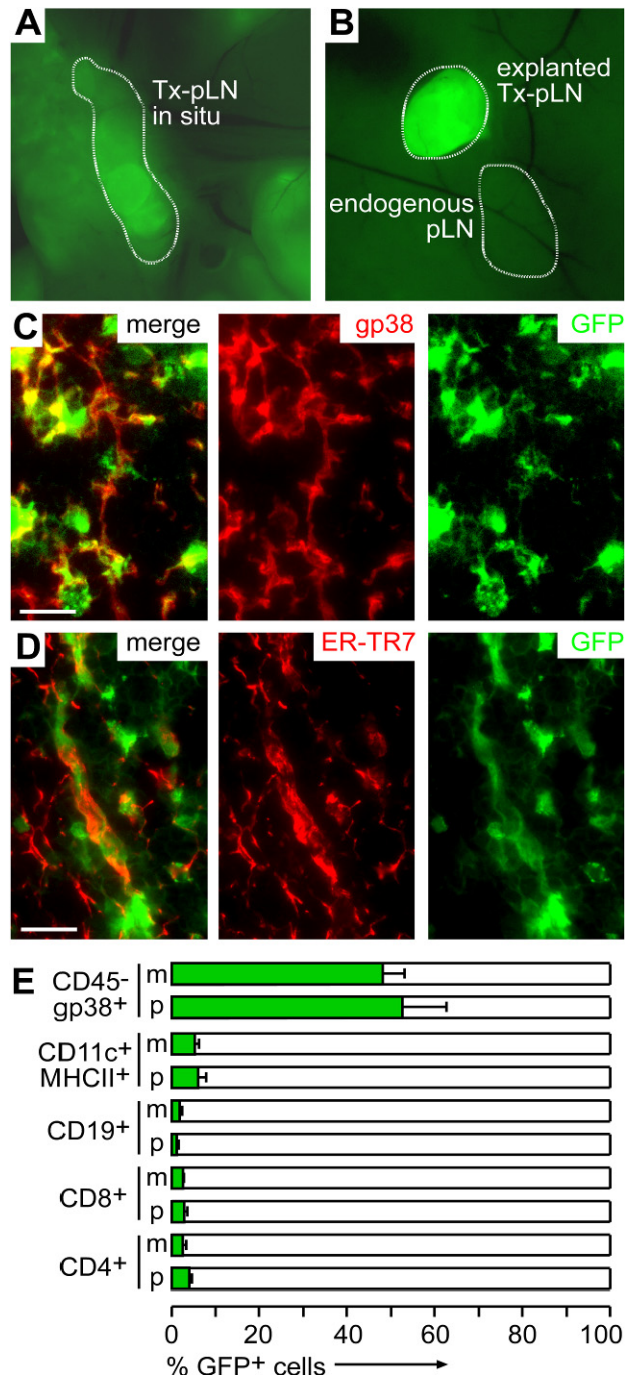


Fig.1: Transplantation of LN fragments yields chimeric lymph nodes

constituted by donor-derived stromal cells and recipient-derived hematopoietic cells.

(A) 8 weeks after transplantation transplanted pLN (Tx-pLN) and transplanted mLN (Tx-mLN) could be identified in situ by expression of EGFP. **(B)** To demonstrate low

auto-fluorescence in endogenous LN an excised Tx-pLN was placed besides the endogenous pLN. **(C, D)** Tx-pLN were analyzed by fluorescence microscopy for EGFP expression (green). Expression of gp38 **(C)** and ER-TR7 **(D)** is depicted in red. Comparable results were obtained for Tx-mLN (data not shown). Bar, 20 μ m. **(E)** Cells were isolated from Tx-LN and EGFP expression by stroma cells, DC, B and T cells was analyzed by flow cytometry (data are pooled from 4 mice analyzed in 2 experiments).

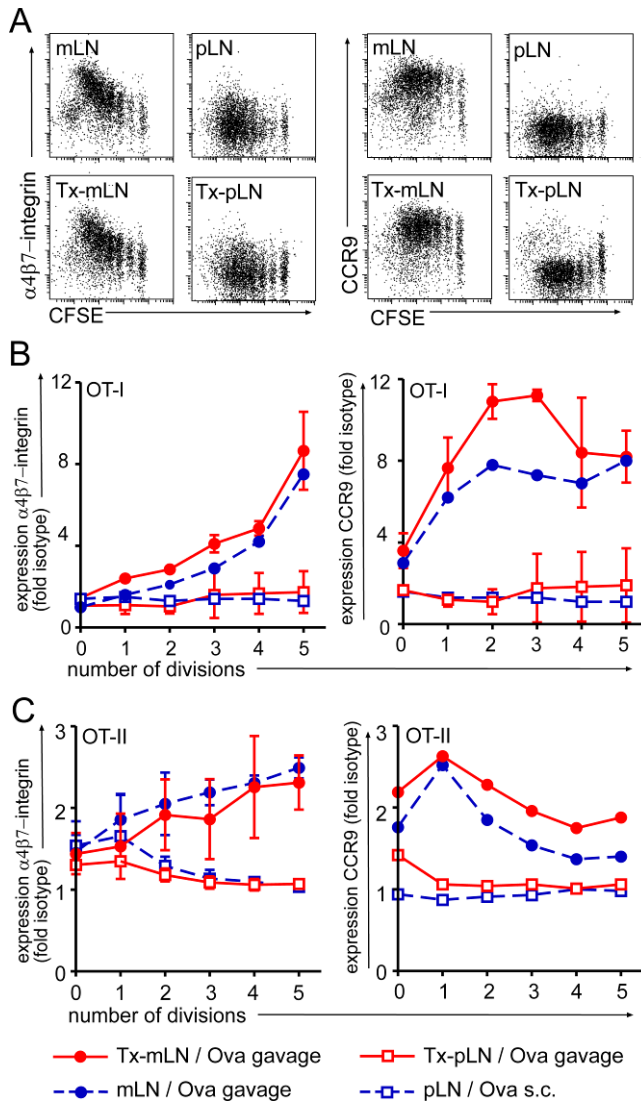


Fig.2: Heterotopic chimeric Tx-pLN but not orthotopic Tx-mLN fail to generate gut-homing T cells *in vivo*.

Cells isolated from OT-I or OT-II Ly5.1 mice were labelled with CFSE and adoptively transferred into mice that received Tx-pLN or Tx-mLN 8 weeks before. One day later, a single dose of Ova was applied orally or injected s.c. (A) Representative results obtained for $\alpha_4\beta_7$ -integrin and CCR9 expression by OT-I T cells (DAPI⁻ V α 2⁺V β 5⁺CD8⁺) activated in the mLN, Tx-mLN and Tx-pLN after oral antigen application and in pLN after s.c. injection of antigen. (B and C) Diagrams depict expression of $\alpha_4\beta_7$ -integrin and CCR9 as fold isotype control for OT-I T cells (DAPI⁻

$V\alpha 2^+V\beta 5^+CD8^+$) (**B**) and OT-II T cells ($DAPI^-Ly5.1^+V\beta 5^+CD4^+$) (**C**). All experiments have been performed at least 3 times with 2 or more mice per group.

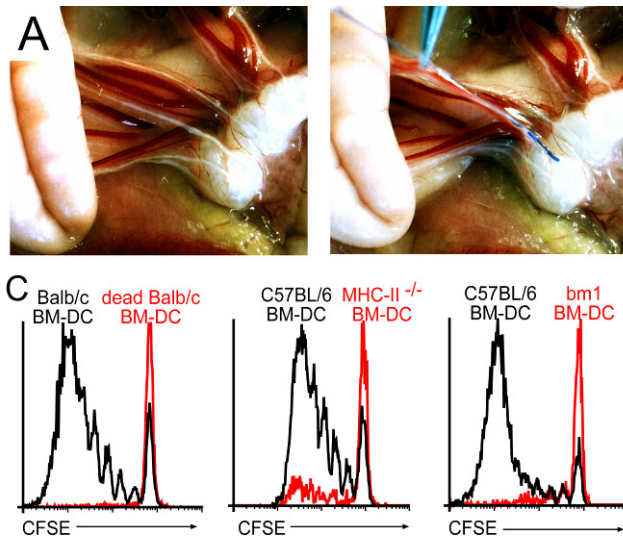


Fig.3: Injection of antigen loaded BM-DC into mLN afferent lymphatics induces proliferation of antigen specific T cells.

Recipient mice received CFSE labelled lymph node cells isolated from DO11.10, OT-I or OT-II donors. One day later these mice received oil by gavage one hour before surgery in order to visualize mLN afferent lymphatics and to facilitate intra lymphatic (i.l.) injection. The small intestine was exposed by surgery and mLN afferent lymphatics identified by their white colour (**A**). To demonstrate the method of i.l. injection approx. 0.3 μ l of blue dye were injected into a single lymph vessel (**B**). Following injection of two times 1 μ l into two separate vessels, as performed for routine injection of DC, the fluid spreads throughout the lymph node sinus (data not shown). (**C**) 10⁵ BM-DC were injected into two separate lymphatic vessels opening into the distal aspect of the mLN chain. Injection of Ova loaded DC (solid black line) but not heat killed DC (red line) induced proliferation of Ova specific DO11.10 T cells ($DAPI^-KJ16-26^+CD4^+$). BM-DC-derived from MHC class II-deficient mice induced only

marginal proliferation of OT-II cells. Similarly, DC derived from bone marrow of bm-1 mice, failed to activate OT-I T cells. All experiments have been performed at least 2 times with 3 or more mice per group.

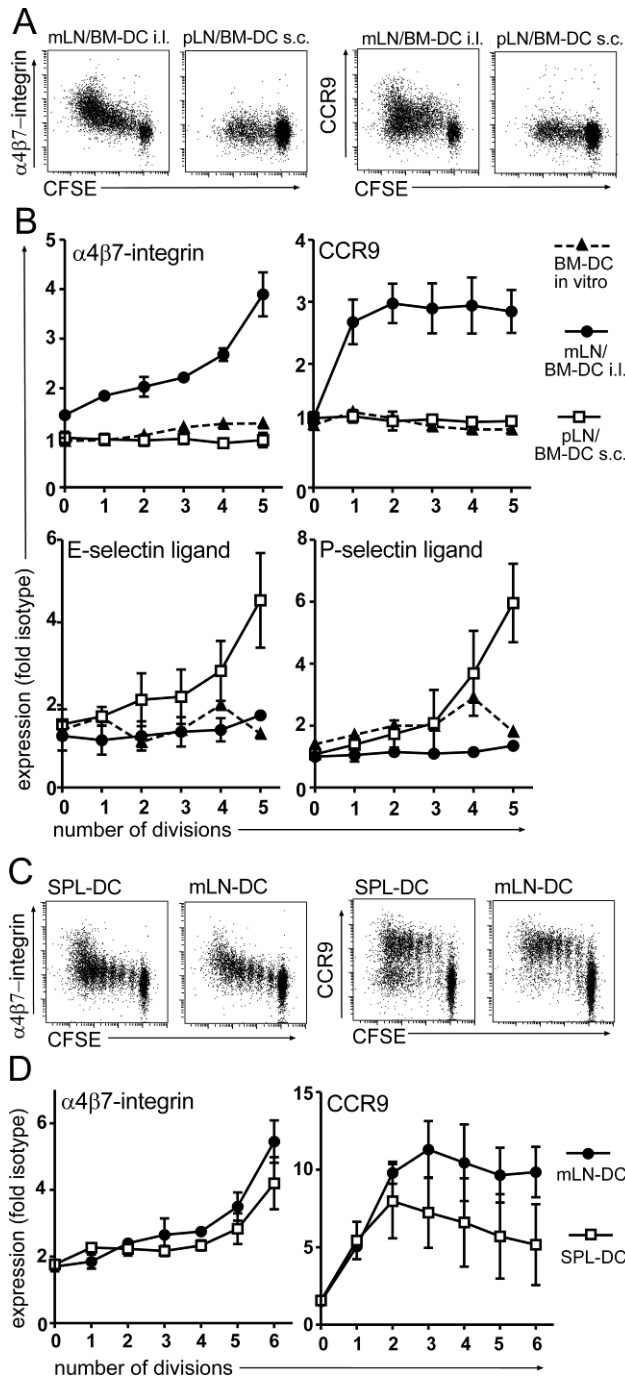


Fig.4: BM-DC and spleen-derived DC generate gut-homing T cells *in vivo* but not *in vitro*.

(A and B) DO11.10 cells were adoptively transferred into wild type recipients. One day later BM-DC were either injected i.i. or s.c. and proliferating DO11.10 T cells in the mLN and pLN were analyzed for expression of $\alpha 4\beta 7$ -integrin, CCR9, E- and P-selectin ligand as indicated. Moreover, expression of these molecules was assessed

following *in vitro* co-culture of antigen-loaded BM-DC with DO11.10 T cells at a 1:10 ratio. BM-DC injected into mLN afferent lymphatics but not injected s.c. or *in vitro* co-cultures led to the up-regulation of $\alpha_4\beta_7$ -integrin and CCR9 on proliferating T cells. Conversely, s.c. but not i.l. injection of BM-DC induced expression of E- and P-selectin ligand. (**C** and **D**) DC were isolated from mLN and spleen, loaded *in vitro* with Ova peptide and injected i.l. into recipient mice as described above. Spleen-derived DC that fail to up-regulate gut-homing factors after three days of co-culture with DO11.10 cells *in vitro* (data not shown) readily induced expression of $\alpha_4\beta_7$ -integrin and modest expression of CCR9 following i.l. injection *in vivo*. All experiments were performed at least 3 times with at least 2 mice per group.

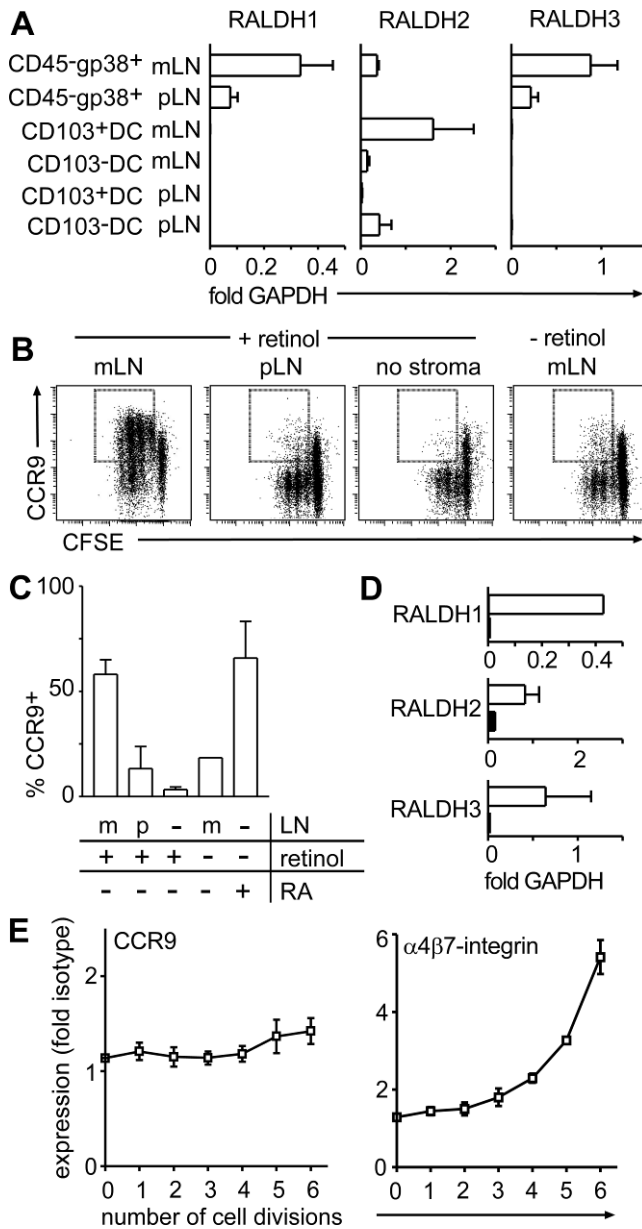
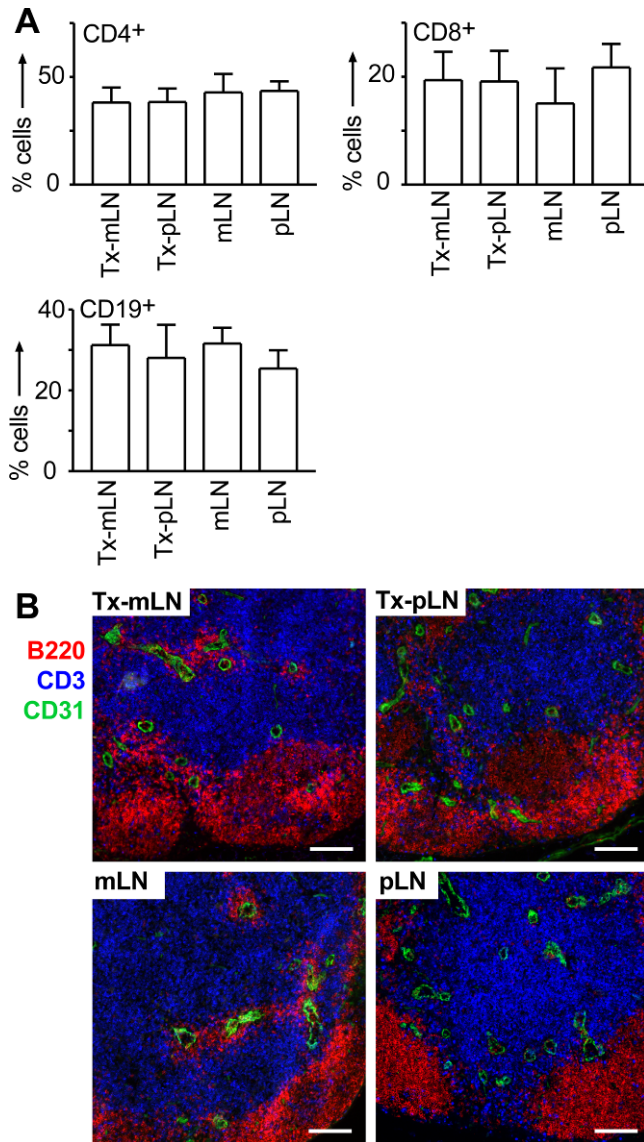


Fig.5: mLN- but not pLN-derived stroma cells express high levels of RALDH and support the induction of CCR9 on proliferating T cells.

(A) cDNA was prepared from sorted CD45⁻CD24⁻gp38⁺ stroma cells and CD103⁺ as well as CD103⁻ DC (CD11c⁺MHCII⁺) purified from pLN and mLN. Expression of RALDH1, 2 and 3 was assessed by real-time PCR and is depicted as fold expression compared to GAPDH. Data depict the mean and SD of 3-5 independent experiments measured in duplicates. (B, C) CFSE labelled OT-I cells were activated by anti-CD3/CD28 treatment in the presence of either pLN- or mLN-derived stroma cells with or without addition of retinol. Stroma cells were enriched by adherence and culture of

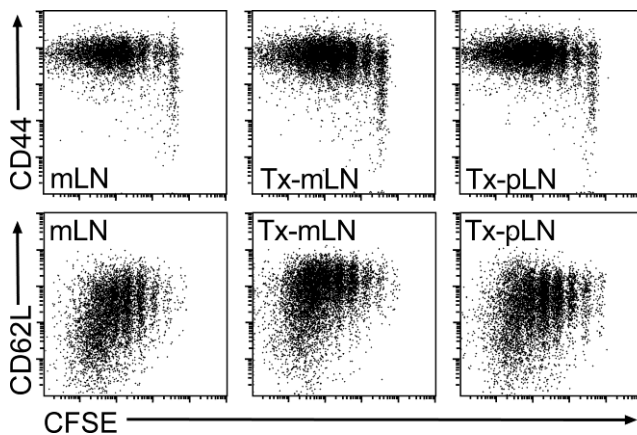
digested lymph node cell suspensions over 10 days. Data shown represent the mean and SD of three independent experiments. **(D)** cDNA was prepared from sorted CD45⁻CD24⁻gp38⁺ stroma cells (open bars) and CD103⁺ DC (closed bars) of CCR7-deficient mLN. Expression of RALDH1, 2 and 3 was assessed by real-time PCR. Bars depict the mean and SD of fold expression compared to GAPDH observed in two independent experiments. **(E)** CCR9 expression was analyzed following i.i. injection of antigen-loaded BM-DC into mLN afferent lymphatics of CCR7-deficient mice. In contrast to the situation in wild type mice, BM-DC failed to support the induction of CCR9 on T cells in CCR7-deficient mice. Expression of $\alpha_4\beta_7$ -integrin was not significantly affected. Results depict data obtained in one out of two experiments performed with 5 mice.



Supplementary Fig.1: Transplanted lymph nodes display normal cellular composition and lymph node architecture.

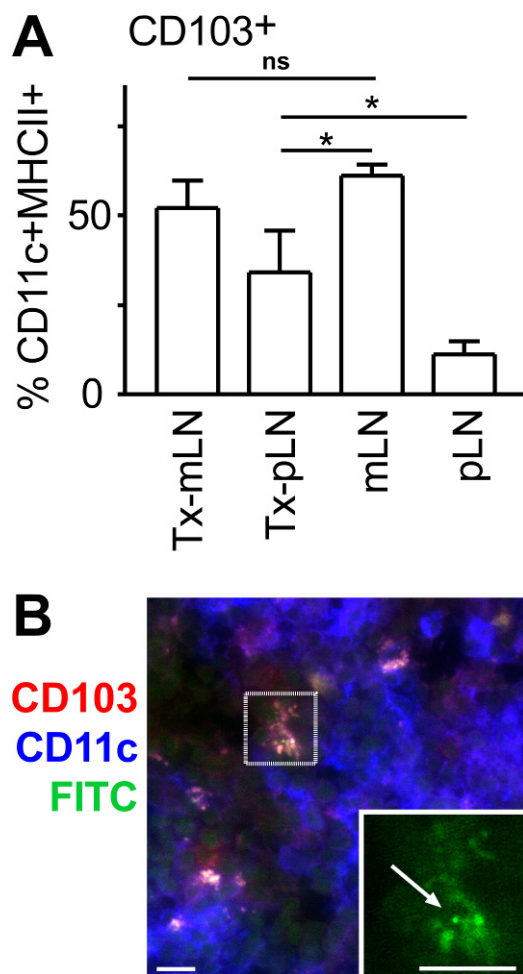
The endogenous mLN was excised and replaced by either pLN or mLN fragments isolated from wild type mice. 8-10 weeks after surgery transplanted pLN (Tx-pLN) and transplanted mLN (Tx-mLN) were isolated and their cellular composition and lymph node architecture analyzed. **(A)** Frequencies of CD4⁺ and CD8⁺ T cells as well as CD19⁺ B cells were comparable between Tx-mLN, Tx-pLN as well as mLN and pLN isolated from non-manipulated wild type mice. Data depict the mean and SD of 4 mice per group analyzed in 2 independent experiments. **(B)** Cryosections of Tx-LN and endogenous LN were stained with anti-B220 (red), anti-CD3 (blue) and anti-

CD31 (green). Tx-LN displayed normal segregation of T and B cell zones and unaltered numbers and distribution of CD31-expressing vessels. Tx-mLN as well as Tx-pLN showed slightly increased frequencies of germinal centres compared to LN isolated from non-manipulated mice (data not shown). Bar, 100 μ m.



Supplementary Fig.2: Proliferating T cells in transplanted lymph nodes gain a phenotype indicative for activated T cells.

10^7 CFSE-labelled lymph node cells isolated from OT-I mice were adoptively transferred into transplanted and non-transplanted recipients. One day after transfer mice received a single gavage of 50mg Ova and after three days expression of CD44 and CD62L was determined by flow cytometry. Proliferating T cells up-regulated CD44 in Tx-mLN, Tx-pLN and mLN to a similar extent and likewise showed no differences in CD62L regulation. Histograms are gated on DAPI⁻CD45.1⁺CD8⁺Va2⁺ cells. Dot plots are representative for five mice per group analyzed in two independent experiments.



Supplementary Fig.3: Gut-derived DC enter Tx-LN.

(A) CD103 is highly expressed by lamina propria DC and thus can be used as a surrogate marker for DC derived from the small intestine. The frequency of CD103⁺ DC among all CD11c⁺MHCII⁺ live cells (DAPI⁻CD45⁺) was determined by flow cytometry and compared to mLN and pLN isolated from non-manipulated mice. Tx-mLN and mLN showed high frequencies of CD103-expressing DC, indicative for their origin in the lamina propria. Notably also Tx-pLN accumulated increased numbers of CD103⁺ DC compared to endogenous pLN, suggesting that small intestinal lamina propria DC enter Tx-LN. Data depict the mean of four mice analyzed in two independent experiments. (B) Gut-derived DC were tracked by the use of fluorescent latex beads. On two consecutive days non-transplanted mice as well as mice receiving either pLN or mLN transplants received two doses of fluorescently labelled

latex beads (approx 10^{11} beads/gavage, bead diameter 200nm, Polysciences). 18h after the second gavage the mice received a single gavage of 10mg Cholera toxin (Sigma) and after one more day Tx-LN and mLN were embedded and examined for the presence of fluorescent latex beads. Immunofluorescent microscopy revealed latex beads in CD11c⁺ cells in Tx-pLN (shown in **(B)**) as well as Tx-mLN and mLN (data not shown). No obvious differences were noted in the frequency of bead-carrying cells between Tx-mLN and Tx-pLN. (at least 4 mice per group were analyzed in two experiments). Bead carrying DC in some but not all cases stained positive for CD103 indicating that beads-carrying DC might originate from Peyer's patches (mostly CD103⁻ DC) as well as the intestinal lamina propria (CD103⁺ DC). Moreover, we noted CD11c⁺CD103⁺ DC displaying prominent autofluorescence in the FITC channel in Tx-mLN, Tx-pLN and mLN but not pLN of non-manipulated mice. The presence of such highly autofluorescent DC is indicative for their gut origin. The inset in B shows a magnification of a bead-carrying CD11c⁺CD103⁺ cells displaying high autofluorescence in the FITC channel. Bar, 10 μ m.

6. The mesenteric lymph nodes exhibit a regulatory function in forming a Cholera-toxin specific IgA response in the intestine, whereas the spleen reacts systemically by specific IgM

Anika Hahn, Nadja Thiessen, Reinhard Pabst, Manuela Ahrendt, Ulrike Bode

Functional and Applied Anatomy, Hannover Medical School, Hannover, Germany

Running Title

Regulation of IgA responses by mesenteric lymph nodes

Keywords

Intestinal immune system; Spleen; mLN; IgA response; Rat

Abbreviations

BrdU-Bromodesoxyuridine; **CT**-cholera toxin; **GALT**-Gut associated lymphatic tissue; **mLN**- mesenteric lymph node; **PALS**- Periarteriolar lymphatic sheath; **PP**-Peyer's patch

Address correspondence to: Dr. Ulrike Bode; Anatomie II, OE 4120; Medizinische Hochschule Hannover; Carl-Neuberg-Str.1; 30625 Hannover, Germany; Phone: +49-511-532-2989; Fax: +49-511-532-2948; E-Mail: Bode.Ulrike@MH-Hannover.de

Abstract

Stimulation of the adaptive immune system in the gut is thought to be mainly initiated in the mesenteric lymph nodes (mLN) and results in an IgA secretion of plasma cells in the lamina propria. However, a detailed role of the mLN in the development of IgA immune responses is poorly understood. Thus, cholera toxin (CT) was applied in mLN resected and mLN bearing animals and the IgA response to CT in the gut lavage and serum was examined. CT-specific IgA antibodies and their producing cells in the intestine were increased in mLN resected rats. The mLN are therefore critical for the expansion of a specific IgA response.

When the mLN of rats are removed, the lymph from the gut flows directly into the blood, whereby the spleen becomes an important lymphoid organ to initiate immune responses. Therefore, a possible involvement of the spleen was examined after oral application of CT.

In the spleen of mLN resected animals proliferation was up-regulated forming germinal centres in the follicles. However, CT-specific IgM⁺ cells, but no IgA⁺ cells were documented. Additionally, the IgM producing marginal zone B cells were decreased after mLN resection, indicating a maturation and mobilization of these cells which leads to an increase of CT-specific IgM in the serum. Thus, the spleen is involved in the immune response against CT after mLN resection, leading to a mobilization and maturation of CT-specific IgM producing cells.

6.1. Introduction

A characteristic feature of the intestinal immune system is a preferential response in the form of producing IgA [1]. There are several ideas about the exact mechanism of plasma cell activation and IgA secretion. On the one hand antigens (Ag) are taken up by antigen-presenting cells (APC) and transported into the mLN [2-4], where CD4⁺ T-cells are activated and start to produce IL-4 and TGF- β . These cytokines lead to a B-cell switch from IgM to IgA [1]. On the other hand, antigens which are taken up by M-cells are presented in the Peyer's patches (PP), where B cell differentiation is also initiated. Afterwards the IgA plasma blasts migrate into the mLN where proliferation and hypermutation take place [5, 6]. The blasts are transported into the blood vessels via the thoracic duct and finally reach the lamina propria where they change into mature IgA-secreting plasma cells [5, 7, 8]. Thus, the mLN seem to be an important site for the development of IgA responses to intestinal antigens. Recently, we auto-transplanted lymph node fragments from peripheral sites (pLNtx) into the mesentery. These pLNtx regenerated, but retained their specific expression pattern (e.g. absence of CCR9, MAdCAM-1) [9, 10]. The pLNtx transplanted animals had a diminished specific IgA response against intestinal antigens, indicating the importance of the mLN-specific properties in an IgA response [9].

In addition, it became clear that the mLN are important for the induction of tolerance [11], as has been shown before for the immune responses to intestinal antigens [12].

In these studies the mLN were removed to define the functional relevance of the mLN. It is well known that lymphatic vessels are able to recover after resection of the mLN developing so-called pseudo-afferent lymphatics, guaranteeing the flow of lymph from the intestine via the thoracic duct into the blood [13, 14]. The mLN act as

a “firewall” against penetrating bacteria coming from the intestine [15]. Thus, the resection of the mLN in mice leads to an accumulation of bacteria in the spleen [12].

The spleen as an organ which is well connected to the blood system has two important functions. Firstly, the red pulp is responsible for removing senescent or defective erythrocytes from the blood. Secondly, the white pulp, as the lymphoid part of the organ, scans the blood for pathogens and is able to induce a specific IgM production as well as a cellular immune response [16]. The white pulp consists of different compartments including the T cell area, the PALS, the B cell enriched follicles and the marginal zone, in which B lymphocytes and macrophages are located. As the marginal zone is situated between the white and red pulp, it is the predominant site where antigens are taken up and initiation of an immune response against blood antigen takes place [17]. The importance of the spleen in defending the body against bacterial antigens is well characterized by observations of patients who had been splenectomised [18-20]. These patients have a high risk of fulminant infection and it is well known that the absence of the spleen leads to several changes in the presence and expression pattern of immune cells in other lymphoid organs [21]. Thus, the spleen plays a central role in the homeostasis of the immune system.

The aim of the present study was to further analyse the functional relevance of the mLN in forming specific IgA responses. A strong IgA response in the intestine can be induced by oral application of cholera toxin (CT), which is known as one of the most potent mucosal immunogens [9, 22-24]. CT is also used as an adjuvant [25]. In this study, the mLN of rats were removed and orally applied CT was used as an example of an immune response in the gut-associated lymphoid tissue (GALT). It was examined whether an adequate IgA immune response against CT could still be

induced. The present study clearly shows that this was not only successful, but that even more specific IgA antibodies were produced in the intestine in the absence of the mLN. Thus, the mLN do not seem to be predominantly the induction site, but exhibit a regulatory function in forming IgA responses.

Furthermore, regarding the fact that without mLN the next station of a circulating APC or soluble Ag is the spleen, the question was whether the spleen would take over the function of the mLN in the specific immune response to CT. The current data illustrate that the spleen is unable to induce an IgA response against orally applied CT, marginal zone B cells are mobilized after CT treatment. Thus, the spleen does not take over the function of the mLN, although this tissue is involved in the recruitment of immune cells fighting against intestinal antigens.

6.2. Material and Methods

Animals

Male rats of the standard inbred strain LEW/Ztm were maintained at the central animal laboratory of Hanover Medical School. Their average weight at the beginning of the experiment was 220- 250g and reached 300- 410g at the end. All animal experiments were performed in accordance with the institutional guidelines and had been approved by the Niedersächsisches Landesamt für Verbraucherschutz und Lebensmittelsicherheit (No. 33-42502-05/960).

Intestinal surgery and cholera administration

Under a combined anaesthesia of Ketamine (Gräub AG, Bern, Switzerland) and Domitor (Pfizer, Karlsruhe, Germany) the intestine was taken out of the peritoneum and replaced after washing with PBS (sham-resection= CT⁻mLN⁺). The mLN resection was performed by micro-dissection along the length of the superior mesenteric artery to the aortic root (CT⁻mLN⁻) [11].

To optimize the protocol to induce an immune response against orally applied antigens, after at least ten days recovery 100µg CT (Sigma, Munich, Germany) were given with a feeding needle under Isofluran anaesthesia to untreated animals on day 0 as a single dose and sacrificed on day 4 or 8. In addition, CT was applied on day 0 and day 14 and the animals were sacrificed on day 15, 17 or 19. To reveal alterations of CT-specific Ig in mLN resected animals compared to mLN bearing animals, we selected the time point, at which the B cell response is increased. Thus, the protocol also reported in [24] was most advantageous where two intragastric doses of CT were given on day 0 and 14 with analysis on day 19. Under these conditions IgA was

found at its highest level in the gut lavage, and a high increase of IgA⁺ cells in the mLN was detected (data not shown).

Therefore, the mLN bearing (CT⁺mLN⁺) and resected (CT⁺mLN⁻) animals were sacrificed on day 19. Before exsanguination 1 mg BrdU/100g body weight was given intravenously as a proliferation marker. One hour later the mLN, PP, spleen, intestine, axillary lymph nodes (axLN), blood and the bone marrow (BM) were removed and analysed (n=8-12).

In order to reveal remaining mLN and to illustrate the formation of the pseudo-afferent lymphatics some rats received Berlin Blue by injection into the subserosa of the intestine at the end of the experiment (data not shown) [9] .

Flow Cytometry

To analyse the memory B cells and marginal zone B cells in the spleen by flow cytometry, three colour staining was performed as previously described [21, 26]. Briefly, memory B cells were identified by a biotinylated anti-IgM mAb (Serotec, Oxford, GB) and an anti-IgD mAb (Ox7, identified by a phycoerythrin conjugated goat anti-mouse Ab, Serotec). Memory B cells were defined as cells with a high expression of IgM and a low expression of IgD [21]. Marginal zone B cells were detected by a biotinylated anti-IgM mAb (Serotec, Oxford, GB) and an anti-CD90 mAb (Ox7, FITC conjugated, Serotec). Marginal zone B cells are defined as IgM high⁽⁺⁺⁾ non migrating (CD90⁻) cells [21].

CT binding cells in cell suspensions of mLN, axLN, spleen, PP, BM and blood were analysed by incubating a blocking buffer enriched with 50% human serum to protect CT binding to GM1 gangliosides. Then, either B cells or IgA⁺ cells were detected by using mAb Mara1 (identified by a phycoerythrin conjugated goat anti- mouse Ab, Serotec). After washing biotinylated CT was incubated and visualized by an

incubation of PerCP conjugated streptavidine. About 1×10^6 cells of the respective cell suspensions were analysed using a FACSCanto (BD Biosciences, Heidelberg, Germany).

ELISA

Total IgA and CT-specific IgA/ IgM were measured in intestinal lavage and serum.

The small intestine was washed with 5 ml of special lavage buffer containing 0.1mg/ml trypsin inhibitor, 50mM EDTA, 0.1% BSA and PBS. The lavage was filtered once on ice and stored at -80°C .

The plates were coated with $0.1\mu\text{g/ml}$ CT (Sigma) in PBS overnight at 4°C . After washing, the plates were blocked with blocking buffer (BD Biosciences) and samples were added and incubated for 90 min at 37°C . After another period of washing, the detection Ab (biotinylated mouse anti-IgA/ biotinylated mouse anti-IgM; BD Biosciences) was added and later detected with horseradish-peroxidase (HRP; BD Biosciences), tetramethylbenzidine (TMB, BD Biosciences) and hydrogen peroxide (1:1) as substrate. The reaction was stopped with $2\text{N H}_2\text{SO}_4$ (Merck, Darmstadt, Germany) and the optical density was analysed in an ELISA-Reader (Bio-TEK Instruments GmbH, Bad Friedrichshall, Germany). Standard rat IgA and IgM (BD Biosciences) at subsequent declining concentrations was used to measure the concentration of the CT-specific IgA/IgM. In detail, the plates were coated with various concentrations of the IgA/IgM. Then, the procedure was carried out as described above and the concentration of CT-specific IgA/IgM was calculated as pg/ml by using the calibration line of standard rat IgA/IgM.

Immunohistology

For immunohistology mLN and spleen were frozen immediately in liquid nitrogen and 7µm thin cryostat sections were made. Proliferation and B-cell areas were detected with anti-BrdU (1:500, Sigma) and BM4013 (1:50, Acris; Hiddenhausen, Germany) respectively, as described before [27]. CT was detected by the Ab VCT (1:100, Biotrend, Köln, Germany).

IgA and IgM positive cells were detected by biotinylated Ab (Mara1, mAbs anti-IgM 1:1000, Serotec). While sections stained for IgM were directly fixed with -20°C methanol/acetone, the sections identifying IgA were blocked with the monoclonal Ab against IgA (Mara-1, 1:100, Serotec) before fixing because of soluble IgA. After one hour of incubation with either biotinylated Abs against IgA or IgM the sections were fixed again with 1% formaldehyde (Sigma) and 0.2% glutaraldehyde (Merck) and then conjugated with streptavidine-peroxidase (Dako, Hamburg, Germany).

Benzidine (Sigma) was used as substrate for the peroxylase.

Immunofluorescence histochemistry was performed according to standard protocols [11]. Briefly, sections were rehydrated in TBST (0.1 M Tris pH 7.5, 0.15 M NaCl, 0.1% Tween-20), pre-incubated with TBST containing 50% rat or mouse serum, incubated with the biotinylated CT and then stained with fluorescent dye-coupled streptavidine (Cy3) in 2.5% serum/TBST. To block the overall GM1-gangliosid binding, blocking buffers were used in the protocol. IgA⁺ cells were stained using the mAbs MARA-1 (Serotec), which was detected by the goat-anti-mouse Abs coupled with FITC (Invitrogen, Karlsruhe, Germany). Nuclei were visualized by 4',6-Diamidino-2-phenylindole (DAPI) staining (1µg/ml DAPI/TBST), and sections were mounted with Fluorescent Mounting Medium (Dako). Images were acquired using an Axiovert 200M microscope with Axiovision software (Carl Zeiss, Jena, Germany).

Data analysis

The software Graph pad Prism 4.0 (Graph pad Software Inc., San Diego, USA) was used for calculations, statistical analysis and graphs. Statistical differences were calculated in the unpaired t-test and are indicated by *, $P < 0.05$; **, $P < 0.01$; ***, $P < 0.001$.

6.3. Results

The mLN are involved in the induction of an IgA response against CT

First of all it was examined how the mLN might be involved in the immune response to CT.

After application of CT the number of proliferating centers increased in follicles that could be defined as secondary follicles (Fig1A). Quantification showed that before CT exposure about 30% of the follicles in the mLN were secondary follicles, while about 49% were counted after CT treatment (Fig.1A). In addition, detection of IgA⁺ cells in the mLN with or without CT administration showed that the number of IgA⁺ cells increased in the medulla after CT exposure (Fig.1B). Next, we questioned whether the IgA⁺ cells in the medulla were CT-specific. Thus, IgA⁺ cells and CT⁺ binding cells were identified via fluorescence staining. IgA⁺ CT binding double positive cells were seen after CT exposure, while the controls did not exhibited CT-specific IgA⁺ cells (Fig.1C). Taken together, these data show that the mLN are involved in the immune response induced by CT.

CT-specific IgA is detected in gut lavage and serum after CT exposition and is increased after resection of the mLN

Furthermore, it was evaluated whether orally applied CT could induce a detectable increase of the IgA titer and whether CT-specific IgA was developed during this experimental procedure.

Regarding the total amount of IgA the titer in the gut lavage and serum did not change (data not shown). Assuming that CT-specific IgA would only be a minority of the total IgA, the CT-specific IgA ELISA is definitely more important for comparing the efficiency of the immune response to the toxin. The level of CT-specific IgA in the gut

lavage after twofold application of the toxin was about 700pg/ml compared to a negligible amount in the control groups (Fig.2). In the serum there was an increase from an also negligible antibody level to about 70pg/ml after CT treatment (Fig.2). Surprisingly, when the mLN were resected the level of CT-specific IgA in the intestinal lavage significantly increased after CT administration. This increase was not seen in the serum (Fig.2).

CT binding IgA⁺ cells are increased in the lamina propria of the small intestine in resected animals

As CT-specific IgA was increased in the gut lavage of mLN resected animals it was analysed whether the presence of CT-specific IgA⁺ cells in the lamina propria of the small intestine differed between the mLN bearing and mLN resected animals.

Therefore, we used an application of CT on sections of the intestine to evaluate the CT-specific Ig bearing cells. As other cells also are able to bind CT, e.g. macrophages and DC, we focused on cells which are IgA⁺. Thus, IgA⁺ cells and CT binding cells were detected by immunofluorescence staining (Fig.3A).

Then, CT binding IgA⁺ cells were quantified and calculated as the percentage of IgA⁺ cells (Fig.3B). After CT administration in both the mLN bearing and mLN resected animals CT binding IgA⁺ cells were seen. Interestingly, in resected animals the percentage of CT binding IgA⁺ cells was increased to that in mLN bearing animals (Fig.3B). Thus, the presence of CT-specific IgA⁺ and its producing cells in the lamina propria of the small intestine were influenced by the mLN.

The spleen is involved in the immune response to orally applied CT

As it is known that resection of the mLN leads to generation of a pseudoafferent lymphatic duct which finally ends in the blood, it is likely that the first station of

antigen arrival is the spleen. Therefore, it was tested whether the spleen is involved in this observed phenomenon after mLN resection. Analysing the proliferating cells in the spleen it became clear that germinal centres increased after CT treatment and mLN resection (Fig.4A). In addition, there was an increase of developing germinal centres among the B cell follicles in the spleen when mLN resected animals were treated with CT compared to non-resected animals (Fig. 4B).

In serial sections with various stainings of an individual secondary follicle IgM⁺ cells (Fig.5) were seen in these structures containing CT, showing that germinal centres in the spleen produced CT-specific IgM⁺ cells (Fig.5A). In contrast to the mLN no IgA⁺ cells were detected in the germinal centres with only a few single ones in the red pulp which was not influenced by CT administration (Fig.5A).

The CT-specific IgM titer was also analyzed in non-resected and mLN resected animals. In the intestinal lavage no detectable titer was seen in any group (data not shown). However, in the serum in mLN resected animals a mean of about 2500 pg/ml was measured, while the CT-specific IgM titer moderately increased after CT administration in mLN bearing animals (Fig.5B). Thus, the data strongly indicate that the increase of developing germinal centres in the spleen after mLN resection leads to an increase of CT-specific IgM in the serum.

The number of marginal zone B cells is decreased after mLN resection

As the spleen is the first station where antigens arrive after mLN resection, we focussed on marginal zone B cells which are the most prominent cells for initial stimulation after antigen exposure. With respect to their function these cells mainly exhibit a long-lived, non-migrating (memory-like) phenotype [17]. Marginal zone B cells were identified by a staining of IgM and CD90 as previously described in [21]. In addition, memory B cells were analysed via their IgM and IgD expression (Fig.6A and

B). Compared to the control groups both memory B cells and marginal zone B cells were increased after CT administration. In contrast, after mLN resection and CT administration the number of these two cell populations was decreased (Fig.6A and B). In the PP marginal zone B cells were significantly increased after mLN resection (CT+mLN+: $4.9\pm 0.8\%$; CT+mLN-: $8.0\pm 0.6\%$ marginal zone B cells among lymphocytes, n=5).

Another important aspect was the appearance of an increased proliferation of marginal zone B cells at the border of the marginal zone and PALS after CT treatment and mLN resection (supplemental data).

Thus, the data show that orally applied CT, which arrives in the spleen via the pseudoafferent lymphatics and the blood stream, leads to a proliferation and mobilisation of marginal zone B cells, which probably accumulate in the PP.

B cell populations in other lymphoid organs are unaffected after CT administration and after mLN resection

As other lymphoid organs are also able to induce B cell maturation and carry IgM and IgA expressing B cells, the bone marrow, the blood, the axillary lymph node (axLN) and the PP were analysed with respect to the presence of CT-specific B cells. As Fig.7A shows, the major sites where CT binding cells develop are the mLN and also to a high extent the PP. Lymphoid organs such as the axLN, spleen, BM or the blood were only marginally involved in the induction of CT-specific B cells (Fig.7A).

Interestingly, after mLN resection no differences were observed in the presence of CT-specific B cells in these organs (Fig.7A).

Then, we focused on the number of CT-specific IgA⁺ B cells in PP, axLN, spleen, BM and blood. Fig.7B shows that the percentage of CT-specific cells among IgA⁺ cells did not change after mLN resection (Fig.7B).

6.4. Discussion

It is well accepted that intestinal antigens are taken up by dendritic cells (DC) or M cells and are either presented in the PP or in the mLN to induce an immune response [1, 2]. Some intestinal antigens solely enter the mLN via the afferent lymphatics, leading to an uptake directly in the mLN [28]. Thus, the mLN is an important site where antigens coming from the gut are filtered [12]. In addition, it was demonstrated in several studies that the mLN plays a central role in tolerance induction and responses to intestinal antigens. After initiation of an immune response antigen-specific IgA is produced in the lamina propria of the gut and transported to the gut lumen [11].

To investigate whether the mLN is involved in the induction and formation of intestinal IgA responses, CT was orally administered to untreated rats and compared to mLN resected rats. CT is known to be one of the most potent mucosal immunogens causing a strong intestinal secretory IgA response to CT after oral application [9, 22-24]. Recent studies have shown an increase of IgA B cell precursors in the GALT after CT feeding. It was concluded that up to 5% of all intestinal antibody-producing plasma cells could be CT-specific [23].

The current study shows that CT-specific IgA⁺ cells were present within the medulla of the mLN, a site where plasma cells are generally found [29]. In addition, by increasing developing germinal centres and IgA production the mLN are directly involved in the immune response against CT. It is generally accepted that activated B cells migrate from the induction site to the lamina propria of the intestine where they produce Ag-specific Ig [30]. Therefore, we analysed the CT-specific Ig in the intestinal lavage. We clearly showed that oral CT treatment results in the presence of CT-specific IgA. Surprisingly, in the absence of the mLN the presence of CT-specific

IgA was greatly enhanced compared with mLN. This was underlined by the observation that CT-specific IgA⁺ cells were also increased in the lamina propria of the intestine after mLN resection. Thus, the mLN is not predominantly the induction site of a CT-specific immune response, but is important for the expansion of the CT-specific reaction. In addition, animals which were transplanted with a pLN (pLNtx) instead of an mLN showed a decreased IgA response against CT, supporting the view that the mLN has a regulatory function in the maintenance of IgA.

To answer the question which other lymphoid tissue might be involved in the increased presence of CT-specific IgA in the absence of the mLN, the present study focused on the spleen. It is well known that lymphatic vessels are able to recover after resection of the mLN developing so-called pseudo-afferent lymphatics, guaranteeing the flow of lymph from the intestine via the thoracic duct into the blood [13, 14]. Thus, without the mLN the spleen is the organ where antigens coming from the intestine arrive.

The current study shows that after CT treatment germinal centres developed in the spleen and they were more prominent in the absence of the mLN. Thus, the spleen is able to react to Ag coming from the intestine in the presence but even more in the absence of mLN.

Our study clearly demonstrates that after CT application and resection of the mLN CT-specific IgM⁺ cells develop within the germinal centres. After resection of the mLN no induction of IgA was seen in the developing germinal centres, showing that the spleen is not able to compensate the role of the mLN.

It is known that marginal zone B cells are the prominent cells that interact with incoming Ag. In response to this stimulation these cells can proliferate quickly and develop into plasma cells which produce high amounts of IgM. Then, these cells migrate into the blood as plasma cells or as memory B cells [17, 31]. In this study a

decrease of both memory B cells and marginal zone B cells was found and CT-specific IgM was detected in the serum after CT treatment and mLN resection. Thus, the data indicate that marginal zone B cells are the prominent cells which recognize the CT first after mLN resection. This results in proliferation, maturation and mobilization of these cells, which leads to an increase of CT-specific IgM in the serum.

Furthermore, we also looked at the involvement of other lymphoid organs in the induction of CT-specific IgA response. Beside the mLN CT-binding cells were also detected in the PP. However, the proportion the CT-binding cells among IgA⁺ cells was lower in the PP compared to the mLN. After mLN resection there was no change in the presence of CT-specific IgA⁺ cells. Thus, the PP does not seem to be the site where the increased CT-specific IgA⁺ cells had come from and where CT-specific IgA was produced.

In addition, it can be excluded that other lymphoid organs are involved in the immune response against CT after its oral application, because the BM, axLN and the blood showed an increase of CT-specific IgA⁺ B cells.

In conclusion, by resecting the mLN and orally applying CT we clearly show that the mLN do not seem to be predominantly the induction site, but exhibit a regulatory function in forming an antigen-specific IgA response. In addition, by removing the “firewall” against antigens coming from the intestine, we showed that the spleen is confronted with these antigens. However, the spleen is not able to assume the role of the mLN in the production of specific IgA. In response to an increased antigen supply from the gut the spleen forms more germinal centres with IgM producers and mobilizes their marginal zone B cells which probably migrate into the lamina propria of the gut.

Acknowledgements

The comments of PD Dr. Oliver Pabst have been of great help. The authors also wish to thank Frauke Weidner and Melanie Paschy for excellent technical assistance and Sheila Fryk for correction of the English. The work was supported by the Deutsche Forschungsgemeinschaft (SFB621/ A10). There is no conflict of interest.

6.5. References

1. Brandtzaeg P. Induction of secretory immunity and memory at mucosal surfaces. *Vaccine* 2007;25:5467-84.
2. Iliev ID, Matteoli G, Rescigno M. The yin and yang of intestinal epithelial cells in controlling dendritic cell function. *J. Exp. Med.* 2007;204:2253-7.
3. Niedergang F, Kweon MN. New trends in antigen uptake in the gut mucosa. *Trends Microbiol.* 2005;13:485-90.
4. Mora JR, von Andrian UH. Differentiation and homing of IgA-secreting cells. *Mucosal Immunol.* 2008;1:96-109.
5. Fagarasan S, Honjo T. Regulation of IgA synthesis at mucosal surfaces. *Curr. Opin. Immunol.* 2004;16:277-83.
6. Suzuki K, Ha SA, Tsuji M, Fagarasan S. Intestinal IgA synthesis: a primitive form of adaptive immunity that regulates microbial communities in the gut. *Semin. Immunol.* 2007;19:127-35.
7. Macpherson AJ, McCoy KD, Johansen FE, Brandtzaeg P. The immune geography of IgA induction and function. *Mucosal Immunol.* 2008;1:11-22.
8. McGhee JR, Kunisawa J, Kiyono H. Gut lymphocyte migration: we are halfway 'home'. *Trends Immunol.* 2007;28:150-3.
9. Ahrendt M, Hammerschmidt SI, Pabst O, Pabst R, Bode U. Stromal cells confer lymph node-specific properties by shaping a unique microenvironment influencing local immune responses. *J. Immunol.* 2008;181:1898-907.
10. Hammerschmidt SI, Ahrendt M, Bode U, et al. Stromal mesenteric lymph node cells are essential for the generation of gut-homing T cells in vivo. *J. Exp. Med.* 2008;205:2483-90.

11. Worbs T, Bode U, Yan S, et al. Oral tolerance originates in the intestinal immune system and relies on antigen carriage by dendritic cells. *J. Exp. Med.* 2006;203:519-27.
12. Macpherson AJ, Uhr T. Induction of protective IgA by intestinal dendritic cells carrying commensal bacteria. *Science* 2004;303:1662-5.
13. Pabst R, Rothkotter HJ. Regeneration of autotransplanted lymph node fragments. *Cell Tissue Res.* 1988;251:597-601.
14. Rothkotter HJ, Pabst R. Autotransplantation of lymph node fragments. Structure and function of regenerated tissue. *Scand. J. Plast. Reconstr. Surg. Hand Surg.* 1990;24:101-5.
15. Macpherson AJ, Smith K. Mesenteric lymph nodes at the center of immune anatomy. *J. Exp. Med.* 2006;203:497-500.
16. Mebius RE, Kraal G. Structure and function of the spleen. *Nat. Rev. Immunol.* 2005;5:606-16.
17. Martin F, Kearney JF. Marginal-zone B cells. *Nat. Rev. Immunol.* 2002;2:323-35.
18. Mourtzoukou EG, Pappas G, Peppas G, Falagas ME. Vaccination of asplenic or hyposplenic adults. *Br. J. Surg.* 2008;95:273-80.
19. Pabst R, Westermann J, Rothkotter HJ. Immunoarchitecture of regenerated splenic and lymph node transplants. *Int. Rev. Cytol.* 1991;128:215-60.
20. Pabst R. Regeneration of autotransplanted splenic fragments: basic immunological and clinical relevance. *Clin. Exp. Immunol.* 1999;117:423-4.
21. Milicevic NM, Luettig B, Trautwein C, et al. Splenectomy of rats selectively reduces lymphocyte function-associated antigen 1 and intercellular adhesion molecule 1 expression on B-cell subsets in blood and lymph nodes. *Blood* 2001;98:3035-41.

22. Elson CO, Ealding W. Cholera toxin feeding did not induce oral tolerance in mice and abrogated oral tolerance to an unrelated protein antigen. *J. Immunol.* 1984;133:2892-7.
23. Elson CO, Ealding W. Generalized systemic and mucosal immunity in mice after mucosal stimulation with cholera toxin. *J. Immunol.* 1984;132:2736-41.
24. Schmucker DL, Daniels CK, Wang RK, Smith K. Mucosal immune response to cholera toxin in ageing rats. I. Antibody and antibody-containing cell response. *Immunology* 1988;64:691-5.
25. Lycke N. Targeted vaccine adjuvants based on modified cholera toxin. *Curr. Mol. Med.* 2005;5:591-7.
26. Bode U, Lorchner M, Ahrendt M, et al. Dendritic cell subsets in lymph nodes are characterized by the specific draining area and influence the phenotype and fate of primed T cells. *Immunology* 2008;123:480-90.
27. Bode U, Wonigeit K, Pabst R, Westermann J. The fate of activated T cells migrating through the body: rescue from apoptosis in the tissue of origin. *Eur. J. Immunol.* 1997;27:2087-93.
28. Sixt M, Kanazawa N, Selg M, et al. The conduit system transports soluble antigens from the afferent lymph to resident dendritic cells in the T cell area of the lymph node. *Immunity* 2005;22:19-29.
29. Willard-Mack CL. Normal structure, function, and histology of lymph nodes. *Toxicol. Pathol.* 2006;34:409-24.
30. Brandtzaeg P, Pabst R. Let's go mucosal: communication on slippery ground. *Trends Immunol.* 2004;25:570-7.
31. Batista FD, Harwood NE. The who, how and where of antigen presentation to B cells. *Nat. Rev. Immunol.* 2009;9:15-27.

6.6. Figures

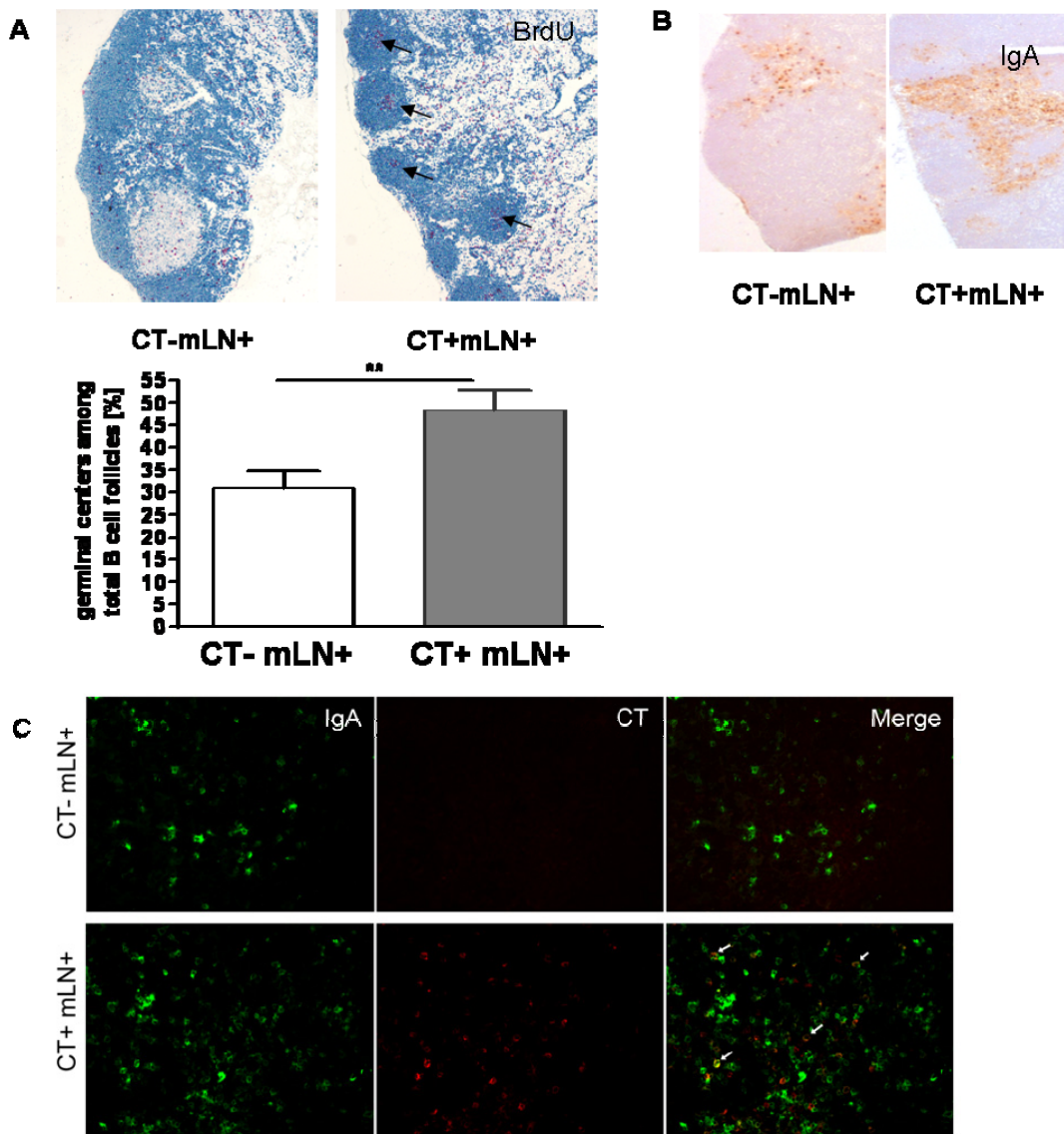


Fig.1: CT administration leads to an increase of secondary follicles and induces higher numbers of germinal centres and IgA in the mLN

A. Cryostat sections of the mLN of CT treated and non-treated animals were made. B cells (blue) and proliferating cells (BrdU⁺, red) were visualized to identify secondary follicles with developing germinal centres in the B cell area of the mLN (Magnification 20X). Secondary follicles were counted in the mLN of untreated and CT treated animals and the percentage of B cell follicles bearing secondary follicles (>28

proliferating cells/follicle) were calculated. Means and standard error are given (n=5-8) and significant differences in the unpaired t-test are indicated by **, P< 0.01. After CT exposure, secondary follicles were increased compared to untreated animals showing that the mLN is involved in the immune response to CT. **B.** After CT administration IgA⁺ cells were visualized in the mLN and compared to the situation without CT (IgA⁺, brown). Mainly in the medulla IgA⁺ cells were increased after CT treatment. The data are representative of 4-5 independent experiments.

C. Immunofluorescence stainings of the mLN after and without CT treatment were carried out with Abs against IgA (green) and with CT to evaluate CT binding cells (red) (20x, n=4-5). Dapi was used to visualize all cells. An increasing number of IgA⁺ CT binding cells were only seen after CT treatment in the medulla of the mLN, while without oral CT administration CT-specific IgA⁺ cells were not present.

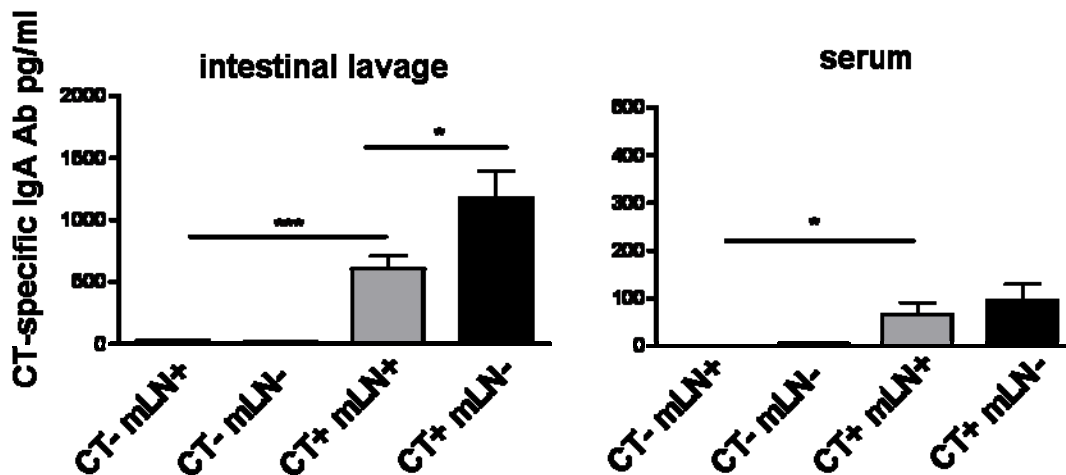


Fig.2: Resection of the mLN leads to an increase of CT-specific IgA in the gut lavage

The intestinal lavage and the serum of untreated and CT treated rats were sampled and analysed for their content of CT-specific IgA in the ELISA. Means and standard error are given (n=4-8) and significant differences in the unpaired t-test are indicated

by *, $P < 0.05$; ***, $P < 0.0001$. CT treatment has no effect on the total amount of IgA in gut lavage and serum while CT-specific IgA in the intestine increases in mLN bearing animals and even more in the mLN resected group.

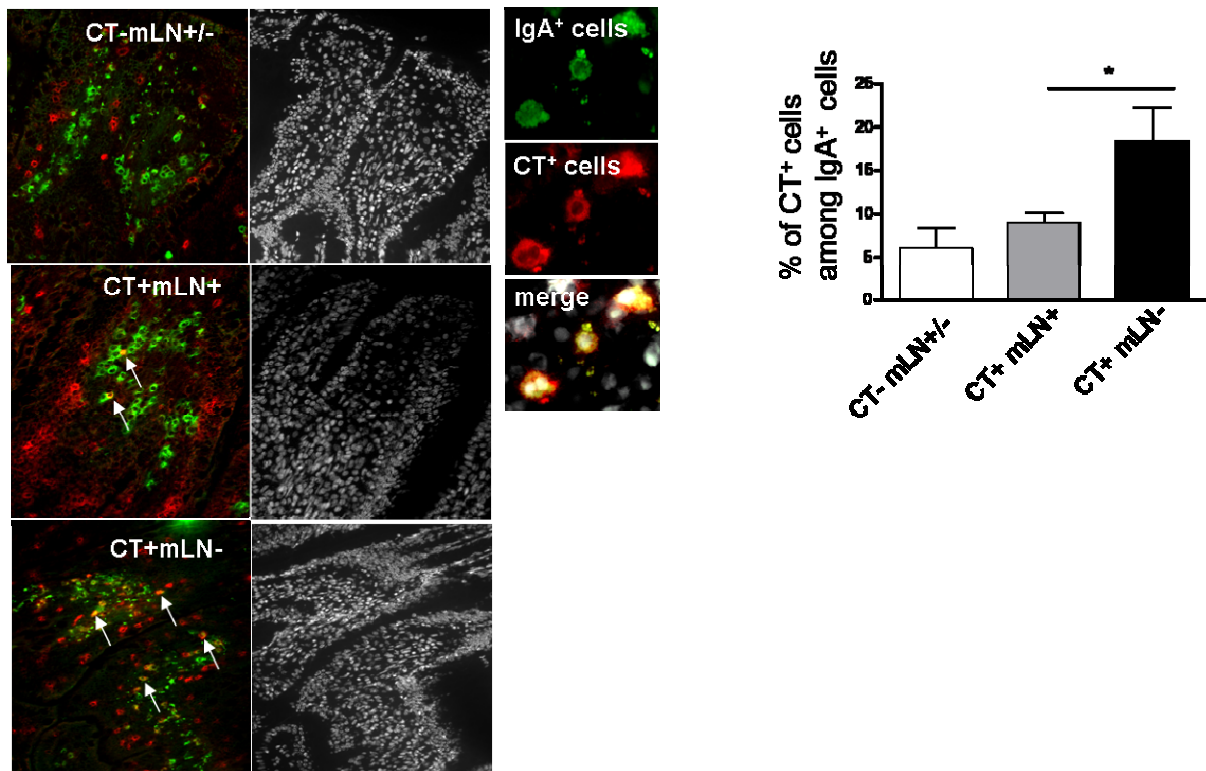


Fig.3: The number of CT-specific IgA⁺ cells in the lamina propria is increased after mLN resection

A. Immunofluorescence stainings of the lamina propria of the gut in mLN bearing and mLN resected rats, which had been treated with CT, were carried out with Abs against IgA (green) and with CT to evaluate CT binding cells (red) (20x, n=4-5). Dapi was used to visualize all cells (20x, white). CT binding IgA⁺ cells were seen in both groups, but even more in mLN resected animals. The right side shows the staining of each cell in detail (100x, green: B cells, CT binding cells: red and merge: CT⁺ IgA⁺ cells. **B.** Ten sections were visualized for each animal. IgA⁺ cells (30-100/section) and CT⁺ binding IgA⁺ cells (1-15/section) were counted on each section and

calculated as the percentage of CT binding IgA⁺ cells. Means and standard error are given and significant differences in the unpaired t-test are indicated by *, P< 0.05.

The data show that the percentage of CT binding IgA⁺ plasma cells in the lamina propria after mLN resection was increased to that of mLN bearing cells.

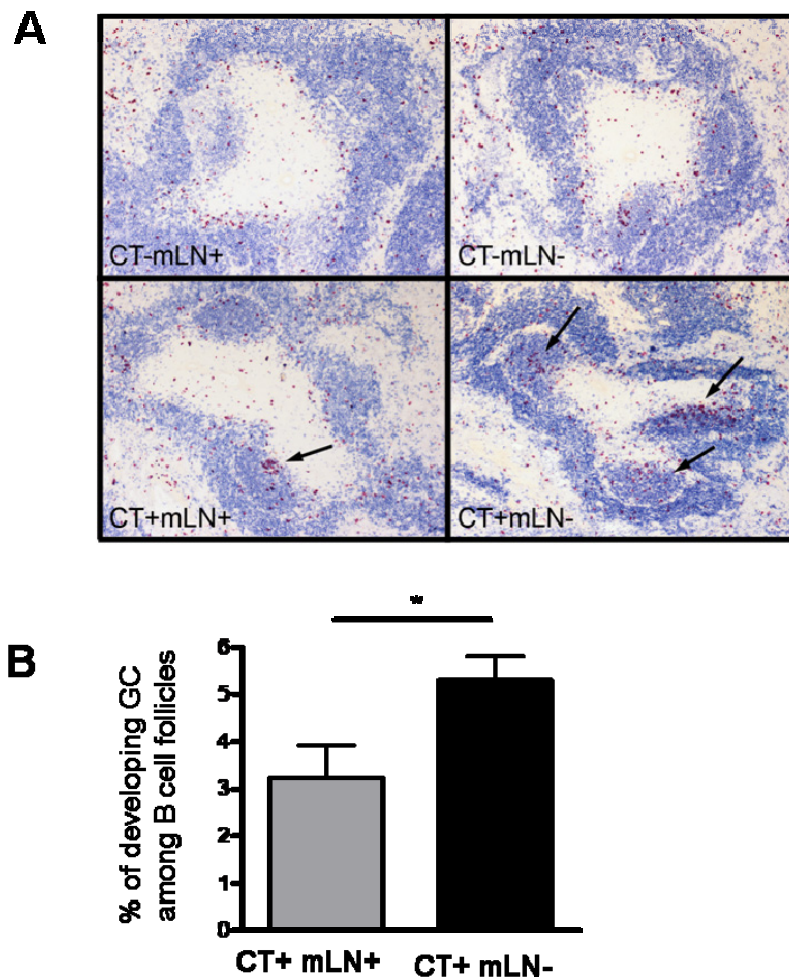


Fig.4: Oral CT treatment leads to an increase of germinal centres

A. The spleens of all four groups were analysed by immunohistology. Cryosections were stained with Abs against B cells (blue) and incorporated BrdU (red) (n=4-5) (Magnification 4X). CT administration and mLN resection lead to an amplification of germinal centres in the follicle of the spleen (arrows) (Magnification 4X). **B.** Germinal centres were counted in the spleen of mLN resected and mLN bearing animals after

and without CT treatment and the percentage of germinal centres (>28 proliferating cells/follicle) in the B cell follicles was calculated. Means and standard error are given (n=5-8) and significant differences in the unpaired t-test are indicated by *, P< 0.05. After CT administration germinal centres were increased in the mLN resected group compared to non-resected animals, showing that the spleen is involved in the immune response against CT in mLN resected animals.

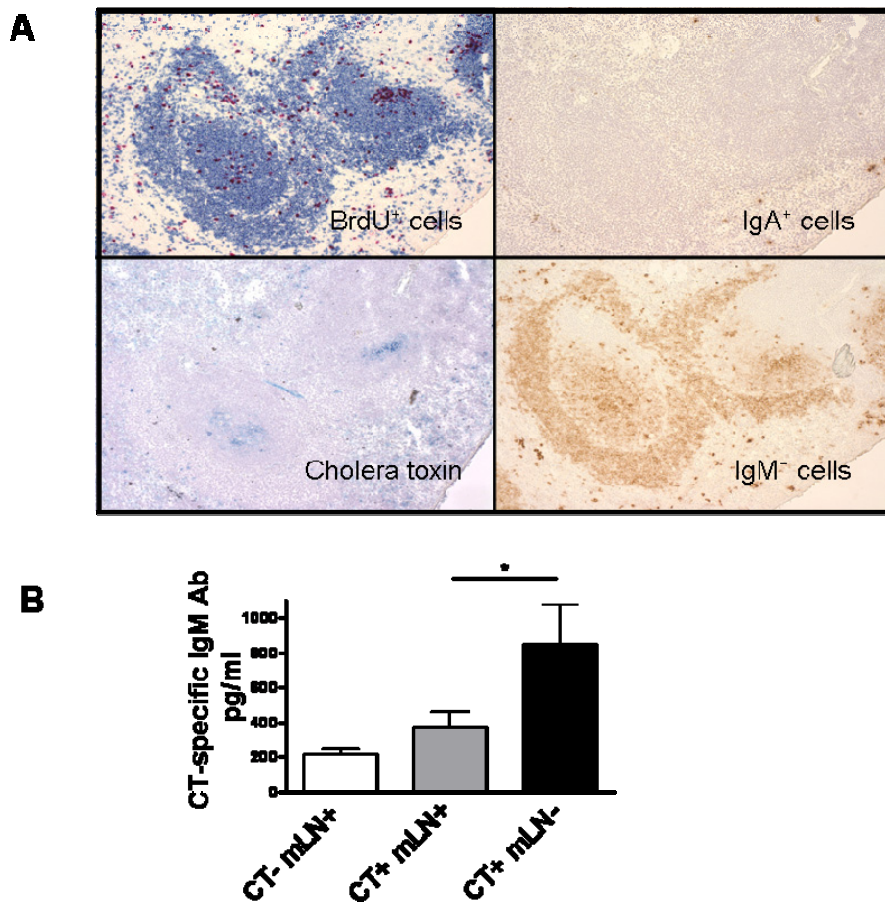


Fig.5: After CT treatment there are CT bearing germinal centres that induce IgM⁺ cells but no IgA⁺ cells

A. Using serial cryostat sections of the spleen of CT treated animals after mLN resection, first, B cells (blue) and proliferating cells (BrdU⁺, red) were visualized to identify developing germinal centres in the B cell follicles of the spleen. Additionally,

CT was identified in some of these germinal centres (blue). Then in germinal centres bearing CT IgA⁺ and IgM⁺ cells were identified. Germinal centres bearing CT were not involved in the IgA response to CT but to a great extent in the development of CT-specific IgM⁺ B cells (Magnification 10X). The data are representative of 4-5 independent experiments. **B.** In the serum there is an increase of CT specific IgM in mLN resected animals compared to mLN bearing rats, indicating that the increase of germinal centers in the spleen is responsible for the elevated levels of IgM in the serum. The serum of untreated and CT treated rats was sampled and analysed for the content of CT specific IgM in the ELISA. Means and standard error are given (n=4-8) and significant differences in the unpaired t-test are indicated by *, P< 0.05.

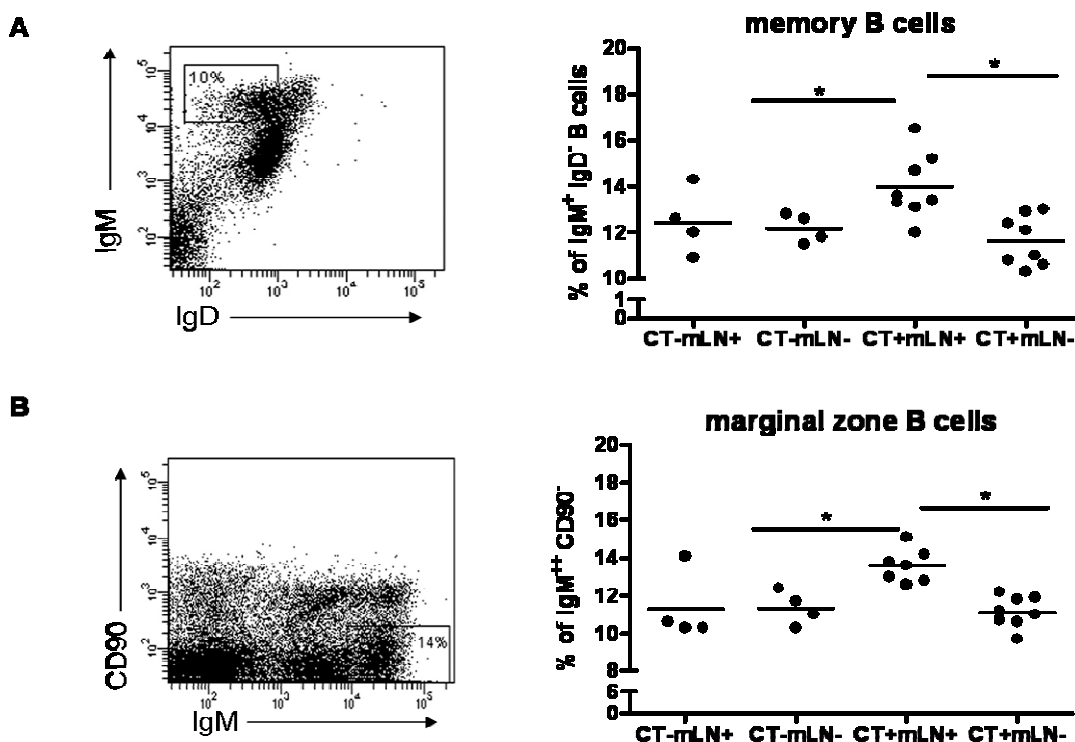


Fig.6: CT treatment and mLN resection leads to changes in the memory and marginal zone B cell population in the spleen

A. The memory B cells were identified by staining against IgM and IgD in the flow cytometry. The dot plot shows that memory B cells were gated by identifying IgM high expressing cells (y-axis) which are IgD^{low} (x-axis). These analyses were done in all groups. The dot plot shown is representative for 4-8 experiments. The graph shows the results of these analyses by flow cytometry. Single values are given and the means are indicated as a solid line. Significant differences in the unpaired t-test are indicated by *, P< 0.05. **B.** Marginal zone B cells were identified by staining against IgM and CD90 in the flow cytometry. The dot plot shows that marginal zone B cells were gated by identifying IgM high expressing cells (x-axis) which are CD90⁻ (y-axis). These analyses were done in all groups. The dot plot shown is representative for 4-8 experiments. The graph shows the results of these analyses by flow cytometry. Single values are given and the means are indicated as a solid line. Significant differences in the unpaired t-test are indicated by *, P< 0.05.

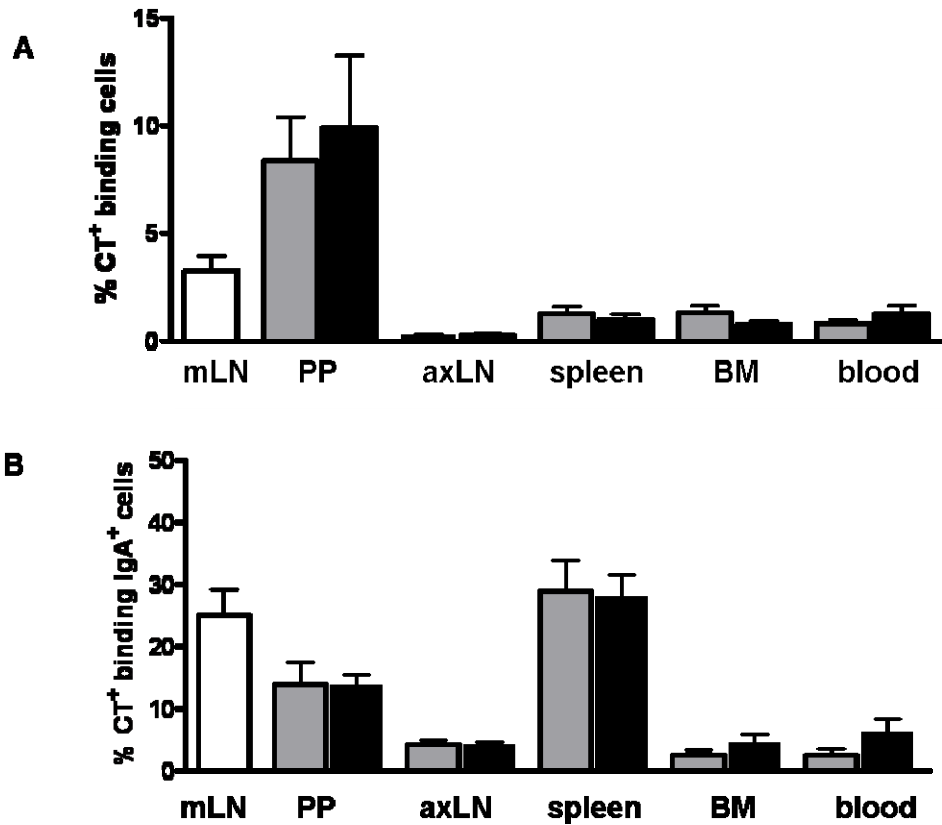
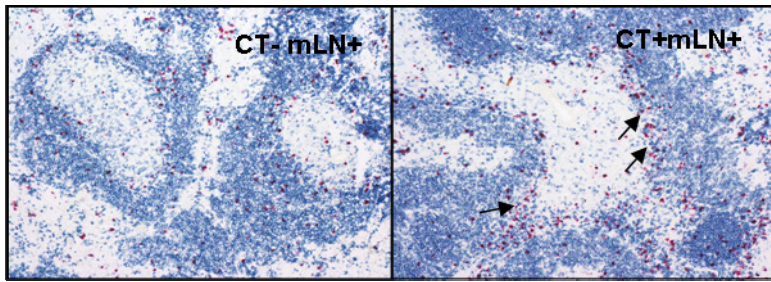


Fig.7: The resection of the mLN has no affect on CT-specific IgA⁺ B cells in secondary lymphoid organs.

After CT treatment the percentages of CT⁺ binding cells (**A**) and CT-specific IgA⁺ (**B**) cells of the PP, axLN, spleen, bone marrow (BM) and blood of mLN bearing and mLN resected animals were analysed by flow cytometry (n=5-8). Means and standard error are given and significant differences were tested in the unpaired t-test. CT treatment also affects the PP, although mLN resection has no effect on the presence of CT-specific IgA⁺ cells in the PP.



Supplemental data: After CT treatment bands of proliferating cells are formed at the border of the PALS and marginal zone

The spleens of all four groups were analysed by immunohistology. Cryosections were stained with Abs against B cells (blue) and incorporated BrdU (red) (n=4-5) (Magnification 4X). An increase of proliferating cells at the border of the PALS and marginal zone was seen after CT administration and mLN resection (arrows) (Magnification 4X).

7. Lymph node stromal cells strongly influence immune response suppression

Manuela Ahrendt*, Reinhard Pabst*, Ulrike Bode*

* Functional and Applied Anatomy, Hannover Medical School, Hannover, Germany

Running Title

Stromal cells influence the induction of oral tolerance

Keywords

Lymph node, tolerance, vaccination, stromal cells, transplantation

Abbreviations

mLN, mesenteric lymph nodes; **mLNtx**, transplanted mesenteric lymph nodes; **pLN**, peripheral lymph nodes; **pLNtx**, transplanted peripheral lymph nodes; **Tregs**, regulatory T cells

Address correspondence to: Dr. Ulrike Bode; Anatomie II, OE 4120; Medizinische Hochschule Hannover; Carl-Neuberg-Str.1; 30625 Hannover, Germany; Phone: +49-511-532-2989; Fax: +49-511-532-2948; E-Mail: Bode.Ulrike@MH-Hannover.de

The work was supported by the German Research Foundation (SFB621/A10).

Abstract

Many pathogens and food antigens are initially encountered in the gut, where the decision is made to mount an immune response or induce tolerance. To analyse the balance between tolerance and immunity, mesenteric or peripheral lymph node fragments (mLNtx or pLNtx) were transplanted into rats and mice. Recently we showed that only stromal cells survived after transplantation, and that they are able to affect T cell function and influence the IgA response after induction of an immune response. In the current study, oral tolerance was induced via OVA in transplanted animals. A reduced delayed-type hypersensitivity response (DTH) was detected in pLNtx compared to mLNtx animals. Reduced IL-10 expression, reduced numbers of regulatory T cells, and increased numbers of B cells were identified within the pLNtx fragments. The increase of B cells results in an immunoglobulin production different from mLNtx.

In pLNtx stromal cells survived after transplantation resulting in a regenerated lymph node which keeps their site-specific environment. Thus, stromal cells have a high impact creating this environment. This environment of pLNtx induces a tolerogenic phenotype not by T cell suppression but by B cell accumulation and antibody production.

7.1. Introduction

The gut, as an important component of the immune system, is the first site of contact and recognition for many antigens (Ag). At initial contact, the decision has to be made if the Ag is a harmless encounter, such as food, or a potentially harmful pathogen. When pathogens enter the gut, they may invade the gut lumen to encounter intramucosal lymphoid cells, or be recognized by luminal immune cells, thus initiating an immune response.

With both the initiation of an immune response as well as oral tolerance it has been shown that mucosal antigen-loaded DC migrate via afferent lymphatics into the mesenteric lymph node (mLN), and that this migration is CCR7 dependent [1, 2]. Within the mLN, DC present antigens to quiescent T cells. In the case of an immune response, this leads to clonal expansion of antigen specific T cells and their differentiation into T helper cells. T helper cells migrate towards the B cell areas [3], where Ag-specific T- and B cells meet at the border between the T- and B cell compartments [4]. Here, T cells activate B cells to proliferate, undergo Ig switching, and differentiate into specific Ab-producing cells. Gut-specific homing molecules, including CCR9, are upregulated and IgA is expressed. IgA⁺ B cells migrate back to the gut and differentiate into plasma cells, where they secrete Ag-specific IgA into the bowel lumen. Furthermore, some B cells differentiate into memory B cells, which are mobilised at subsequent presentation of the same Ag, allowing faster elimination. In contrast to this response, oral tolerance results from stimulation of regulatory cytokine-secreting T cells or anergy.

Over the years it has been suggested that suppressor CD8⁺ T cells are required for the induction of oral tolerance by cross-presentation with DC [5]. However, depletion of CD8⁺ T cells showed no effect on the induction of oral tolerance, whereas depletion of CD4⁺ T cells did prevent oral tolerance [6]. Later studies showed that CD4⁺ regulatory T cells (Tregs), which are FoxP3⁺, are involved in the induction of oral tolerance [5, 7]. It is generally accepted that feeding high- or low doses of Ag can induce oral tolerance. High doses of Ag result in T cell anergy and deletion whereas low doses of Ag favor tolerance induced by regulatory cells [5, 8]. Induction of oral tolerance by a high oral dose of Ag without previous Ag challenge results in the inability of T cells to proliferate and enter the B cell follicles, thus failing to induce B cell activation [9]. Later it was reported that Ag-tolerant T cells were able to migrate to the B cell area after challenge, but remained unable to support B cell proliferation [10]. It is suggested that these Ag-tolerant T cells are inefficient in cytokine production. This suppression of immune response is mLN-dependent, as shown in studies demonstrating that tolerance cannot be induced in the absence of mLN, but transfer of mLN T cells from Ag-tolerant mice results in the development of tolerance [11-13].

The mechanism by which the gastrointestinal immune system chooses to develop tolerance versus mounting an immune response is poorly understood, and is an area of active research.

In order to evaluate this phenomenon, we established a transplantation model in which peripheral lymph node fragments (pLNtx) were transplanted into the mesentery. We have shown previously that transplanted pLNtx regenerate within eight weeks. The LN compartment structure, which is destroyed during excision and transplantation, becomes rebuild and repopulated with host-derived immune cells.

Over the period of regeneration, donor stromal cells, which are the structural components of LN, survive. Expression of cytokines, including IL-4, was found to be comparable to the expression pattern of normal mLN; the expression of some cytokines is influenced by the area of lymphatic drainage, whereas other are LN-specific and are expressed by all mLN, e.g. IL-2 or CCR9. Stromal cells have been shown to be involved in the regulation of immune responses by upregulation of gut homing molecules and modulation of IgA concentration [14]. With this chimeric model we can now analyze the influence of stromal cells on site-specific LN variations, immune responses, and tolerance induction. In this study LNtx transplanted animals were fed with OVA to induce oral tolerance, which was measured by the delayed type hypersensitivity (DTH) response. We found that in pLNtx transplanted animals lower ear swelling could be identified together with a change in LN lymphocyte subset composition. We also determined a change in cytokine and Ig production in the pLNtx compared to mLNtx after oral tolerance induction. Thus, stromal cells seem to have a potent influence in the development of Ag-induced immune responses.

7.2. Material and Methods

Animals

Male LEW rats or female C57/Bl6 mice were bred at the central animal laboratory of Hannover Medical School and were used at a weight of 180-250g or 18-25g, respectively. All animal experiments were performed in accordance with the institutional guidelines and were approved by the Niedersächsisches Landesamt für Verbraucherschutz und Lebensmittelsicherheit (No 33-42502-05/960).

Intestinal surgery

As described earlier [14], mLN and pLN were isolated from LEW rats or C57/Bl6 mice and used as donors for LEW rats or C57/Bl6 mice, respectively. Under combined anesthesia with ketamine (Gräub AG, Bern, Switzerland) and xylazine 2% (Bayer Health Care, Leverkusen, Germany), the mLN of the small and large intestine of the host were removed and donor mLNtx or axillary and brachial (pLNtx) were transplanted into this region.

Immunofluorescence histochemistry

Staining was performed according to standard protocols [11]. Briefly, sections were rehydrated in TBST (0.1 M Tris (pH 7.5), 0.15 M NaCl, and 0.1% Tween 20), preincubated with TBST containing 5% rat or mouse serum, and stained with fluorescent dye-coupled Abs (CD45-APC, laminin-Cy3) in 2.5% serum/TBST. Nuclei were visualized by 4',6-diamidino-2-phenylindole staining (1 µg/ml 4',6-diamidino-2-phenylindole/ TBST), and sections were mounted with Fluorescent Mounting Medium (DakoCytomation). Images were analyzed and recorded using an Axiovert 200M microscope with Axiovision software (Zeiss).

Quantification of mRNA expression in mLNtx and pLNtx

Total RNA was isolated according to the manufacturer's protocol (Rneasy Kit, Qiagen, Hilden, Germany) and cDNA synthesis was performed with 50 mM oligo primer, 0.1 M DTT, 5x first strand buffer, 10mM dNTP, 35 U/ μ l Rnase inhibitor, and 200U/ μ l M-MLV reverse transcriptase (all obtained from Invitrogen, Karlsruhe, Germany) in a total volume of 20 μ l at 37°C for 50 min. With this cDNA quantitative real time PCR was performed using the QuantiTect SYBR-Green protocol from Qiagen. The primer sequences and amplicon sizes were as follows: CCR7 (5'-GTGTGCTTCTGCCAAGATGA -3' and 5'-CCACGAAGCAGATGACAGAA -3'; 154 bp), CCL19 (5'-AGACTGCTGCCTGTCTGTGA -3' and 5'-GCCTTTGTTCTTGGCAGAAG -3'; 205 bp), CCL21 (5'-ATGTGCAAACCCTGAGGAAG -3' and 5'-TCCTCTTGAGGGCTGTGTCT -3'; 178 bp), IL-10 (5'-ATGCTGCCTGCTCTTACTGACTG -3' and 5'-CCCAAGTAACCCTTAAAGTCCTGC -3'; 216 bp), IL-4 (5'-ACGAGGTCACAGGAGAAGGGA -3' and 5'-AGCCCTACAGACGAGCTCACTC -3'; 101 bp), and β -Actin (5'-AGCCATGTACGTAGCCATCC -3' and 5'-CTCTCAGCTGTGGTGGTGAA -3'; 228 bp; housekeeping gene).

Immune response induction

Purified cholera toxin (CT) (Sigma-Aldrich, St. Luis, USA) was administered as described previously [14, 15], with some modifications: Eight weeks after transplantation, LEW rats with mLNtx or pLNtx were immunized orally with 100 μ g of CT (in 0.5 ml of 0.01 M PBS containing 0.2% gelatin) on days 0 and 14. On day 19, the rats were exsanguinated and cell suspensions were made (n = 4–5). Analysis via flow cytometry was performed as described below.

Induction and measurement of DTH responses

Eight weeks after transplantation mice were fed with 25 mg ovalbumin (Grade III; Sigma-Aldrich) in 200µl PBS or PBS only as a control on day 0, 3, 6, and 8 by gavage. On day 16 mice were immunized by subcutaneously injection of 300µg ovalbumin (Grade VI; Sigma-Aldrich) in 200µl PBS/CFA emulsion. On day 34 mice were challenged by subcutaneous injection of 50µg ovalbumin (Grade VI) in 10 µl PBS into the right ear and PBS only into the left ear. Ear swelling was measured before challenge and 48h later. DTH response was calculated as described previously [11].

Antibodies for flow cytometry

Cell suspensions from mLNTx and pLNTx were made and 1×10^6 cells were incubated with biotinylated anti-rat R73 revealed by PerCP (T lymphocytes) and anti-rat mAb W3/25 APC conjugated (CD4⁺ T cells). B cells were characterized by anti-rat OX12; a PE-conjugated Ab was used as the secondary step. All antibodies were purchased from Serotec, Oxford, GB. Cells from mLNTx and pLNTx of C57BL/6 mice were examined in the same way and the following antibodies were used: anti-CD3-FITC, anti-B220-FITC (both kindly provided by R. Förster, Hannover, Germany), anti-CD4-APC, anti-CD25-PE (both acquired from Serotec), and anti-FoxP3-FITC (eBiosciences, San Diego, USA). All FACS analyses were performed on a FACSCanto. Isotype matched mAb served as controls.

Serum ELISA

ELISA was performed using the mouse immunoglobulin isotyping ELISA Kit (BD Biosciences, San Diego, USA). Samples were diluted at a concentration of 1:2000.

The optical density was analyzed in an ELISA-Reader (Bio-TEK Instruments GmbH, Bad Friedrichshall, Germany).

Data analysis

Calculations, statistical analysis, and graphs were performed with Graphpad Prism 4.0 (Graphpad Software Inc., San Diego, USA).

7.3. Results

Stromal cells survive after transplantation of LNtx fragments

The mLN of wt mice were removed and mLN or pLN fragments (mLNtx or pLNtx) from EGFP⁺ mice were transplanted into this region. Eight weeks after transplantation mLNtx or pLNtx fragments were removed and analyzed.

Hematopoietic cells were detected by staining with anti-CD45 (Fig.1A-C). CD45⁺ cells were observed in both transplanted LN (LNtx) but the majority were negative for GFP. Thus, immune cells in the LNtx are host derived cells which migrated into the LNtx. Within both LNtx fragments GFP⁺ cells were detected and identified as stromal cells, building the backbone of the LN, by positive staining with laminin, demonstrating that host stromal cells survived during regeneration (Fig.1D-F).

Expression of CCR7 and its ligands, CCL19 and CCL21, is normal in LNtx

The presence of CCR7 and its ligands CCL19 and CCL21 were analyzed in transplanted LNtx fragments in order to detect the migration capacity of immune cells. Via real time polymerase chain reaction (PCR), expression of CCR7 in mLNtx and pLNtx fragments was found to be similar to that in control mLN (Fig.2A). The ligands CCL21 and CCL19 were also expressed to the same degree in LNtx in comparison to mLN control (Fig.2B, C). Therefore, the regenerated transplanted LN is comparable to a normal LN based on expression of CCR7 and its ligands and also by immune cell distribution.

Transplantation of pLNtx produced less ear swelling after tolerance induction

One function of the mLN is the induction of oral tolerance. After LN regeneration, transplanted mice were fed with OVA several times to induce tolerance. Tolerance

induction was evaluated by the DTH response. The DTH reaction has been well characterized as an influx of immune cells and resultant swelling at the Ag injection site [16, 17]. Control animals as well as LNtx mice, fed with PBS, showed a high DTH response (ear swelling) after immunization and challenge with OVA; in contrast, OVA fed animals showed reduced ear swelling. Surprisingly, in pLNtx animals a lower DTH response was found than in mLNtx (Fig.3). These results demonstrate that LNtx are able to induce immune tolerance. Furthermore, pLNtx transplanted animals seem to be more sufficient at inducing oral tolerance than mLNtx.

A different cellular composition was found in pLNtx compared to mLNtx

LNtx were analyzed after tolerance induction to determine their composite cell subsets. It was found that mLNtx fragments showed similar cell subsets compared to control mLN, whereas pLNtx showed diminished T cell numbers and fewer CD4⁺ T cells (Fig.4A). By contrast, more B cells could be identified in pLNtx-transplanted animals (Fig.4A). The same proportion of decreased T cells and increased B cell numbers were found after induction of an immune response by Cholera toxin (CT) administration in pLNtx compared to mLNtx animals (Fig.4B).

Furthermore, we analyzed the LNtx fragments and control LN for the presence of CD4⁺ FoxP3⁺ Tregs. Previous analysis demonstrated that CD4⁺ Tregs are responsible for the induction of oral tolerance [5, 7]. These cells were first identified by their secretion of inhibitory cytokines such as IL-10 and TGF- β [18, 19]. In mLNtx and control LN we found comparable induction of FoxP3⁺ Tregs (data not shown). In pLNtx we detected reduced numbers of FoxP3⁺ Tregs and also reduced expression of IL-10 mRNA (Fig.5A-C).

Th1 cytokine-induced immunoglobulins were found in pLNtx

The mLN were shown to induce a prominent Th2 immune responses by producing IL-4 and TGF- β whereas pLN produce a stronger Th1 response via cytokines such as IFN γ [20]. LNtx fragments from Ag-tolerant mice were removed and mRNA was isolated to determine the expression pattern of Th1 and Th2 cytokines. The expression of Th2-specific cytokine mRNA, including IL-4, was found to be higher in mLNtx compared to pLNtx (Fig.6A). Furthermore cytokines were shown to manipulate B cell class switching from IgM to other Ig isotypes. Typical Th2 cytokines are able to induce class switch to IgG₁ or IgG_{2b}, while IL-2 and IFN γ are involved in the class switch to IgG_{2a} and IgG₃ [21-24]. We analyzed the serum of Ag-tolerant transplanted mice for Ig subclasses. In pLNtx high levels of λ light chain Ab were observed in the serum, whereas in mLNtx or mLN control no increased Ab production was detectable. Furthermore, reduced IgG_{2b} levels but increased IgG₃ were found in pLNtx Ab-tolerant mice compared to mLNtx (Fig.6B). Nevertheless, these data indicate that within pLNtx a different and increased antibody induction takes place after tolerance induction compared to mLNtx.

7.4. Discussion

In the current study GFP⁺ lymph node fragments were transplanted into the mesentery of mice and after regeneration of these transplanted LN fragments (LNtx) the majority of GFP⁺ hematopoietic cells were replaced by GFP⁻ recipient cells. However, non-hematopoietic cells, including stromal cells were found to remain within the LNtx. Thus, LNtx recipient immune cells arriving by afferent lymphatics or cardiovascular circulation were replaced by donor lymphoid cells. By contrast, stromal cells from the donor survived and provide the structural support for the transplanted LN.

We previously showed that LN implanted from the periphery into the mesentery consists of both migrating immune cells and resident stromal cells building the backbone of the LN. When a peripheral LN was implanted into the mesentery, the immune cells disappeared from the transplanted LN, but the skeletal backbone survived after transplantation. We were able to show the survival of stromal cells after LN transplantation by staining GFP⁺ cells with the stromal cell markers gp38 and ERTR7 [14, 25]. Hence, this leads to the situation that a regenerated pLN despite being perfused by the gut still has the lymph node specific properties of a pLN. Stromal cells were not only shown to build the backbone of the LN, furthermore, these cells were identified to support the survival of immune cells via IL-7 and BAFF [26, 27], and seem to express CCL19 and CCL21, which are important chemokines for the migration of immune cells into and within the LN [28, 29]. Their receptor, CCR7, is found on lymphocytes and DC, and is reported to have an important role in the migration of immune cells into secondary lymphoid organs and positioning within the various LN compartments [2, 30]. Furthermore, it was reported that in CCR7-deficient mice oral tolerance cannot be induced [11]. Therefore, the normal

expression pattern of these chemokines is important for the migration of immune cells and thus for triggering oral tolerance. In the present study equal mRNA expression of these chemokines was found in control LN as well as mLNTx or pLNTx transplanted fragments. This chemokine pattern suggested a normal migration capacity, which was supported by the finding that lymphocytes and DC were detected in normal numbers within the LNTx [14]. However, differences between mLNTx and pLNTx were found in the LN specific expression pattern of cytokines including IL-4 and chemokines including CCR9 [14]. With this chimeric model of regenerated LN with survived stromal cells, replaced immune cells, normal migration capacity and remained LN-specific generation of tissue tropism we are now able to analyse the importance of stromal cells for the induction of immune responses or oral tolerance. In order to generate oral tolerance, previous studies showed that CD4⁺ cells must be presented Ag by antigen presenting cells and that there is no reduction in the DTH response after depletion of CD4⁺ cells [6, 31]. It was also shown that Ag-tolerant T cells are unable to induce B cell activation and Ab production [9]. Previous analysis demonstrated that CD4⁺ Tregs are responsible for the induction of oral tolerance [5, 7]. These cells were first identified by their secretion of inhibitory cytokines such as IL-10 and TGF- β [18, 19]. Secretion of these cytokines enables Tregs to suppress effector T cell proliferation and B cell Ig production [32]. In our study, we showed that FoxP3⁺ Tregs and IL-10 expression levels were diminished in animals transplanted with pLNTx, whereby the DTH response was lower than in mLNTx animals. However, in these pLNTx animals a humoral response was triggered followed by a different Ig pattern compared to mLNTx animals. Thus, pLNTx transplanted animals with reduced levels of Tregs and induction of the humoral response seem to be more sufficient at inducing oral tolerance than mLNTx.

FoxP3⁺ Tregs were previously shown to be induced by mucosal DC via retinoic acid

(RA) [33-35]. We have shown previously that in the LNtx similar DC subsets are present compared to control mLN. Gut specific CD103⁺ DC arriving via afferent lymphatics into the LNtx could be identified in pLNtx as well as mLNtx. However, in pLNtx less RALDH2 mRNA expression was observed [14]. This enzyme was shown to be produced by gut CD103⁺ DC and to be necessary for the production of RA [36]. Analyzing the stromal cells of mLN and pLN, mRNA of RALDH2 was found only in the mLN [25]. Therefore, stromal cells seem to be able to effect host immune cells by their RALDH2 production. Furthermore, stromal cells appear to cooperate with incoming DC in order to build a site-specific expression pattern via downregulation of RALDH2. Thus, the reduced number of FoxP3⁺ Tregs and the decreased expression of IL-10 in pLNtx animals seem to originate from this lymph node specific environment including RALDH2. Furthermore, this situation results in the non-suppression of B cells, which is in turn triggered by stromal cells.

The mLN were shown to induce a prominent Th2 immune responses by producing IL-4 and TGF- β whereas pLN produce a stronger Th1 response via cytokines such as IFN γ [20]. Previously we showed that pLNtx retain their expression pattern, exhibiting higher levels of IL-2 and IFN γ after transplantation [14]. Furthermore, cytokines were shown to manipulate B cell class switching from IgM to other Ig isotypes. Typical Th2 cytokines are able to induce class switch to IgG₁ or IgG_{2b}, while IL-2 and IFN γ are involved in the class switch to IgG_{2a} and IgG₃ [21-24]. Also, Tregs have been shown to initiate a switch from IgM to IgA, thus inhibiting the production of IgG₁ after tolerance induction [5, 37, 38]. In line with these findings, we found after oral tolerance induction in mLNtx higher IL-4 mRNA expression and an Ig subclass pattern different from pLNtx. Additionally, Ig isotypes typical for cytokines induces by pLN were detected in the serum of pLNtx transplanted animals.

Furthermore, higher levels of λ chain Abs were identified in these pLNtx mice. Mature B cells express a single class of Ig heavy chain and either λ or κ light chains, which are important for diversity of the B cell repertoire [39, 40]. Functional differences between these two light chains are not known. Higher frequency of one Ig light chains is associated with increased production of one kind of Ig. Thus, high levels of the λ light chain Abs in pLNtx indicated a strong proliferation of only one kind of a B cell clone. Indeed, as described above we have found an increased number of B cells in pLNtx supporting the view that a humoral immune response is induced during oral tolerance induction. Thus, the regenerated environment facilitated by the survived stromal cells decides whether Treg or B cell expansion is induced.

In the current study, OVA feeding resulted in a tolerogenic phenotype, which is characterized by a low DTH response. pLNtx transplanted animals were unable to induce similar numbers of Tregs compared to mLNtx and therefore there was no inhibition of an Ab response in pLNtx. However, pLNtx induced an effect that resulted in a low DTH response against OVA, showing B cell expansion and Ab production. Thus, a humoral immune response was induced in pLNtx. Thereafter, a faster immune response was initiated upon repeated Ag identification. This phenomenon is utilized by vaccination where Ag is given repeatedly to induce a humoral immune response with memory B cells producing Ag-specific Ab. Therefore, pLNtx seem to induce such a humoral immune response comparable to a vaccination by an increased Ab production after repeated OVA feedings.

In pLNtx the immune cells disappeared from the transplanted LN, but the stromal cells survived after transplantation. This leads to the situation that the regenerated lymph node remains their side-specific environment. Thus, stromal cells have a high impact creating this environment; thereby they have a strong influence on the

operation of immunological responses and are important for the balance between tolerance and immunity.

Acknowledgment

The comments of Astrid Westendorf have been a great help. We also wish to thank Melanie Paschy for excellent technical assistance and Tim Worbs for advice with DTH reaction. The work was supported by the Deutsche Forschungsgemeinschaft (SFB621/ A10).

7.5. References

1. Jang, M. H., N. Sougawa, T. Tanaka, T. Hirata, T. Hiroi, K. Tohya, Z. Guo, E. Umemoto, Y. Ebisuno, B. G. Yang, J. Y. Seoh, M. Lipp, H. Kiyono, and M. Miyasaka. 2006. CCR7 is critically important for migration of dendritic cells in intestinal lamina propria to mesenteric lymph nodes. *J. Immunol.* 176:803-810.
2. Forster, R., A. C. Valos-Misslitz, and A. Rot. 2008. CCR7 and its ligands: balancing immunity and tolerance. *Nat. Rev. Immunol.* 8:362-371.
3. Ansel, K. M., L. J. Heyzer-Williams, V. N. Ngo, M. G. Heyzer-Williams, and J. G. Cyster. 1999. In vivo-activated CD4 T cells upregulate CXC chemokine receptor 5 and reprogram their response to lymphoid chemokines. *J. Exp. Med.* 190:1123-1134.
4. Garside, P., E. Ingulli, R. R. Merica, J. G. Johnson, R. J. Noelle, and M. K. Jenkins. 1998. Visualization of specific B and T lymphocyte interactions in the lymph node. *Science* 281:96-99.
5. Faria, A. M., and H. L. Weiner. 2005. Oral tolerance. *Immunol. Rev.* 206:232-259.
6. Garside, P., M. Steel, F. Y. Liew, and A. M. Mowat. 1995. CD4+ but not CD8+ T cells are required for the induction of oral tolerance. *Int. Immunol.* 7:501-504.
7. Nagatani, K., K. Sagawa, Y. Komagata, and K. Yamamoto. 2004. Peyer's patch dendritic cells capturing oral antigen interact with antigen-specific T cells and induce gut-homing CD4(+)CD25(+) regulatory T cells in Peyer's patches. *Ann. N. Y. Acad. Sci.* 1029:366-370.
8. Garside, P., and A. M. Mowat. 2001. Oral tolerance. *Semin. Immunol.* 13:177-185.
9. Kobets, N., K. Kennedy, D. O'Donnell, and P. Garside. 2004. An investigation of the ability of orally primed and tolerised T cells to help B cells upon mucosal challenge. *Immunology* 112:550-558.

10. Smith, K. M., F. McAskill, and P. Garside. 2002. Orally tolerized T cells are only able to enter B cell follicles following challenge with antigen in adjuvant, but they remain unable to provide B cell help. *J. Immunol.* 168:4318-4325.
11. Worbs, T., U. Bode, S. Yan, M. W. Hoffmann, G. Hintzen, G. Bernhardt, R. Forster, and O. Pabst. 2006. Oral tolerance originates in the intestinal immune system and relies on antigen carriage by dendritic cells. *J. Exp. Med.* 203:519-527.
12. Spahn, T. W., H. L. Weiner, P. D. Rennert, N. Lugering, A. Fontana, W. Domschke, and T. Kucharzik. 2002. Mesenteric lymph nodes are critical for the induction of high-dose oral tolerance in the absence of Peyer's patches. *Eur. J. Immunol.* 32:1109-1113.
13. Challacombe, S. J., and T. B. Tomasi, Jr. 1980. Systemic tolerance and secretory immunity after oral immunization. *J. Exp. Med.* 152:1459-1472.
14. Ahrendt, M., S. I. Hammerschmidt, O. Pabst, R. Pabst, and U. Bode. 2008. Stromal cells confer lymph node-specific properties by shaping a unique microenvironment influencing local immune responses. *J. Immunol.* 181:1898-1907.
15. Schmucker, D. L., C. K. Daniels, R. K. Wang, and K. Smith. 1988. Mucosal immune response to cholera toxin in ageing rats. I. Antibody and antibody-containing cell response. *Immunology* 64:691-695.
16. Poulter, L. W., G. J. Seymour, O. Duke, G. Janossy, and G. Panayi. 1982. Immunohistological analysis of delayed-type hypersensitivity in man. *Cell Immunol* 74:358-369.
17. Waksman, B. H. 1979. Cellular hypersensitivity and immunity: conceptual changes in last decade. *Cell Immunol* 42:155-169.
18. Dubois, B., A. Goubier, G. Joubert, and D. Kaiserlian. 2005. Oral tolerance and regulation of mucosal immunity. *Cell Mol. Life Sci.* 62:1322-1332.

19. Mowat, A. M., L. A. Parker, H. Beacock-Sharp, O. R. Millington, and F. Chirido. 2004. Oral tolerance: overview and historical perspectives. *Ann. N. Y. Acad. Sci.* 1029:1-8.
20. Bode, U., G. Sparmann, and J. Westermann. 2001. Gut-derived effector T cells circulating in the blood of the rat: preferential re-distribution by TGF beta-1 and IL-4 maintained proliferation. *Eur. J. Immunol.* 31:2116-2125.
21. Snapper, C. M., K. B. Marcu, and P. Zelazowski. 1997. The immunoglobulin class switch: beyond "accessibility". *Immunity.* 6:217-223.
22. McIntyre, T. M., D. R. Klinman, P. Rothman, M. Lugo, J. R. Dasch, J. J. Mond, and C. M. Snapper. 1993. Transforming growth factor beta 1 selectivity stimulates immunoglobulin G2b secretion by lipopolysaccharide-activated murine B cells. *J. Exp. Med.* 177:1031-1037.
23. Snapper, C. M., T. M. McIntyre, R. Mandler, L. M. Pecanha, F. D. Finkelman, A. Lees, and J. J. Mond. 1992. Induction of IgG3 secretion by interferon gamma: a model for T cell-independent class switching in response to T cell-independent type 2 antigens. *J. Exp. Med.* 175:1367-1371.
24. Estes, D. M., and W. C. Brown. 2002. Type 1 and type 2 responses in regulation of Ig isotype expression in cattle. *Vet. Immunol. Immunopathol.* 90:1-10.
25. Hammerschmidt, S. I., M. Ahrendt, U. Bode, B. Wahl, E. Kremmer, R. Forster, and O. Pabst. 2008. Stromal mesenteric lymph node cells are essential for the generation of gut-homing T cells in vivo. *J. Exp. Med.* 205:2483-2490.
26. Link, A., T. K. Vogt, S. Favre, M. R. Britschgi, H. cha-Orbea, B. Hinz, J. G. Cyster, and S. A. Luther. 2007. Fibroblastic reticular cells in lymph nodes regulate the homeostasis of naive T cells. *Nat. Immunol.* 8:1255-1265.
27. Schiemann, B., J. L. Gommerman, K. Vora, T. G. Cachero, S. Shulga-Morskaya, M. Dobles, E. Frew, and M. L. Scott. 2001. An essential role for BAFF in the normal development of B cells through a BCMA-independent pathway. *Science* 293:2111-2114.

28. Zlotnik, A., and O. Yoshie. 2000. Chemokines: A new classification system and their role in immunity. *Immunity* 12:121-127.
29. Mori, S., H. Nakano, K. Aritomi, C. R. Wang, M. D. Gunn, and T. Kakiuchi. 2001. Mice lacking expression of the chemokines CCL21-ser and CCL19 (plt mice) demonstrate delayed but enhanced T cell immune responses. *J. Exp. Med.* 193:207-218.
30. Ohl, L., M. Mohaupt, N. Czeloth, G. Hintzen, Z. Kiafard, J. Zwirner, T. Blankenstein, G. Henning, and R. Forster. 2004. CCR7 governs skin dendritic cell migration under inflammatory and steady-state conditions. *Immunity*. 21:279-288.
31. Barone, K. S., S. L. Jain, and J. G. Michael. 1995. Effect of in vivo depletion of CD4+ and CD8+ cells on the induction and maintenance of oral tolerance. *Cell Immunol.* 163:19-29.
32. Lim, H. W., P. Hillsamer, A. H. Banham, and C. H. Kim. 2005. Cutting edge: direct suppression of B cells by CD4+ CD25+ regulatory T cells. *J. Immunol.* 175:4180-4183.
33. Strober, W. 2008. Vitamin A rewrites the ABCs of oral tolerance. *Mucosal Immunol.* 1:92-95.
34. Siddiqui, K. R. R., and F. Powrie. 0 AD. CD103+ GALT DCs promote Foxp3+ regulatory T cells. *Mucosal Immunol.* 1:S34-S38.
35. Sun, C. M., J. A. Hall, R. B. Blank, N. Bouladoux, M. Oukka, J. R. Mora, and Y. Belkaid. 2007. Small intestine lamina propria dendritic cells promote de novo generation of Foxp3 T reg cells via retinoic acid. *J. Exp. Med.* 204:1775-1785.
36. Iwata, M., A. Hirakiyama, Y. Eshima, H. Kagechika, C. Kato, and S. Y. Song. 2004. Retinoic acid imprints gut-homing specificity on T cells. *Immunity*. 21:527-538.
37. Mestecky, J., M. W. Russell, and C. O. Elson. 2007. Perspectives on mucosal vaccines: is mucosal tolerance a barrier? *J. Immunol.* 179:5633-5638.

38. Ngan, J., and L. S. Kind. 1978. Suppressor T cells for IgE and IgG in Peyer's patches of mice made tolerant by the oral administration of ovalbumin. *J. Immunol.* 120:861-865.
39. Xu, D. 2006. Dual surface immunoglobulin light-chain expression in B-cell lymphoproliferative disorders. *Arch. Pathol. Lab Med.* 130:853-856.
40. Hardy, R. R., J. L. Dangl, K. Hayakawa, G. Jager, L. A. Herzenberg, and L. A. Herzenberg. 1986. Frequent lambda light chain gene rearrangement and expression in a Ly-1 B lymphoma with a productive kappa chain allele. *Proc. Natl. Acad. Sci. U. S. A* 83:1438-1442.

7.6. Figures

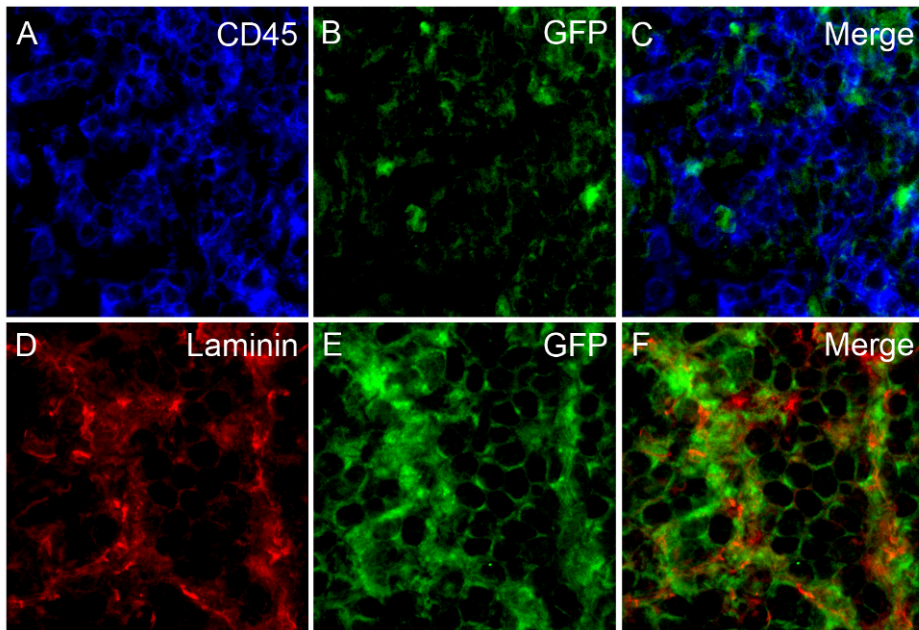


Fig.1: Immune cells were replaced while stromal cells survived

LN fragments of EGFP mice were transplanted into C57BL/6 mice. After regeneration LNtx were removed, cryosections were made and stained with anti-CD45. Only singly positive CD45⁺ cells or GFP⁺ cells could be identified, double positive cells were not seen (**A-C**). Stromal cells were identified using anti-laminin (**D**). Donor cells are GFP⁺ cells (**E**) and merging of the laminin staining and GFP⁺ cells showed that all stromal cells are donor derived (**F**).

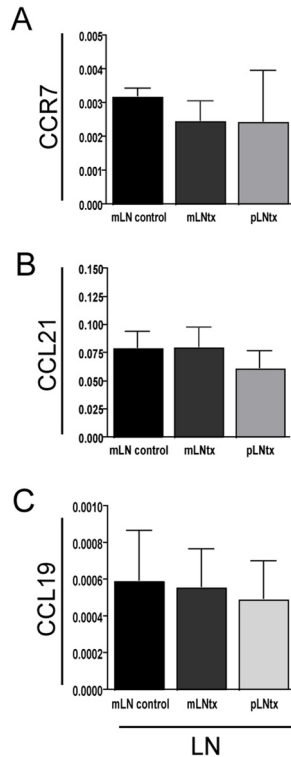


Fig.2: Expression of CCR7, CCL19, and CCL21 are comparable in LNtx

mLNtx or pLNtx fragments were transplanted into the mesentery of C57BL/6 mice and removed after eight weeks. mRNA was isolated and real time PCR were performed in triplet. Control animals were analysed in the same way. **A.** CCR7 mRNA expressed by immune cells and CCL21 and CCL19 (**B, C**) expressed by stromal cells are important chemokines involved in the migration of lymphocytes and DC into different LN compartments. mLNtx and pLNtx showed similar expression levels of all three chemokines and similar mRNA expression compared to control mLN. The data are normalized to the housekeeping gene β -Actin and are shown from 3-8 animals. Means and SEM are given and significant differences in the unpaired t test are included.

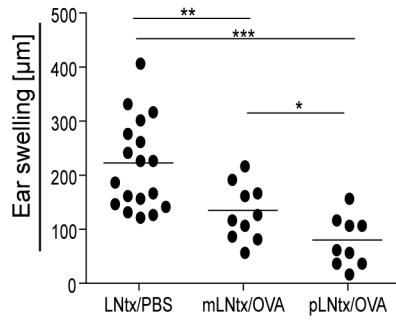


Fig.3: LNtx are able to induce a tolerogenic phenotype

Eight weeks after transplantation mLNtx and pLNtx animals were fed four times with ovalbumin or PBS as a control. Eight days later mice were immunized by subcutaneously injection of OVA in PBS/CFA emulsion and challenged on day 34 by injection of OVA into the right ear and PBS into the left ear. Ear swelling was measured before challenging and 48h later. DTH responses were calculated and each animal is shown as a dot (PBS fed LNtx, n=18; OVA fed LNtx, n=9-10). Significant differences in the unpaired t-test are indicated by * $P < 0.05$; ** $P < 0.01$; *** $P < 0.001$.

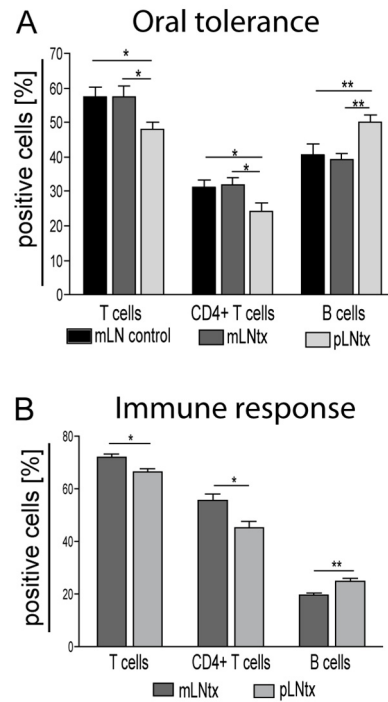


Fig.4: The cell subset composition in pLNtx after tolerance induction is comparable to Cholera toxin treated pLNtx animals

A. After induction of oral tolerance by feeding OVA to mLNtx or pLNtx transplanted mice and control animals, the control mLN and LNtx were analysed via flow cytometry. CD3⁺ and CD4⁺ T cells were found in similar numbers in mLNtx compared to control mLN, whereas in pLNtx decreased numbers were identified. pLNtx showed an increased number of B cells. Means and standard error are given (n= 4-10) and significant differences in the unpaired t-test are indicated by *P< 0.05; **P<0.01. **B.** Cholera toxin was given orally to mLNtx and pLNtx transplanted rats after LN regeneration. LNtx were removed and cell suspensions were made for flow cytometry analyses. In pLNtx a lower percentage of CD3⁺ cells was found, which resulted in decreased numbers of CD4⁺ cells. In contrast more B cells were identified in pLNtx compared to mLNtx. Means and SE are given (n = 4) and significant differences in the unpaired t test are indicated *P < 0.05. **P = 0.01.

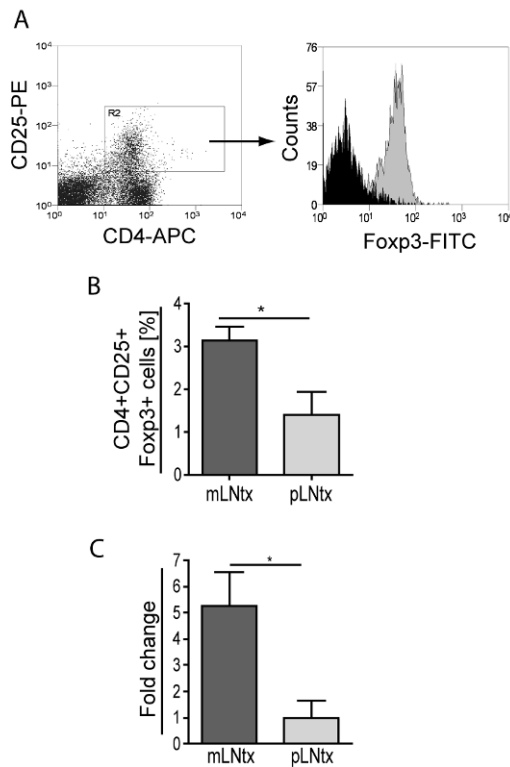


Fig.5: CD4⁺ CD25⁺ FoxP3⁺ Tregs and IL-10 expression are reduced in pLNtx

mLNtx and pLNtx were removed and flow cytometry and real time PCR were performed after tolerance induction. **A-B**. Cell suspensions were made and cells were stained for CD4, CD25, and FoxP3. **A**. Dot plot of a characteristic CD4, CD25 staining. CD4⁺ CD25⁺ cells were gated and FoxP3⁺ cells were measured. Isotype control (black) and FoxP3 staining (grey) are shown in the histogram. **B**. Percentage of the CD4⁺ CD25⁺ FoxP3⁺ cells in mLNtx and pLNtx Ag-tolerant mice. Means and SEM are given (n = 5) and significant differences in the unpaired t test are indicated *P < 0.05. **C**. mRNA of OVA fed LNtx was isolated and real time PCR in triplets was performed. Decreased IL-10 mRNA expression was found in pLNtx compared to mLNtx. Relative mRNA levels were normalized with respect to expression level of pLNtx (fold change set to 1). The data are normalized to the housekeeping gene β -Actin and given from 3-5 animals. Means and SEM are given and significant differences in the unpaired t test are indicated *P < 0.05.

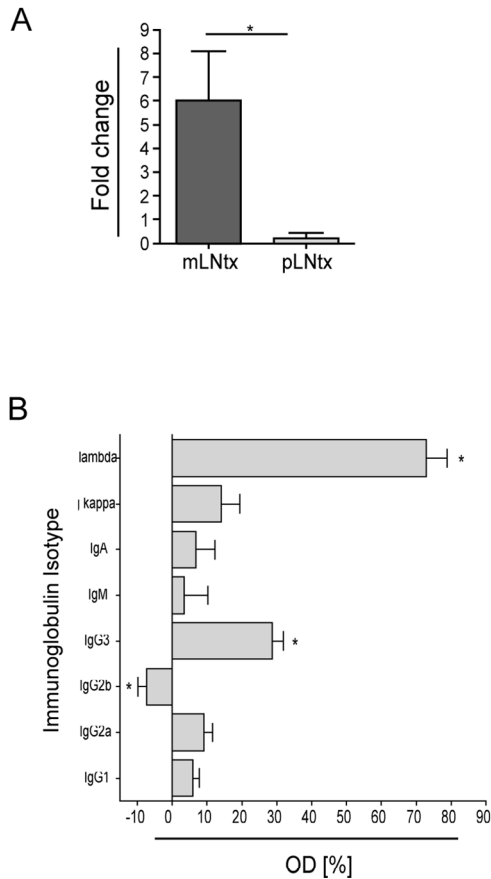


Fig.6: pLNtx showed reduced IL-4 expression and an altered immunoglobulin pattern

A. mRNA of OVA fed LNtx was isolated and real time PCR was performed in triplet. Decreased IL-4 mRNA expression was found in pLNtx compared to mLNtx. The data are normalized to the housekeeping gene β -Actin and given from 3-5 animals. Means and SEM are given and significant differences in the unpaired t test are indicated * $P < 0.05$. **B.** After tolerance induction immunoglobulin isotyping ELISA for the serum was performed in control and transplanted mice. Plates were coated with different immunoglobulin Ab, later on the serum in a dilution to 1:2000; a positive control was included and the optical density (OD) was measured. Calculated to the positive control the data of the OVA fed LNtx were compared with mLNtx as 100%. Increased levels of Ab with a λ chain and also higher levels of IgG₃ were identified whereas IgG_{2b} were found in reduced levels in pLNtx compared to mLNtx Ag-tolerant mice.

Means and standard error are given from 6-8 animals and significant differences in the unpaired t-test are indicated by * $P < 0.05$.

8. General discussion

The gut is a special organ system in the body, colonized by commensals and traversed by pathogens and food antigens. DC pick up different kinds of Ag from the gut and migrate to the mLN via the afferent lymphatics. Therefore, the mLN is different to other LN in the body, for example pLN [5, 6]. Although they have the same architecture based on T and B cell compartments, different cell subsets and differences in the expression of various molecules have been identified. CD103⁺ DC can only be detected in the area of the gut, whereas skin DC show specific expression markers of other regions [17, 19, 24]. Furthermore, DC in the mLN produce RALDH2, an enzyme found to be necessary for the oxidation of vitamin A to retinoic acid, whereby homing molecules on lymphocytes are upregulated [21]. After priming, naïve lymphocytes upregulate CCR9 and $\alpha_4\beta_7$ integrin for gut specific migration [17, 22]. On the other hand MAdCAM-1, the ligand for $\alpha_4\beta_7$ integrin, is exclusively expressed on HEV in mLN and gut associated tissues [7]. Differences in the cytokine pattern between mLN and pLN have also been found. IL-2 and IFN γ are detectable at higher mRNA levels in pLN than in mLN. On the other hand IL-4 and TGF β are expressed to a greater extent in mLN [26].

It is still unclear, how these differences develop and which factors are involved. Antigens, proteins and cells coming from the afferent lymphatics may have a great influence on the formation of the LN environment whereas other components, such as the stromal cells, forming the backbone of the LN, may also have a role in the different outcomes.

To analyze these differences, we established a transplantation model in which mLN of rats and mice were removed from the mesentery and fragments of mLN or pLN were inserted into this region. This chimera was used for further experiments to analyze the influence of the lymph coming from the gut and the sessile stromal cells on creating the unique microenvironment of the mLN. With this work, we are able to show the importance of stromal cells concerning the induction of specific immune responses and oral tolerance.

There are two possible ways how cells enter the mLN. One of these options is the entry via the blood stream by HEV, where naïve T and B cells as well as some activated T cells migrate directly into the LN [5]. On the other hand a mixture of immune cells, soluble Ag and molecules arrive in the paracortical regions of the LN via the afferent lymphatics. Using the transplantation system, we showed that shortly after transplantation the LN are reconnected to the lymph and the blood stream, and immune cells can enter the LNtx by both ways (chapter 4). Further studies showed that transplanted lymph node fragments adhere and connect to the blood system and the lymphatic vessels shortly after transplantation [63, 64]. Chemokines are equally essential for migration of immune cells, especially DC, from the tissue into the LN. CCL19 and CCL21 are produced by HEV and stromal cells in the T cell area which allowed CCR7⁺ immune cells to migrate into the compartments within the LN [12, 65]. In LNtx the normal mRNA expression of these chemokines as well as a comparable composition of immune cells to control LN can be detected (chapter 7). The importance of CCR7, CCL19 and CCL21 had been shown earlier. Förster et al. [66] showed that migration and declined homing as well as positioning of lymphocytes can be disturbed by using CCR7 knock out mice. Additionally, decreased migration of immune cells and a lack of T cell areas were found in plt mice lacking CCL19 and

CCL21 expression in secondary lymphoid organs [9]. HEV are important structures for lymphocyte recirculation from the blood vasculature into the LN. Characteristic endothelial cells make massive immune cell migration possible. Furthermore, HEV express MAdCAM-1, which is exclusively found in mucosal tissues [7]. Peripheral LN are negative for MAdCAM-1 staining. MAdCAM-1 blocking experiments lead to a steep drop in emigration into the HEV [7, 67]. After regeneration of both LNtx, HEV are observed and lymphocytes are recovered in normal numbers (chapter 4). Hence, HEV of transplanted LN fragments are found to be survived, functional and immune cells can migrate into the organ. MAdCAM-1 is found in mLNtx whereas pLNtx show no expression of MAdCAM-1 (chapter 4). Furthermore, stromal cells of the T cell area shown to be podoplanin positive, also survive the transplantation (chapter 4). They rearrange and ensheath the RF, which survive too. In addition, this is also true for stromal cells of the B cell area. Thus, stromal cells of the transplanted LN fragments create the conditions for immune cells to migrate into their specific compartment, whereby they keep their developmental characteristics.

In rats we showed that mLN DC are positive for MHCII and CD103. This unique property makes it easy to identify DC as specific for the gut, whereas pLN DC are detectable through their MHCII^{hi}, CD103⁻ expression [19, 68]. These pLN DC cannot be found in the mLN (chapter 3). In further investigations of pLN and mLN DC it became evident that there are more phenotypic differences, e.g. higher CD11c expression on mLN DC and CD172a (SIRP) on pLN DC (chapter 3). A similar phenotype could be found by analyzing DC from the gut especially from the LP [20, 69] and Langerhans cells from the skin [68, 70, 71]. Also the cytokine pattern produced by DC is tissue specific. The DC from mLN produce higher mRNA levels of IL-4, whereas pLN DC express TGF β to a higher extent (chapter 3). This different

cytokine production of DC results in variable T cell priming. We demonstrated that mLN DC induce more IL-2 receptor positive CD4⁺ T cells and furthermore that mLN primed T cells produce more IFN γ compared to pLN (chapter 3).

However, after transplantation of pLN into the mesentery MHCII⁺ CD103⁺ DC are found in the LNtx but no longer MHCII^{hi} CD103⁻ cells (chapter 4). Thus, DC migrate from the gut to the draining transplanted lymphoid organ. These unique DC coming from the draining area migrate into the LN to present Ag for a successful immune response induction. Furthermore, we showed that these tissue specific DC are highly qualified in binding superantigens and therefore are the main population, responsible for the induction of tissue specific immune responses (chapter 3). Another factor in inducing a tissue specific immune response by CD103⁺ DC is the ability of mLN DC to induce $\alpha_4\beta_7$ integrin and CCR9 on lymphocytes [22, 69]. Lymphocytes which express $\alpha_4\beta_7$ integrin and CCR9 migrate predominantly to the gut system. The ligand of $\alpha_4\beta_7$ integrin, MAdCAM-1, and the ligand of CCR9, CCL25 can only be found on HEV in the gastrointestinal tract [8, 17, 72]. These homing properties are induced by CD103⁺ DC which produce RALDH2 [21]. RALDH2 is an enzyme for the oxidation process of vitamin A to retinoic acid and is expressed by mLN DC but only weakly by pLN DC [21]. After regeneration of transplanted mLN and pLN the mRNA level of RALDH2 was analyzed. Compared to control mLN the mLNtx show a similar expression pattern, though in pLNtx only marginal RALDH2 expression is observed (chapter 4). Since the DC populations from both LNtx are host derived and recruited from the gut, it can be concluded that stromal cells also produce RALDH2. To prove this, stromal cells were isolated from mLN and pLN and analyzed to reveal the mRNA expression. RALDH2 can be identified in the stromal cells of mLN, whereas pLN stromal cells show no expression (chapter 5). The absence of RALDH2 in pLN can lead in pLNtx in a failure to induce a gut homing potential on Ag specific T cells.

In contrast, mLNtx as well as control mLN DC and stromal cells are able to promote lymphocytes to upregulate $\alpha_4\beta_7$ integrin and CCR9 (chapter 4, 5). Thus, stromal cells have a great influence on the migration pattern of immune cells independent of DC. These results suggest that stromal cells are able to instruct DC to change or neglect their tissue specific effect, whereby the migration capacity of immune cells is altered. The influence of stromal cells on the immune system is now spotlighted by many other groups. Therefore, stromal cells have been analyzed via two-photon laser scanning microscopy for their interaction with lymphocytes. These studies showed that stromal cells get into closer contact with immune cells, whereby they can control the migration of T cells as well as B cells to their compartment [12, 15, 65]. Furthermore, on isolated gut epithelial cells mRNA of RALDH1 can be found. Co-cultured with bone marrow-DC, epithelial cells can induce CD103 expression on these DC [73]. Thus, not only mLN DC are able to induce homing properties on immune cells but also stromal cells have the potential to influence these cells.

Differences can also be found in the cytokine pattern between mLN and pLN. IL-2 and IFN γ are detectable in high mRNA levels in pLN to provoke more Th1 dependent responses. In contrast, mLN induce prevalent Th2 immune responses by producing IL-4 and TGF β [26]. After transplantation of pLN into the mesentery, the expression level of IL-4 changes to the level of normal mLN (chapter 4). We also showed that mLN DC are able to produce IL-4 to induce Th2 immune responses (chapter 3). In vivo studies by others have shown recently, that isolated mouse DC from the PP promote the differentiation of Th2 cells [30]. Thus, cytokines such as IL-4 seem to be unaffected by stromal cells but greatly influenced by migrating cells coming from the lymph or the blood.

IL-2 and IFN γ are expressed in pLNtx at the same level as in normal pLN (chapter 4). Incoming host derived immune cells do not seem to be responsible for the expression pattern of these two cytokines; whereas donor derived stromal cells seem to be able to influence the expression. Other studies showed that stromal cells in the T cell area produce IL-7 to support the survival of naïve T cells [74] or CD257 for the B cell endurance [75]. Thus, cytokines seem to be manipulated or produced by stromal cells, possibly through the interaction of immune cells with stromal cells or through the existing LN specific microenvironment.

We demonstrated that under steady state conditions LN show tissue specific differences. These differences were due to stromal cells, and have an impact on the cytokine pattern of the LN and also on the homing properties of lymphocytes. But how important are these differences after Ag recognition and induction of a specific immune response or mucosal tolerance?

First of all we investigated the general role of the mLN for the gastrointestinal tract. The important function of the mLN in mucosal tolerance was shown after removing the mLN when tolerance cannot be induced [60]. Similar to this experimental design, we removed the mLN in rats and induced an immune response by oral CT administration (chapter 6). CT is taken up by DC and transported via the afferent lymphatics to the mLN or reaches the mLN as soluble Ag where it is picked up and presented by resident DC. T cells which recognize the Ag differentiate and proliferate. Effector T cells leave the mLN and home to the gut where they fight CT present in the lumen or infected cells. Other T cells migrate to the border between the T and B cell area to help B cells become IgA producing B cells. After CT administration, increased numbers of secondary follicles and increased numbers of B cells, positive for IgM or IgA were found (chapter 6). Analyzing the gut lavage and the

serum, high levels of CT specific IgA antibodies can be discovered in comparison to untreated animals. Furthermore, we determined the CT specific IgA titer of rats which lack the mLN after resection. Compared to CT treated control animals, increased levels of CT specific IgA were identified in mLN resected animals, in the gut lavage (chapter 6). In line with this a higher number of IgA⁺ CT⁺ cells were detected in the LP of resected CT treated rats (chapter 6). Thus, the mLN is not the only place where the differentiation of antibody producing B cells is induced, but it appears to be the place where the regulation occurs. The mLN may have a regulatory function in the productive efficiency of Ab producing B cells and therefore in regulating the amplitude of immune responses. This argumentation was supported by the finding that mLN transplanted animals show normal CT specific IgA levels in the gut lavage (chapter 4). However, the level in pLNtx animals is reduced. Additionally, we found reduced IgA producing B cells in pLNtx which expressed decreased amounts of CCR9 (chapter 4). Due to this, differentiated B cells from the pLNtx appear to be unprivileged in their migration to the gut and their production of adequate amounts of Ag specific IgA. Hence, stromal cells are able to influence the specificity of immune responses by producing enzymes such as RALDH2 and also by contacting immune cells to influence their cytokine (e.g. IL-2), chemokine (e.g. CCR9) and antibody generation.

As described above, the mLN was shown to be necessary to induce mucosal tolerance. Mucosal or oral tolerance is the absence of an immune response after Ag recognition and presentation. It is known that DC and regulatory T cells are involved, by suppressing the proliferation and differentiation of T and B cells, but how this happens in detail is still unclear. Only the function of DC in this system is well established. DC take up Ag from the gut lumen and migrate to the mLN via the

afferent lymphatics. There they present the harmless Ag to T cells, which leads to deletion or anergy of T cells or to the stimulation of regulatory T cells, whereby an immune response is prevented [47]. Further studies showed that the mLN is an important organ for the induction of oral tolerance [60]. After removing the mLN or blocking its development by $LT\beta R$ antibodies, tolerance cannot be induced [60, 76]. However, the injection of T cells isolated from the mLN of tolerized mice, showed also tolerance in the recipient [62]. Tolerance was detected by measurement of ear swelling after feeding the antigen, immunization and challenge. It is known that DC migrate into the mLN where $CD4^+$ T cells are induced by RALDH2 to upregulate FoxP3, a transcription factor expressed in regulatory T cells [53, 54]. We showed that tolerance can be induced in both LNtx transplanted animals, whereby pLNtx tolerized mice show improved oral tolerance induction, compared to mLNtx mice (chapter 7). However, different cell subset compositions are found in mLNtx and pLNtx. In pLNtx, decreased percentages of $CD4^+$ T cells and more relevant for tolerance reduced numbers of regulatory T cells are seen compared to control mLN and mLNtx. The presence of regulatory T cells is associated with the production of the suppressor cytokines, such as IL-10 [77] and therefore a lower mRNA expression of IL-10 is found in pLNtx (chapter 7). In contrast, B cells are increased in pLNtx mice. Furthermore, in the serum of pLNtx animals, increased levels of IgG_3 are found compared to mLNtx (chapter 7). Thus, in pLNtx animals no RALDH2 production is detected (chapter 4, 5) and therefore in these LNtx, the induction of regulatory T cells is reduced and this results in an increased number of B cells and immunoglobulin production. Increased B cell numbers and the production of Ab after Ag recognition are found during humoral immune responses. Thereby, a faster immune response is initiated by repeated Ag identification and this is utilized by vaccination, when Ag is given several times. Therefore, after feeding OVA several times pLNtx animals show

a tolerogenic phenotype, but it seems to be induced by a humoral immune response comparable to a vaccination by an increased Ab production. Thus, stromal cells have a great influence on the decision how an immunological reaction works.

In conclusion, we demonstrated that cells and molecules arriving via the lymph or the blood have only a minor effect on the environment of mLN. In contrast, we showed that stromal cells of LN are very important in regulating the intensity and the direction of an efficient immune response. Lymphocytes and DC migrate into the LN, showing a tissue specific phenotype, whereby DC in mLN are able to induce the upregulation of homing molecules on lymphocytes. However, DC, which come from the gut, are not able to induce homing properties in pLNtx. In addition, stromal cells control the migration of immune cells expressing MAdCAM-1. They are involved in inducing homing molecules on lymphocytes by producing RALDH2. Additionally, stromal cells influence the production of cytokines, whereby the direction of an immune response is defined. If tolerance or immune responses are initiated is also stromal cell dependent. Thus, stromal cells are important player in the regulation of tolerance and immunity. Therefore, stromal cells are greatly responsible for forming an LN specific microenvironment.

9. References

1. Blum, K. S., and R. Pabst. 2006. Keystones in lymph node development. *J. Anat.* 209:585-595.
2. Pabst, R. 2007. Plasticity and heterogeneity of lymphoid organs. What are the criteria to call a lymphoid organ primary, secondary or tertiary? *Immunol. Lett.* 112:1-8.
3. Cyster, J. G., K. M. Ansel, K. Reif, E. H. Ekland, P. L. Hyman, H. L. Tang, S. A. Luther, and V. N. Ngo. 2000. Follicular stromal cells and lymphocyte homing to follicles. *Immunol. Rev.* 176:181-193.
4. Brandtzaeg, P., and F. E. Johansen. 2005. Mucosal B cells: phenotypic characteristics, transcriptional regulation, and homing properties. *Immunol. Rev.* 206:32-63.
5. Bode, U., C. Duda, F. Weidner, M. Rodriguez-Palmero, K. Wonigeit, R. Pabst, and J. Westermann. 1999. Activated T cells enter rat lymph nodes and Peyer's patches via high endothelial venules: survival by tissue-specific proliferation and preferential exit of CD8(+) T cell progeny. *Eur. J. Immunol.* 29:1487-1495.
6. Gretz, J. E., A. O. Anderson, and S. Shaw. 1997. Cords, channels, corridors and conduits: Critical architectural elements facilitating cell interactions in the lymph node cortex. *Immunol. Rev.* 156:11-24.
7. Girard, J. P., and T. A. Springer. 1995. High endothelial venules (HEVs): specialized endothelium for lymphocyte migration. *Immunol. Today* 16:449-457.
8. Tanaka, T., Y. Ebisuno, N. Kanemitsu, E. Umemoto, B. G. Yang, M. H. Jang, and M. Miyasaka. 2004. Molecular determinants controlling homeostatic recirculation and tissue-specific trafficking of lymphocytes. *Int. Arch. Allergy Immunol.* 134:120-134.

9. Mori, S., H. Nakano, K. Aritomi, C. R. Wang, M. D. Gunn, and T. Kakiuchi. 2001. Mice lacking expression of the chemokines CCL21-ser and CCL19 (plt mice) demonstrate delayed but enhanced T cell immune responses. *J. Exp. Med.* 193:207-218.
10. Crivellato, E., A. Vacca, and D. Ribatti. 2004. Setting the stage: an anatomist's view of the immune system. *Trends Immunol.* 25:210-217.
11. Westermann, J., and R. Pabst. 1996. How organ-specific is the migration of 'naive' and 'memory' T cells? *Immunol. Today* 17:278-282.
12. Bajenoff, M., J. G. Egen, L. Y. Koo, J. P. Laugier, F. Brau, N. Glaichenhaus, and R. N. Germain. 2006. Stromal cell networks regulate lymphocyte entry, migration, and territoriality in lymph nodes. *Immunity.* 25:989-1001.
13. Crivellato, E., and F. Mallardi. 1997. Stromal cell organisation in the mouse lymph node. A light and electron microscopic investigation using the zinc iodide-osmium technique. *Journal of Anatomy* 190:85-92.
14. Ushiki, T., O. Ohtani, and K. Abe. 1995. Scanning Electron-Microscopic Studies of Reticular Framework in the Rat Mesenteric Lymph-Node. *Anat. Rec.* 241:113-122.
15. Katakai, T., T. Hara, M. Sugai, H. Gonda, and A. Shimuzu. 2004. Lymph node fibroblastic reticular cells construct the stromal reticulum via contact with lymphocytes. *J. Exp. Med.* 200:783-795.
16. Sixt, M., N. Kanazawa, M. Seig, T. Samson, G. Roos, D. P. Reinhardt, R. Pabst, M. B. Lutz, and L. Sorokin. 2005. The conduit system transports soluble antigens from the afferent lymph to resident dendritic cells in the T cell area of the lymph node. *Immunity* 22:19-29.
17. Sigmundsdottir, H., and E. C. Butcher. 2008. Environmental cues, dendritic cells and the programming of tissue-selective lymphocyte trafficking. *Nat. Immunol.* 9:981-987.

18. Brenan, M., and M. Puklavec. 1992. The MRC OX-62 antigen: a useful marker in the purification of rat veiled cells with the biochemical properties of an integrin. *J. Exp. Med.* 175:1457-1465.
19. Yrlid, U., and G. MacPherson. 2003. Phenotype and function of rat dendritic cell subsets. *APMIS* 111:756-765.
20. Iwasaki, A. 2007. Mucosal dendritic cells. *Annu. Rev. Immunol.* 25:381-418.
21. Iwata, M., A. Hirakiyama, Y. Eshima, H. Kagechika, C. Kato, and S. Y. Song. 2004. Retinoic acid imprints gut-homing specificity on T cells. *Immunity* 21:527-538.
22. Stagg, A. J., M. A. Kamm, and S. C. Knight. 2002. Intestinal dendritic cells increase T cell expression of alpha 4 beta 7 integrin. *Eur. J. Immunol.* 32:1445-1454.
23. Svensson, M., B. Johansson-Lindbom, F. Zapata, E. Jaensson, L. M. Austenaa, R. Blomhoff, and W. W. Agace. 0 AD. Retinoic acid receptor signaling levels and antigen dose regulate gut homing receptor expression on CD8⁺ T cells. *Mucosal Immunol.* 1:38-48.
24. Mebius, R. E. 2007. Vitamins in control of lymphocyte migration. *Nature Immunol.* 8:229-230.
25. Mora, J. R., M. Iwata, B. Eksteen, S. Y. Song, T. Junt, B. Senman, K. L. Otipoby, A. Yokota, H. Takeuchi, P. Ricciardi-Castagnoli, K. Rajewsky, D. H. Adams, and U. H. von Andrian. 2006. Generation of gut-homing IgA-secreting B cells by intestinal dendritic cells. *Science* 314:1157-1160.
26. Bode, U., G. Sparmann, and J. Westermann. 2001. Gut-derived effector T cells circulating in the blood of the rat: preferential re-distribution by TGF beta-1 and IL-4 maintained proliferation. *Eur. J. Immunol.* 31:2116-2125.
27. Elgueta, R., F. E. Sepulveda, F. Vilches, L. Vargas, J. R. Mora, M. R. Bono, and M. Roseblatt. 2008. Imprinting of CCR9 on CD4 T cells requires IL-4 signaling on mesenteric lymph node dendritic cells. *J. Immunol.* 180:6501-6507.

28. Ertesvag, A., L. M. Austenaa, H. Carlsen, R. Blomhoff, and H. K. Blomhoff. 2008. Retinoic acid inhibits in vivo interleukin-2 gene expression and T-cell activation in mice. *Immunology*.
29. Gaffen, S. L., and G. Hajishengallis. 2008. A new inflammatory cytokine on the block: re-thinking periodontal disease and the Th1/Th2 paradigm in the context of Th17 cells and IL-17. *J. Dent. Res.* 87:817-828.
30. Coombes, J. L., and F. Powrie. 2008. Dendritic cells in intestinal immune regulation. *Nat. Rev. Immunol.* 8:435-446.
31. Lanzavecchia, A., and F. Sallusto. 2001. Regulation of T cell immunity by dendritic cells. *Cell* 106:263-266.
32. Banchereau, J., and R. M. Steinman. 1998. Dendritic cells and the control of immunity. *Nature* 392:245-252.
33. Sallusto, F., A. Lanzavecchia, and C. R. Mackay. 1998. Chemokines and chemokine receptors in T-cell priming and Th1/Th2-mediated responses. *Immunol. Today* 19:568-574.
34. Sallusto, F., J. Geginat, and A. Lanzavecchia. 2004. Central memory and effector memory T cell subsets: function, generation, and maintenance. *Annu. Rev. Immunol.* 22:745-763.
35. Mempel, T. R., S. E. Henrickson, and U. H. von Andrian. 2004. T-cell priming by dendritic cells in lymph nodes occurs in three distinct phases. *Nature* 427:154-159.
36. Mora, J. R., and U. H. von Andrian. 2006. T-cell homing specificity and plasticity: new concepts and future challenges. *Trends Immunol.* 27:235-243.
37. Mora, J. R., and U. H. von Andrian. 2008. Differentiation and homing of IgA-secreting cells. *Mucosal Immunol* 1:96-109.
38. Mcghee, J. R., J. Kunisawa, and H. Kiyono. 2007. Gut lymphocyte migration: we are halfway 'home'. *Trends Immunol.* 28:150-153.

39. Lamm, M. E., and J. M. Phillips-Quagliata. 2002. Origin and homing of intestinal IgA antibody-secreting cells. *J. Exp. Med.* 195:F5-F8.
40. Ganusov, V. V., and R. J. De Boer. 2007. Do most lymphocytes in humans really reside in the gut? *Trends Immunol.* 28:514-518.
41. Johansson-Lindbom, B., and W. W. Agace. 2007. Generation of gut-homing T cells and their localization to the small intestinal mucosa. *Immunol Rev.* 215:226-242.
42. Kunisawa, J., and H. Kiyono. 2005. A marvel of mucosal T cells and secretory antibodies for the creation of first lines of defense. *Cell Mol. Life Sci.* 62:1308-1321.
43. Cerutti, A., and M. Rescigno. 2008. The biology of intestinal immunoglobulin A responses. *Immunity.* 28:740-750.
44. Macpherson, A. J., and E. Slack. 2007. The functional interactions of commensal bacteria with intestinal secretory IgA. *Curr. Opin. Gastroenterol.* 23:673-678.
45. Macpherson, A. J., K. D. McCoy, F. E. Johansen, and P. Brandtzaeg. 0 AD. The immune geography of IgA induction and function. *Mucosal Immunol.* 1:11-22.
46. Snoeck, V., I. R. Peters, and E. Cox. 2006. The IgA system: a comparison of structure and function in different species. *Vet. Res.* 37:455-467.
47. Faria, A. M., and H. L. Weiner. 2005. Oral tolerance. *Immunol Rev.* 206:232-259.
48. Tsuji, N. M., and A. Kosaka. 2008. Oral tolerance: intestinal homeostasis and antigen-specific regulatory T cells. *Trends Immunol.*
49. Mowat, A. M. 2003. Anatomical basis of tolerance and immunity to intestinal antigens. *Nat. Rev. Immunol* 3:331-341.
50. Garside, P., and A. M. Mowat. 2001. Oral tolerance. *Semin. Immunol.* 13:177-185.

51. Garside, P., M. Steel, F. Y. Liew, and A. M. Mowat. 1995. CD4+ but not CD8+ T cells are required for the induction of oral tolerance. *Int. Immunol.* 7:501-504.
52. Barone, K. S., S. L. Jain, and J. G. Michael. 1995. Effect of in vivo depletion of CD4+ and CD8+ cells on the induction and maintenance of oral tolerance. *Cell Immunol.* 163:19-29.
53. Siddiqui, K. R. R., and F. Powrie. 0 AD. CD103+ GALT DCs promote Foxp3+ regulatory T cells. *Mucosal Immunol.* 1:S34-S38.
54. Sun, C. M., J. A. Hall, R. B. Blank, N. Bouladoux, M. Oukka, J. R. Mora, and Y. Belkaid. 2007. Small intestine lamina propria dendritic cells promote de novo generation of Foxp3 T reg cells via retinoic acid. *J. Exp. Med.* 204:1775-1785.
55. Nagatani, K., K. Sagawa, Y. Komagata, and K. Yamamoto. 2004. Peyer's patch dendritic cells capturing oral antigen interact with antigen-specific T cells and induce gut-homing CD4(+)CD25(+) regulatory T cells in Peyer's patches. *Ann. N. Y. Acad. Sci.* 1029:366-370.
56. Lim, H. W., P. Hillsamer, A. H. Banham, and C. H. Kim. 2005. Cutting edge: direct suppression of B cells by CD4+ CD25+ regulatory T cells. *J. Immunol.* 175:4180-4183.
57. Kobets, N., K. Kennedy, D. O'Donnell, and P. Garside. 2004. An investigation of the ability of orally primed and tolerised T cells to help B cells upon mucosal challenge. *Immunology* 112:550-558.
58. Smith, K. M., F. McAskill, and P. Garside. 2002. Orally tolerized T cells are only able to enter B cell follicles following challenge with antigen in adjuvant, but they remain unable to provide B cell help. *J. Immunol.* 168:4318-4325.
59. Gonnella, P. A., H. P. Waldner, and H. L. Weiner. 2001. B cell-deficient (mu MT) mice have alterations in the cytokine microenvironment of the gut-associated lymphoid tissue (GALT) and a defect in the low dose mechanism of oral tolerance. *J. Immunol.* 166:4456-4464.

60. Worbs, T., U. Bode, S. Yan, M. W. Hoffmann, G. Hintzen, G. Bernhardt, R. Forster, and O. Pabst. 2006. Oral tolerance originates in the intestinal immune system and relies on antigen carriage by dendritic cells. *J. Exp. Med.* 203:519-527.
61. Spahn, T. W., H. L. Weiner, P. D. Rennert, N. Lugering, A. Fontana, W. Domschke, and T. Kucharzik. 2002. Mesenteric lymph nodes are critical for the induction of high-dose oral tolerance in the absence of Peyer's patches. *Eur. J. Immunol.* 32:1109-1113.
62. Challacombe, S. J., and T. B. Tomasi, Jr. 1980. Systemic tolerance and secretory immunity after oral immunization. *J. Exp. Med.* 152:1459-1472.
63. Mebius, R. E., J. Breve, G. Kraal, and P. R. Streeter. 1993. Developmental Regulation of Vascular Addressin Expression - A Possible Role for Site-Associated Environments. *Int. Immunol.* 5:443-449.
64. Pabst, R., and H. J. Rothkotter. 1988. Regeneration of autotransplanted lymph node fragments. *Cell Tissue Res.* 251:597-601.
65. Katakai, T., T. Hara, J. H. Lee, H. Gonda, M. Sugai, and A. Shimizu. 2004. A novel reticular stromal structure in lymph node cortex: an immuno-platform for interactions among dendritic cells, T cells and B cells. *Int. Immunol.* 16:1133-1142.
66. Forster, R., A. C. Valos-Misslitz, and A. Rot. 2008. CCR7 and its ligands: balancing immunity and tolerance. *Nat. Rev. Immunol.* 8:362-371.
67. Ihara, Y., S. Miyagawa, T. Hasegawa, T. Kimura, H. Xu, and M. Fukuzawa. 2007. Effect of blocking the mucosal addressin cell adhesion molecule-1 (MAdCAM-1) in a rat small intestinal transplantation model. *Transpl. Immunol* 17:271-277.
68. Itano, A. A., S. J. McSorley, R. L. Reinhardt, B. D. Ehst, E. Ingulli, A. Y. Rudensky, and M. K. Jenkins. 2003. Distinct dendritic cell populations sequentially present antigen to CD4 T cells and stimulate different aspects of cell-mediated immunity. *Immunity.* 19:47-57.

69. Johansson-Lindbom, B., M. Svensson, O. Pabst, C. Palmqvist, G. Marquez, R. Forster, and W. W. Agace. 2005. Functional specialization of gut CD103(+) dendritic cells in the regulation of tissue-selective T cell homing. *J. Exp. Med.* 202:1063-1073.
70. Ohl, L., M. Mohaupt, N. Czeloth, G. Hintzen, Z. Kiafard, J. Zwirner, T. Blankenstein, G. Henning, and R. Forster. 2004. CCR7 governs skin dendritic cell migration under inflammatory and steady-state conditions. *Immunity.* 21:279-288.
71. Hagnerud, S., P. P. Manna, M. Cella, A. Stenberg, W. A. Frazier, M. Colonna, and P. A. Oldenborg. 2006. Deficit of CD47 results in a defect of marginal zone dendritic cells, blunted immune response to particulate antigen and impairment of skin dendritic cell migration. *J. Immunol.* 176:5772-5778.
72. Johansson-Lindbom, B., and W. W. Agace. 2004. Vitamin A helps gut T cells find their way in the dark. *Nature Medicine* 10:1300-1301.
73. Edele, F., R. Molenaar, D. Gutle, J. C. Dudda, T. Jakob, B. Homey, R. Mebius, M. Hornef, and S. F. Martin. 2008. Cutting edge: instructive role of peripheral tissue cells in the imprinting of T cell homing receptor patterns. *J. Immunol.* 181:3745-3749.
74. Link, A., T. K. Vogt, S. Favre, M. R. Britschgi, H. cha-Orbea, B. Hinz, J. G. Cyster, and S. A. Luther. 2007. Fibroblastic reticular cells in lymph nodes regulate the homeostasis of naive T cells. *Nat. Immunol.* 8:1255-1265.
75. Schiemann, B., J. L. Gommerman, K. Vora, T. G. Cachero, S. Shulga-Morskaya, M. Dobles, E. Frew, and M. L. Scott. 2001. An essential role for BAFF in the normal development of B cells through a BCMA-independent pathway. *Science* 293:2111-2114.
76. Spahn, T. W., M. K. Muller, W. Domschke, and T. Kucharzik. 2006. Role of lymphotoxins in the development of Peyer's patches and mesenteric lymph nodes: relevance to intestinal inflammation and treatment. *Ann. N. Y. Acad. Sci.* 1072:187-193.

77. Dubois, B., A. Goubier, G. Joubert, and D. Kaiserlian. 2005. Oral tolerance and regulation of mucosal immunity. *Cell Mol. Life Sci.* 62:1322-1332.

10. Contribution

I contributed to all studies by performing the transplantation model.

In the publication “Dendritic cell subsets in lymph nodes are characterized by the specific draining area and influence the phenotype and fate of primed T cells” I analyzed the dendritic cell subpopulation of transplanted lymph node fragments (mLNtx and pLNtx) for their composition pattern.

In “Stromal cells confer lymph node-specific properties by shaping a unique microenvironment influencing local immune responses” most of the work was done by myself. I received technical help with flow cytometry and histochemical staining.

For “Stromal mesenteric lymph node cells are essential for the generation of gut-homing T cells in vivo” I carried out the animal studies including the transplantation.

The work for the publication “Lymph node stromal cells strongly influence immune response suppression” was also done by myself with technical help with flow cytometry and histochemical staining as well as the ELISA technique.

In “The mesenteric lymph nodes exhibit a regulatory function in forming a Cholera-toxin specific IgA response in the intestine, whereas the spleen reacts systemically by specific IgM” I performed the animal studies including the surgery and the cholera toxin administration. Furthermore, fluorescence staining analysis was also done by myself.

11. Curriculum vitae

I. General Information

Name: Manuela Ahrendt
Date of birth: July 27th, 1977
Place of birth: Magdeburg, Germany
Citizenship: German
Address: Gellertstr.57
30175 Hannover, Germany

II. Education

1984 – 1998 Primary and Grammar School
June 1998 Abitur (high school diploma), Gymnasium Bad Zwischenahn/
Edeweicht, Germany

1998 - 2000 Study of Biology, Martin Luther University, Halle/Saale, Germany
2000 - 2004 Study of Biology, Carl von Ossietzky University, Oldenburg,
Germany

Since 2005 Scientific assistant; Medical School Hannover, Institute for
Functional and Applied Anatomy, Germany

III. Conferences and Workshops

- 4th -5th September 2006 Development and Function of Secondary and Tertiary
Lymphoid Tissues; Institute Pasteur, Paris, France
Poster
- 4th -5th September 2007 “Annual Meeting 2007“ des Arbeitskreises
Adhäsionsmoleküle; Heidelberg, Germany
Poster
- 5th -7th September 2007 37th Annual Meeting of the German Society for
Immunology; Heidelberg, Germany
Poster
- 2nd -7th March 2008 4th Spring School on Immunology; Ettal, Germany
Poster
Talk
- 3rd -6th September 2008 Joint Annual Meeting of Immunology; Vienna, Austria
Poster
- 14th November 2008 DC Workshop; Hannover, Germany
Talk

12. Publication list

Original Publications

Langhans B and **Ahrendt M**, Nattermann J, Sauerbruch T, Spengler U (2005) Comparative study of NK cell-mediated cytotoxicity using radioactive and flow cytometric cytotoxicity assays. *J. Immunol. Methods.* 306:161-8.

Gerhardt T, Pöge U, Stoffel-Wagner B, **Ahrendt M**, Wolff M, Spengler U, Palmedo H, Sauerbruch T, Woitas RP (2006) Estimation of glomerular filtration rates after orthotopic liver transplantation: Evaluation of cystatin C-based equations. *Liver Transpl.* 12:1667-72.

Bode U, Lorchner M, **Ahrendt M**, Blessenohl M, Kalies K, Claus A, Overbeck S, Rink L, Pabst R (2008) Dendritic cell subsets in lymph nodes are characterized by the specific draining area and influence the phenotype and fate of primed T cells. *Immunology.* 123:480-90.

Ahrendt M, Hammerschmidt SI, Pabst O, Pabst R, Bode U. (2008) Stromal cells confer lymph node-specific properties by shaping a unique microenvironment influencing local immune responses. *J. Immunol.* 181:1898-907

Hammerschmidt SI, **Ahrendt M**, Bode U, Kremmer E, Förster R, Pabst O. (2008) Stromal mesenteric lymph node cells are essential for the generation of gut-homing T cells in vivo. *J. Exp. Med.* 205:2483-90

Hahn A, Thiessen N, Pabst R, **Ahrendt M**, Bode U. (2009) The mesenteric lymph nodes exhibit a regulatory function in forming a Cholera-toxin specific IgA response in the intestine, whereas the spleen reacts systemically by specific IgM (submitted at *Immunology*)

Ahrendt M, Pabst R, Bode U. (2009) The effect of immune response suppression is strongly influenced by stromal cells of lymph nodes (submitted at *J. Immunol.*)

Abstract publications

Ahrendt M, Hammerschmidt SI, Pabst O, Pabst R, Bode U; „Stromal cells confer lymph node-specific properties by shaping a unique microenvironment influencing local immune responses“ in: Wiener klinische Wochenschrift Suppl 01/08; „Joint annual Meeting of Immunology“ Vienna, Austria, 3.-6. September 2008

Fleissner D, **Ahrendt M**, Bode U, Buer J, Westendorf AM; „Initiation of cytotoxic epithelial-specific CD8⁺ T cell responses in the intestinal mucosa“ in: Wiener klinische Wochenschrift Suppl 01/08; „Joint annual Meeting of Immunology“ Vienna, Austria, 3.-6. September 2008

Hahn A, Thiessen N, Pabst R, **Ahrendt M**, Bode U; „ The mesenteric lymph node regulates the amplitude of IgA secretion in the drained area: potential role of the spleen in the immune response against orally applied cholera toxin“ in: Wiener klinische Wochenschrift Suppl 01/08; „Joint annual Meeting of Immunology“ Vienna, Austria, 3.-6. September 2008

13. Erklärung zur Dissertation

Hierdurch erkläre ich, dass die Dissertation „The role of afferent lymph from the gut in the regulation of the microenvironment and the immune response in the mesenteric lymph node“ selbstständig verfasst und alle benutzten Hilfsmittel sowie evtl. zur Hilfeleistung herangezogene Institutionen vollständig angegeben wurden.

Die Dissertation wurde nicht schon als Diplom- oder ähnliche Prüfungsarbeit verwendet.

Hannover, den

Name: Manuela Ahrendt

14. Danksagung

Es sei mir an dieser Stelle gestattet all jenen Personen zu danken, die mich in den vergangenen Jahren unterstützt haben.

An erster Stelle möchte ich mich ganz herzlich bei Frau Dr. Ulrike Bode für die erstklassige Betreuung der Arbeit bedanken. Sie hat durch ihre fachliche Kompetenz, ihre ständige Diskussionsbereitschaft, ihre Geduld und nicht zuletzt durch ihre moralische Unterstützung ganz wesentlich zum Gelingen dieser Arbeit beigetragen.

Mein besonderer Dank gilt auch Herrn Prof. Dr. Reinhard Pabst für die freundliche Aufnahme am Institut für Funktionelle und Angewandte Anatomie, die Bereitstellung des Arbeitsplatzes und das meiner Arbeit entgegengebrachte Interesse.

Frau Frauke Weidner und Frau Melanie Paschy danke ich für die technische Unterstützung. Des Weiteren möchte ich mich ganz herzlich bei allen Mitarbeitern des Instituts für Funktionelle und Angewandte Anatomie für das gute Arbeitsklima und die große Hilfsbereitschaft bedanken.

Ich danke allen meinen Freunden für ihr Verständnis und ihre moralische Unterstützung. Ganz besonders danke Jutta Schade und Katrin Blum für ihre aufmunternden Worte und Taten während und nach der Arbeitszeit, Christiane Pietzsch für ihr offenes Ohr und Henning Büttner für die Ruhe und Entspannung in aufregenden Zeiten.

Besonderer Dank gilt natürlich nicht zuletzt auch meiner Familie, vor allem meinen Eltern, die mich mit Liebe und Unterstützung begleitet haben.

Diese Arbeit wurde unterstützt von der Deutschen Forschungsgemeinschaft (DFG).